Multi-modality imaging assessment of native valvular regurgitation: an EACVI and ESC council of valvular heart disease position paper

Lancellotti, P.; Pibarot, P.; Chambers, J.; Canna, G. la; Pepi, M.; Dulgheru, R.; ... ; European Association Cardiovasculair Imaging

EACVI DOCUMENT

Multi-modality imaging assessment of native valvular regurgitation: an EACVI and ESC council of valvular heart disease position paper

Patrizio Lancellotti [1,2,3]*, Philippe Pibarot [4], John Chambers[5],
Giovanni La Canna[6], Mauro Pepi[7], Raluca Dulgheru[1], Mark Dweck[8],
Victoria Delgado [9], Madalina Garbi[10], Mani A. Vannan[11], David Montaigne [12],
Luigi Badano[13,14], Pal Maurovich-Horvat[15], Gianluca Pontone [16],
Alec Vahanian [17,18], Erwan Donal [19], and Bernard Cosyns [20]; On behalf of the
Scientific Document Committee of the European Association of Cardiovascular
Imaging

[1]Department of Cardiology, Valvular Disease Clinic, University of Liège Hospital, GIGA Cardiovascular Sciences, CHU Sart Tilman, 4000 Liège, Belgium; [2]Gruppo Villa Maria Care and Research, Maria Cecilia Hospital, Cotignola, Italy; [3]Anthea Hospital, Via Camillo Rosalba, 35, Bari, Italy; [4]Department of Medicine, Québec Heart & Lung Institute, Laval University, 2725, chemin Sainte-Foy, Québec, Canada; [5]Emeritus Professor of Clinical Cardiology, Guy's and St Thomas' Hospital, London SE1 7EH, UK; [6]Cardiovascular Department, IRCCS Humanitas Clinical and Research Hospital, Applied Diagnostic Echocardiography, 20089 Rozzano, Milan, Italy; [7]Department of Cardiovascular Imaging, Centro Cardiologico Monzino IRCCS, 20138 Milan, Italy; [8]BHF Centre for Cardiovascular Science, University of Edinburgh, Little France Crescent, Edinburgh EH16 4SB, UK; [9]Department of Cardiology, Leiden University Medical Center, Albinusdreef 2 2300 RC Leiden, The Netherlands; [10]Royal Papworth Hospital, Cambridge University Health Partner, Cambridge Biomedical Campus, CB2 0AY Cambridge, UK; [11]Marcus Heart Valve Center, Piedmont Heart Institute, Atlanta, GA, USA; [12]University of Lille, Inserm, CHU Lille, Institut Pasteur de Lille, U1011-EGID, F-59000 Lille, France; [13]Department of Medicine and Surgery, University of Milano-Bicocca, 20089 Milan, Italy; [14]Department of Cardiac, Metabolic and Neural Sciences, Istituto Auxologico Italiano, IRCCS, 20089 Milan, Italy; [15]MTA-SE Cardiovascular Imaging Research Group, Medical Imaging Centre, Semmelweis University, 1083 Budapest, Hungary; [16]Centro Cardiologico Monzino, IRCCS, 20138 Milan, Italy; [17]UFR Medecine, Université de Paris, Site Bichat, 16 rue Huchard, 75018 Paris, France; [18]LVTS INSERM U1148, GH Bichat, 46, rue Henri Huchard, 75018 Paris, France; [19]University of Rennes, CHU Rennes, Inserm, LTSI—UMR 1099, Rennes, France; and [20]Department of Cardiology, CHVZ (Centrum voor Hart en Vaatziekten), ICMI (In Vivo Cellular and Molecular Imaging) Laboratory, Universitair Ziekenhuis Brussel, 101 Laarbeeklaan, 1090 Brussels, Belgium

Valvular regurgitation represents an important cause of cardiovascular morbidity and mortality. Imaging is pivotal in the evaluation of native valve regurgitation and echocardiography is the primary imaging modality for this purpose. The imaging assessment of valvular regurgitation should integrate quantification of the regurgitation, assessment of the valve anatomy and function, and the consequences of valvular disease on cardiac chambers. In clinical practice, the management of patients with valvular regurgitation largely relies on the results of imaging. It is crucial to provide standards that aim at establishing a baseline list of measurements to be performed when assessing native valve regurgitation. The present document aims to present clinical guidance for the multi-modality imaging assessment of native valvular regurgitation.

Keywords   valvular regurgitation • echocardiography • cardiac magnetic resonance imaging • computed tomography • expert's consensus • aortic valve • mitral valve • tricuspid valve • pulmonary valve

Introduction

Imaging and especially Doppler echocardiography is critical to initial and longitudinal assessment of patients with native valvular regurgitation. It provides detailed anatomic and functional information and clarifies the mechanisms underlying valvular regurgitation.

Non-invasive cardiac imaging not only detects the presence of regurgitation but also provides an understanding of the mechanisms of regurgitation, quantification of its severity, and haemodynamic consequences.[1–4] In clinical practice, the management of patients with native valvular regurgitation largely integrates the results of imaging. It is thus crucial to provide standards that aim at

---

establishing a baseline list of measurements to be performed when assessing regurgitation. Practically, the evaluation of valvular regurgitation requires the use of different imaging modalities, should integrate multiple parameters, should be performed under optimized medical therapy, and should be combined with clinical data. The present document, based on the thorough review and interpretation of the literature by experts in the field, aims to present clinical guidance for the multi-modality imaging assessment of native valvular regurgitation and to complement the 2021 ESC guidelines on valvular heart diseases.[5]

General imaging considerations

Echocardiography

Two-dimensional (2D) transthoracic echocardiography (TTE) is the first-line imaging in valvular regurgitation and is often sufficient for diagnosis. Two-dimensional transoesophageal echocardiography (TOE) is indicated when TTE is insufficient or when further diagnostic refinement is required. Three-dimensional (3D) echocardiography provides realistic and intuitive anatomic images of valvular apparatus, which may provide additional information, particularly in patients with complex valve lesions, and allows more accurate quantitation of haemodynamic consequences of the regurgitation on cardiac chambers.[6]

Valve assessment: key points

(1) TTE is the first-line imaging modality in valvular regurgitation.
(2) TOE is advocated when TTE is of non-diagnostic value or when further diagnostic refinement is required.
(3) TOE is not indicated in patients with a good-quality TTE except before planning valvular repair or in the operating room at the time of surgery.
(4) 3D echo provides additional information in patients with complex valve lesions and is increasingly used for assessing repair suitability.

In practice, the evaluation of valvular regurgitation starts with 2D TTE, which can orient readily to a severe regurgitation in the presence of a major valvular defect or to a minor leak when the valve anatomy and leaflet motion are normal. The aetiology (cause of the valve disease) and mechanism of the regurgitation (lesion/deformation resulting in valve dysfunction) including the dysfunction type (cusp motion abnormality) are described according to the Carpentier's classification of leaflet motion: Type I: normal leaflet motion, Type II: excessive motion, and Type III: restrictive motion.[7]

Then, a careful assessment of the *regurgitant jet* by colour Doppler, using multiple views, can rapidly diagnose minimal regurgitation, which requires a priori no further quantification (*Figure 1*). In all other cases, the use of a more quantitative method is advised when feasible (vena contracta, VC; proximal isovelocity surface area, PISA).

### Estimation of the severity of valvular regurgitation: key points

(1) The colour Doppler flow area of the regurgitant jet is not appropriate to quantify the severity of valvular regurgitation.
(2) Both VC measurement and the PISA method are the preferred methods to evaluate the severity of regurgitation when feasible.
(3) Adjunctive parameters should be used when there is discordance between the quantified degree of regurgitation and the clinical context.

In the second step, the impact of the regurgitation on the ventricles, the atria and the pulmonary artery pressures is estimated. Mode of acquisition, advantages, and limitations of the various echo Doppler parameters used for the assessment of valvular regurgitation severity are detailed in *Tables 1 and 2*. *Finally*, all the collected data are compared with the individual clinical context in order to stratify the management and the follow-up.[5] When uncertainty persists alternative imaging modalities can be used for example TOE and cardiac magnetic resonance (CMR) and stress echocardiography. The use of stress echocardiography in valvular heart disease is the subject of a different document.[8] Briefly for left-sided valves, a quantitative exercise echocardiography can help identify valvular lesion that have been underestimated on baseline imaging as well as the ventricular and pulmonary consequences of the regurgitation. According to the clinical context and the grade of regurgitation, *appropriate monitoring* will be delivered.[5,9,10]

Cardiac magnetic resonance

CMR adds important advantages to the assessment of native valvular regurgitation (provides a view of the entire heart without limitations of body habitus or imaging windows, allows free choice of imaging planes, is free of ionizing radiation, does not require contrast administration).[11] This becomes particularly relevant when uncertainty exists as to the severity or aetiology of regurgitant valve lesions particularly in the presence of eccentric valve lesions, multiple regurgitant jets, right-sided valve lesions, and in patients with poor echocardiographic windows.[5] In these situations, CMR has emerged as a useful second line investigation providing quantitative assessments of valve regurgitation, heart chamber size, and systolic function that helps in the adjudication of valve severity. The ability of CMR to accurately assess the right ventricle, pulmonary, and tricuspid valves (TVs) lends itself to the assessment of right-sided valve lesions.[1,3,4]

The scan protocol in regurgitant valve disease evaluation is based around cine images [using balanced steady-state free precession (bSSFP) or fast spoiled gradient echo (FSPGR) sequences] to assess cardiac structure and function as well as velocity encoded phase-contrast pulse sequences that assess blood flow through the heart.[12] Long-axis cines images are acquired in two-, three-, and four-chamber views for assessments of left-sided valve lesions with equivalent views of the right ventricle to assess the tricuspid and pulmonary valves. Further modified valve views can be acquired in any plane to provide a detailed assessment of valve function and morphology. A
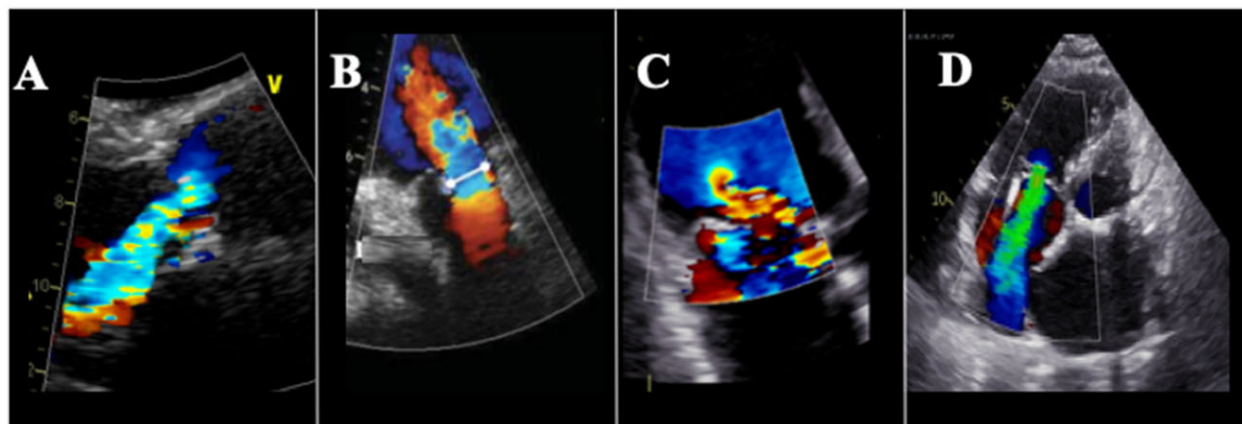
Figure 1 Assessment of the regurgitant jet by colour flow Doppler (*A*: aortic; *B*: pulmonary; *C*: mitral; *D*: tricuspid).

ventricular short-axis cine-stack is acquired from atrioventricular plane to the apex. This allows gold standard assessment of left and right ventricular volumes in both diastole and systole and calculation of stroke volumes and ejection fractions. Whilst bSSFP sequences provide the highest signal to noise ratio, FSPGR acquired in the same views can improve jet localization and minimize artefact. In addition, appropriately orientated cine images allow precise measurement of atrial size and aortic dimensions. Phase-contrast sequences are used for direct flow measurements. In the standard protocol, they are acquired in the aortic root (at the level of the sinotubular junction or just below) and main pulmonary artery perpendicular to the desired vessel. Through plane views allow precise assessment of both forward and reverse flow through the plane of the valves or vessels in questions.[13,14] More recently, tissue characterization has emerged as key point in several scenarios of valve disease. In this regard, T1 mapping and late gadolinium enhancement techniques can also provide relevant additional information in order to detect early myocardial damage in these patients as evidence of ventricular decompensation.[15] These techniques can also help evaluate myocardial pathologies underlying functional valve lesions.

In practice, a stepwise approach using qualitative, semi-quantitative or quantitative methods is prone for the CMR evaluation of valvular regurgitation. CMR can provide useful anatomic information regarding valve lesions and the nature of its dysfunction. Whilst the spatial resolution is inferior to echocardiography, CMR cine images can readily assess valve morphology and help in understanding the aetiology of valve regurgitation. Similar to echocardiography visualization of the size of the regurgitant defect frequently provides an early guide to the likely severity of the valve lesion.

As a crude guide to severity, the extent of signal loss (visualization of signal voids) due to spin dephasing can be visually observed in the receiving chamber on cine image acquisitions[16] (*Figure 2*). It should be noted that calculation of the regurgitant jet area or length are not reliable indices of disease severity and are therefore not usually performed; however, patients with regurgitant lesions that demonstrate central laminar flow usually have at least moderate regurgitation. Alternatively, planimetry of the anatomical regurgitant orifice area

(ROA) from the cine CMR acquisitions of the valve can be performed.[17] Such a planimetry is however time-consuming and remains challenging because of appropriate plane alignment and angulation.

Quantitative methods are the recommended approaches for CMR assessment of regurgitation (*Figure 3*). Regurgitant volumes (R Vols) can be measured directly or calculated, and used to derive the regurgitant fraction (RF = R Vol/forward stroke volume × 100). R Vols are assessed by two major CMR methods depending on the valve being interrogated. Direct quantification of the regurgitant blood flow by phase-contrast velocity mapping [phase-contrast technique; preferred method for aortic and pulmonary regurgitation (PR)], or indirectly from the difference between left ventricular (LV) total stroke volume (using planimetry of short-axis ventricular cine images) and forward stroke volume across the aortic or pulmonary valve (using phase-contrast velocity mapping) [preferred method for mitral and tricuspid regurgitation (TR)].[18,19] Blood that is ejected from the ventricles and not moving forward must be leaking back through the atrioventricular valves. Alternative quantitative CMR methods allow confirmation of these two preferred assessments. For example, the R Vol can be calculated by cine assessment and compared with the LV and right ventricular (RV) stroke volumes. The difference in ventricular stroke volumes represents the R Vol, assuming no other valve disease is present. The calculation of RV stroke volume is however less reproducible due to the presence of extensive trabeculation.[20] Also, the R Vol can be obtained by the difference between the mitral or tricuspid inflow stroke volume and aortic or pulmonary stroke volume by phase-contrast imaging. The pattern of flow in the aorta can be examined using 4D flow imaging, with further work required to assess methods of quantification based upon this emerging technique.[13]

Importantly, CMR provides gold-standard assessments of cardiac chamber size to assess the impact of the regurgitant lesion on the myocardium. Similar to echocardiography patients without cardiac dilatation are unlikely to have severe chronic regurgitation. In patients with aortic regurgitation (AR), aortic dilatation can point to the underlying aetiology, whilst the presence of diastolic flow reversal in the descending aorta is easily appreciated and measured on CMR.[21]

Table I Echocardiographic parameters used to quantify regurgitation severity: recordings

Parameters	Aortic regurgitation (AR)	Pulmonary regurgitation (PR)	Mitral regurgitation (MR)	Tricuspid regurgitation (TR)
Valve morphology	• Visual assessment • Multiple views	• Visual assessment • Multiple views	• Visual assessment • Multiple views	• Visual assessment • Multiple views
Annulus diameter	• Measured on three-chamber view on echocardiography • Co-axial short-axis view on CMR or CT			• Apical four-chamber view • Lateral inner edge to septal inner edge
Colour flow regurgitant jet	• Optimize colour gain/scale. Recommended Nyquist settings: 50–70 cm/s • Parasternal long- and short-axis views	• Optimize colour gain/scale. Recommended Nyquist settings: 50–70 cm/s • Evaluate in parasternal short-axis view	• Optimize colour gain/scale. Recommended Nyquist settings: 50–70 cm/s • Evaluate in two views • Measure blood pressure	• Optimize colour gain/scale. Recommended Nyquist settings: 50–70 cm/s • Evaluate in two views • Measure blood pressure
VC width and area	• PT-LAX is preferred (apical four-chamber view if not available) • Optimize colour gain/scale. Recommended Nyquist settings: 50–70 cm/s • Identify the three components of the regurgitant jet (VC, PISA, jet into LV) • Reduce the colour sector size and imaging depth to maximize frame rate • Expand the selected zone (Zoom) • Use the cine-loop to find the best frame for measurement • Measure the smallest VC (immediately distal to the regurgitant orifice, perpendicular to the direction of the jet) • Tracing of VC cross-sectional area by 3D imaging using cropping planes to locate the VC	• Parasternal short-axis view • Optimize colour gain/scale. Recommended Nyquist settings: • Identify the three components of the regurgitant jet • Reduce the colour sector size and imaging depth to maximize frame rate • Expand the selected zone (Zoom) and find the best frame for measurement • Measure the smallest VC • Tracing of VC cross-sectional area by 3D imaging using cropping planes to locate the VC	• Two orthogonal planes (PT-LAX, apical four-chamber view) • Optimize colour gain/scale. Recommended Nyquist settings: 50–70 cm/s • Identify the three components of the regurgitant jet (VC, PISA, jet into LA) • Reduce the colour sector size and imaging depth to maximize frame rate • Expand the selected zone (Zoom) • Use the cine-loop to find the best frame for measurement • Measure the smallest VC (immediately distal to the regurgitant orifice, perpendicular to the direction of the jet)	• Apical four-chamber view • Optimize colour gain/scale. Recommended Nyquist settings: 50–70 cm/s • Identify the three components of the regurgitant jet (VC, PISA, jet into RA) • Reduce the colour sector size and imaging depth to maximize frame rate • Expand the selected zone (Zoom) • Use the cine-loop to find the best frame for measurement • Measure the smallest VC (immediately distal to the regurgitant orifice, perpendicular to the direction of the jet)
PISA method	• Apical five-chamber for central jets (PT-LAX for eccentric jets) • Optimize colour flow imaging of AR. • Zoom the image of the regurgitant aortic valve • Increase the Nyquist limit in apical views decrease or increase in PT-LAX • With the cine mode select the best PISA • Display the colour off and on to visualize the AR orifice	• Parasternal short-axis view • Optimize colour flow imaging of PR. • Zoom the selected region • Increase the Nyquist limit (colour flow zero baseline). Recommended Nyquist settings: 25–40 cm/s • Measure the PISA radius at mid-systole using the first aliasing and along the direction of the ultrasound beam	• Apical four-chamber • Optimize colour flow imaging of MR. Recommended Nyquist settings: 25–40 cm/s • Zoom the image of the regurgitant mitral valve • Decrease the Nyquist limit (colour flow zero baseline) • With the cine mode select the best PISA	• Apical four-chamber • Optimize colour flow imaging of TR • Zoom the image of the regurgitant tricuspid valve • Decrease the Nyquist limit (colour flow zero baseline). Recommended Nyquist settings: 25–40 cm/s • With the cine mode select the best PISA

Continued

Table I   Continued

Parameters	Aortic regurgitation (AR)	Pulmonary regurgitation (PR)	Mitral regurgitation (MR)	Tricuspid regurgitation (TR)
	• Measure the PISA radius at diastole using the first aliasing and along the direction of the ultrasound beam • Measure AR peak velocity and TVI (CW) • Calculate flow rate, EROA, R Vol	• Measure PR peak velocity and TVI (CW) • Calculate flow rate, EROA, R Vol	• Display the colour off and on to visualize the MR orifice • Measure the PISA radius at mid-systole using the first aliasing and along the direction of the ultrasound beam • Measure MR peak velocity and TVI (CW) • Calculate flow rate, EROA, R Vol	• Display the colour off and on to visualize the TR orifice • Measure the PISA radius at mid-systole using the first aliasing and along the direction of the ultrasound beam • Measure TR peak velocity and TVI (CW) • Calculate flow rate, EROA, R Vol
CW regurgitant jet profile	• Apical five-chamber • CW AR jet • Avoid over gaining or incomplete spectral traces	• Parasternal short-axis view • Avoid over gaining or incomplete spectral traces	• Apical four-chamber • Avoid over gaining or incomplete spectral traces	• Apical four-chamber • Avoid over gaining or incomplete spectral traces
Pressure half-time	• Apical five-chamber • CW AR Doppler • Avoid over gaining or incomplete spectral traces	• CW PR Doppler • Avoid over gaining or incomplete spectral traces	—	—
Diastolic flow reversal in descending aorta	• PW Doppler • Proximal descending aorta/abdominal aorta	—	—	—
Pulmonary vein flow	—	—	• Apical four-chamber • Sample volume of PW placed into the right upper pulmonary vein • Interrogate the different pulmonary veins when possible	—
Hepatic vein flow	—	—	—	• Subcostal view • Sample volume of PW placed into the hepatic vein
Peak E velocity	—	—	• Apical four-chamber • Sample volume of PW placed at mitral leaflet tips	• Apical four-chamber • Sample volume of PW placed at tricuspid leaflet tips
Ventricular size	• Use preferably the Simpson method to assess the LV	• Use preferably the RV dimension from the apical four-chamber view	• Use preferably the Simpson method to assess the LV	• Use preferably the RV volume using 3D Echo or CMR

AR, aortic regurgitation; CW, continuous wave; EROA, effective regurgitant orifice area; LA, left atrium; LV, left ventricle; MR, mitral regurgitation; PR, pulmonary regurgitation; PT-LAX, parasternal long-axis view; PW, pulsed wave; RA, right atrium; RV, right ventricle; R Vol, regurgitant volume; TR, tricuspid regurgitation; TVI, time–velocity integral; VC, vena contracta.

Table 2 Echocardiographic parameters used to quantify valvular regurgitation severity: advantages and limitations

Parameters	Usefulness/advantages	Limitations
Valve morphology	• Flail valve is specific for severe regurgitation (i.e. ruptured PMs in MR)	• Other abnormalities are non-specific for severe valvular regurgitation
Annulus diameter	• **Dilatation sensitive for severe TR** • **Isolated dilatation suggests secondary MR** • **Dilatation suggests secondary AR due to aortic root dilatation**	• **Dilatation seen in other conditions** • **Need to be confirmed in further studies**
Colour flow regurgitant jet	• Ease of use • Evaluates the spatial orientation of regurgitant jet • Good screening test for mild vs. severe regurgitation	• Can be inaccurate for estimation of regurgitation severity • Influenced by technical and haemodynamic factors • **Expands unpredictably below the orifice in AR or PR** • **Underestimates eccentric jet adhering the atrial wall (Coanda effect) in MR or TR**
VC size	• Relatively quick and easy • Relatively independent of haemodynamic and instrumentation factors • Not affected by other valve leak • Good for extremes regurgitation: mild vs. severe • Can be used in eccentric jet	• Not valid for multiple jets • Small values; small measurement errors leads to large % error • Intermediate values need confirmation • Affected by systolic/diastolic changes in regurgitant flow • Lacks published data in PR

PISA method	• Can be used in eccentric jets
	• Not affected by the aetiology of regurgitation or other valve leak
	• Quantitative: estimates lesion severity (EROA) and volume overload (R Vol)
	• **Flow convergence at 50 cm/s suggests to significant MR**
	• **Large flow convergence at 28 cm/s suggests to significant TR**
		• PISA shape affected
		  • by the aliasing velocity
		  • in case of non-circular orifice
		  • by systolic changes in regurgitant flow
		  • by adjacent structures (flow constraints)
		• PISA radius is more a hemi-ellipse
		• Errors in PISA measurement are squared
		• Inter-observer variability
		• Not validated for multiple jets
		• **Feasibility limited by aortic valve calcifications in AR**
		• **Validated in only few studies in TR**
		• **Lacks published data in PR**

CW regurgitant jet profile	• Simple, easily available • More difficult in eccentric jets	• Qualitative, complementary finding • Complete signal difficult to obtain in eccentric jet
Pressure half-time in AR or PR	• **Simple** • **More difficult in eccentric jets**	• **Affected by LV compliance, blood pressure, acuity**
Diastolic flow reversal in descending aorta in AR	• **Simple**	• **Affected by sample volume location and acuteness of AR** • **Affected by aortic compliance.** • **Brief velocity reversal is normal** • **Cut-off validated for distal aortic arch**
Pulmonary vein flow in MR	• **Simple** • **Systolic flow reversal is specific for severe MR**	• **Affected by LA pressure, atrial fibrillation** • **Not accurate if MR jet is directed into the sampled vein**
Hepatic vein flow in TR	• **Simple** • **Systolic flow reversal is specific for severe TR**	• **Affected by RA pressure, atrial fibrillation**

Continued

Table 2 *Continued*

Parameters	Usefulness/advantages	Limitations
Peak E velocity in MR or TR	• **Simple, easily available** • **Usually increased in severe regurgitation**	• **Affected by atrial pressure, atrial fibrillation, ventricular relaxation** • **Complementary finding**
Atrial and ventricular size	• Dilatation is sensitive for chronic severe regurgitation • Normal size almost excludes severe chronic regurgitation	• Dilatation observed in other conditions (nonspecific) • May be normal in acute severe regurgitation

In Bold: parameters specific to a valvular regurgitation.

AR, aortic regurgitation; CW, continuous wave; EROA, effective regurgitant orifice area; MR, mitral regurgitation; PISA, proximal isovelocity surface area; PM, papillary muscle; PR, pulmonary regurgitation; RA, right atrium; R Vol, regurgitant volume; TR, tricuspid regurgitation; VC, vena contracta.
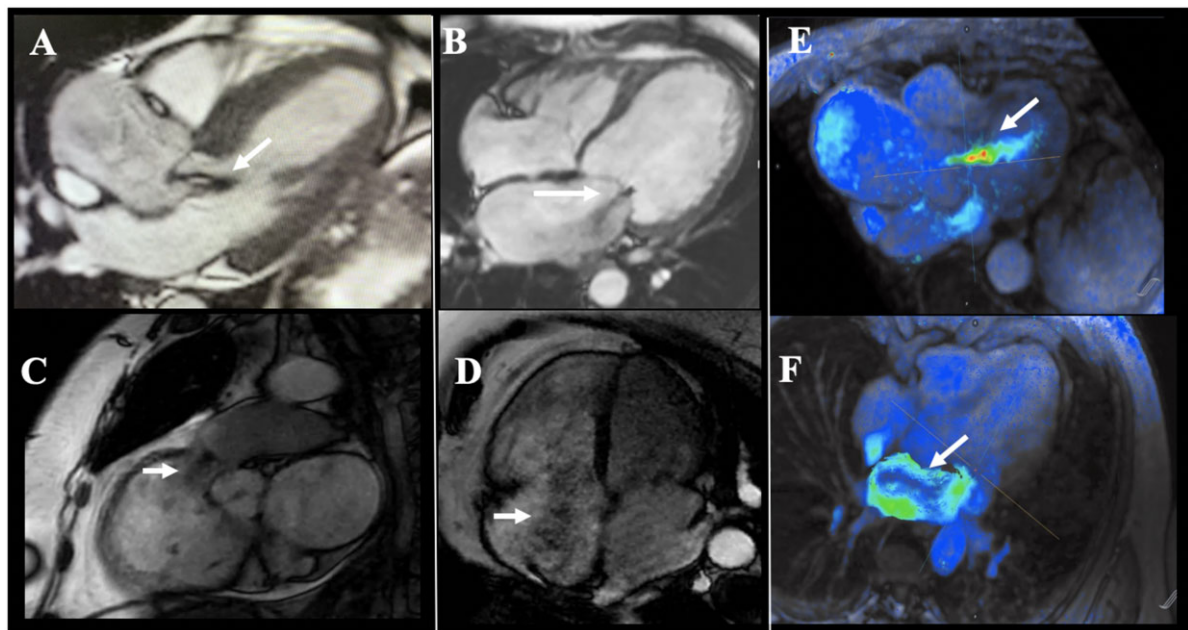
Figure 2 Cardiac magnetic resonance (CMR) imaging evaluation of valvular regurgitation (*A*: aortic; *B*: mitral; *C*: pulmonary; *D*: tricuspid). White arrows: extent of the signal loss on cine CMR acquisitions. (*E*) 4D flow image of aortic regurgitation in a patient with dilatation of the ascending aorta. (*F*) 4D flow of mitral regurgitation: eccentric mitral jet directed towards the interatrial septum contouring the LA wall.

Finally, myocardial tissue characterization has emerged in the field of valve disease. Late gadolinium enhancement detects replacement fibrosis, whilst T1 mapping techniques (native T1, extracellular volume fraction), facilitate quantification of interstitial fibrosis. Whilst these have been extensively investigated in patients with aortic stenosis, data are emerging in regurgitant lesions assessments[22,23] particularly patients with mitral valve (MV) prolapse.[24] Further work required to define the clinical role of such assessments.

CMR is also not as readily available and cheap as echocardiography and cannot be performed at the bedside (*Table 3*). CMR is not possible in some patients with severe claustrophobia; however, cardiac devices are no longer considered an absolute contraindication.[12] Since most CMR acquisitions are acquired over multiple cardiac cycles, arrhythmias such as atrial fibrillation or premature ventricular contractions may pose a challenge for standard breath-held phase-contrast velocity encoded CMR sequences.[12] Whilst initial data suggest CMR provides powerful prognostic information, further research in larger patient cohorts is required for confirmation. Moreover, the low spatial resolution as compared to echocardiography, means that CMR provides less detailed visualization of thin structures such as the cardiac valves (which are usually 1–2 mm thick) and subvalvular apparatus.[14]

Cardiac computed tomography

Standard cardiac computed tomography (CCT) technology requires acquisition of dynamic datasets over multiple heart cycles to fully image cardiac structure and function using electrocardiogram (ECG)
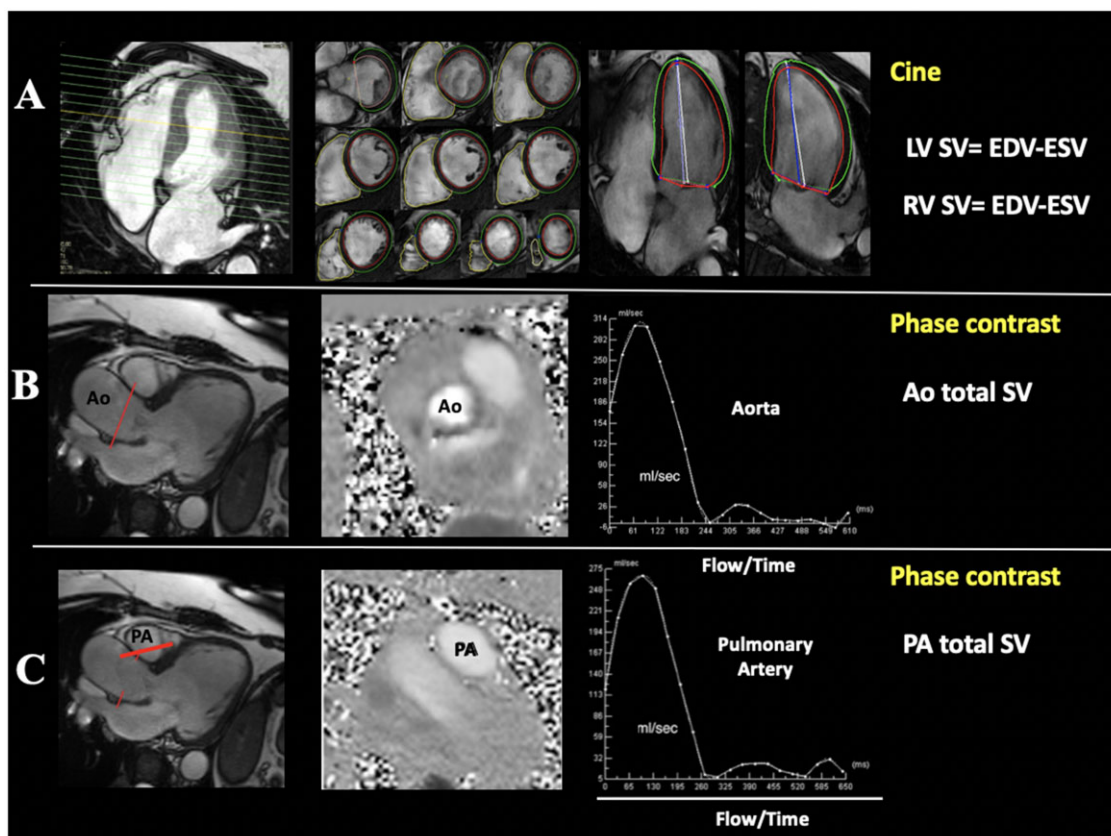
Figure 3 Methods of quantification of valvular regurgitation by cardiac magnetic resonance imaging (CMR). *A*: evaluation of left ventricular (LV) and right ventricular (RV) stroke volume (SV) using cine CMR acquisitions. LV and RV endocardial contours are traced in systole and diastole from a short-axis stack from base to apex; Aortic (Ao) (*B*) and pulmonary (PA) (*C*) flow assessed using phase-contrast sequence and the analysis of the flow time plot.

synchronized acquisitions. Recent technical innovations, improvement of spatial resolution down to 0.5 mm, and the introduction of wide coverage scanners have allowed the acquisition of the entire heart including all cardiac cycles in one beat with high spatial resolution and low radiation exposure.[25] Nevertheless, the current role of CCT in the assessment of patients with valve regurgitation remains limited. There is no current clinically validated method for measuring flow velocity or flow volume using CCT.[5] The main indications for CCT in these patients include assessments of aortic dilatation; rapid rule out of aortic dissection; assessment of valve morphology, calcifications, and non-calcific thickening; and the rule out significant coronary artery disease in patients with an indication for surgery and low probability of coronary atherosclerosis. Finally, CCT could be used for LV and RV volumes and function evaluation or to planimeter ROAs when both echocardiography and CMR are not available or contra-indicated.[26]

Assessment of cardiac chambers size and function

Ventricular size and function are measured using diameters and/or volumes (*Figure 4*) (*Tables 4 and 5*). By echocardiography,

Simpson's biplane method provides an estimate of both diastolic and systolic volume (with indexing to body surface area) and systolic contractile function (LV ejection fraction, LVEF) and should be performed in all cases where image quality permits. RV focused apical four-chamber view is the preferred view for RV dimension assessment.[27] Given its improved accuracy, 3D estimates of chamber volume and function are best for the assessment and surveillance of chamber size, function, and adverse remodelling.[6] CMR evaluation of LV or RV function represents a valuable alternative in case of poor acoustic window or when data obtained by echocardiography are inconclusive.[20] When available, CMR is the preferred method to assess the right ventricle due to its high accuracy and reproducibility, particularly in patients with tricuspid and PR.[5] Of note, ejection fraction (EF) is load dependent and often overestimates ventricular systolic performance. New parameters [myocardial velocities and global longitudinal strain (GLS)] are currently available for assessment of ventricular function and are entering routine clinical practice. Cut-off values are however yet to be validated in larger series. Atrial volumes can be reliably measured by the 2D echo biplane area-length method, 3D echocardiography, CMR, or computed tomography (CT) scan.[11,26]

Table 3 CMR evaluation of valvular regurgitation: advantages and technical limitations

Parameters	Usefulness/advantages	Limitations
Cine imaging **Assessment of valve morphology as well as cardiac chambers size and function** **(bSSFB is the preferred sequence)**	• Provides assessment of valve morphology and regurgitant jet visualization in any plane • Allows assessment of the impact of regurgitant lesions on cardiac chambers • Assessment of diastolic flow reversal in the descending aorta can aid assessment of AR severity • High diagnostic accuracy • High reproducibility • Not based on geometric assumptions	• Time consuming • It requires multiple breath hold • Limited accuracy and reproducibility in patients with arrhythmic disorders during acquisition
AR and PR **Direct quantitative regurgitant flow measurements** **(phase-contrast sequence)**	• Direct measurement of forward and reverse flow through the plane of the valve or vessel • Not based on geometric assumptions • Accurate in aortic regurgitation and pulmonary regurgitation quantification • Contribute to the calculation of MR and TR alongside ventricular stroke volumes outlined below	• Time-consuming • It could require additional dedicates scan acquisition • Challenging in the identification of appropriate plane alignment and angulation outside of the setting of aortic regurgitation or pulmonary regurgitation
MR and TR **Indirect quantitative regurgitant flow measurements as difference between left and right ventricle stroke volumes versus anterograde aorta and pulmonary flow, respectively (both bSSFB and PhC sequence are required)**	• Second line test to confirm findings from direct and indirect methods described above. • High accuracy and reproducibility • It does not require additional acquisition	• Limited accuracy and reproducibility in patients with arrhythmic disorders during acquisition • Background or phantom corrections could be useful wiyth additional scan time
Confirmatory Techniques		
Indirect quantitative regurgitant flow measurements as difference between left and right ventricle stroke volumes **(bSSFB is the preferred sequence)**	• High accuracy and reproducibility for the assessment of MR and TR (not required for AR and MR) • It does not require additional acquisition	• It can be applied only in patients with single valve disease
Direct visualization of regurgitant jet **(FSPGR is the preferred sequence)**	• Linear relationship between dephasing spin velocity and signal loss • Laminar flow suggests at least moderate aortic regurgitation	• Time-consuming • It requires multiple breath hold • Limited spatial resolution in chambers evaluation as compared to bSSFP • They should be acquired on top of bSSFP sequences • Visual estimation of jet with limited correlation with semi-quantitative or quantitative method
Planimetry of the anatomical regurgitant orifice area **(bSSFB is the preferred sequence)**	• High in-plane spatial resolution allowing accurate detection of regurgitant orifice	• Time-consuming • Challenging in the identification of appropriate plane alignment and angulation • Based on geometric assumptions

AR, aortic regurgitation; bSSFP, balanced steady-state free precession; FSPGR, fast spoiled gradient echo; MR, mitral regurgitation; PhC, velocity encoded phase-contrast; PR, pulmonary regurgitation; TR, tricuspid regurgitation.
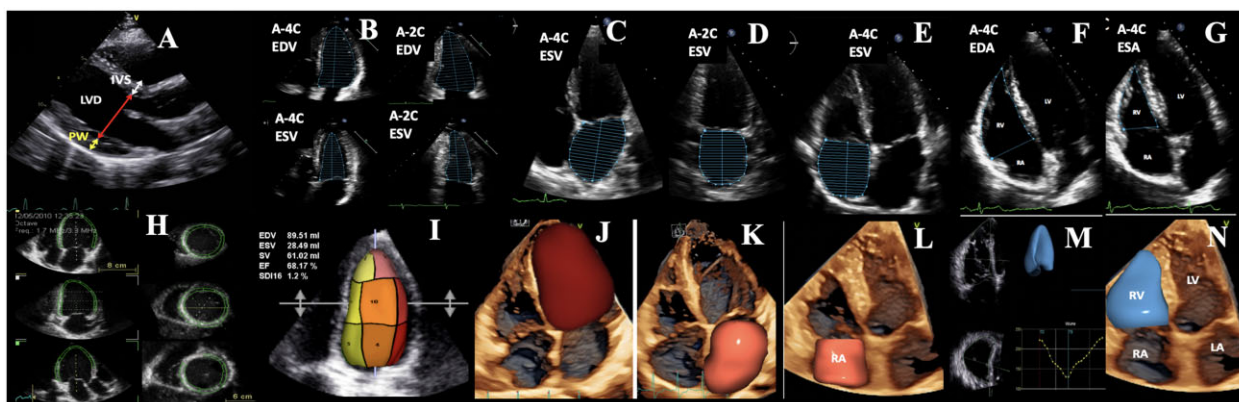
Figure 4 Assessment of cardiac chambers size and function by 2D and 3D echocardiography. (*A*) 2D measurement of LV diameters. (*B–E*) Estimation of cardiac volumes by summation method of disc (*B*: LV, *C* and *D*: LA, *E*: RA). (*F* and *G*) RV fractional area change assessment. (*H–N*) 3D echo assessment of cardiac chamber volumes (*H–J*: LV; *K*: LA; *L*: RA; *M* and *N*: RV).

Table 4　Heart chamber size and function: key points

(1) Quantitative assessment of left ventricular (LV) diameters, volumes, and ejection fraction (EF) is mandatory

(2) 2D measurement of LV/RV diameters is mandatory

(3) The 2D-based biplane summation method of discs is the standard approach for the estimation of LV volumes and ejection fraction

(4) 3D echo assessment of LV/RV function provides more accurate and reproducible data

(5) Contrast echo is indicated in patients with poor acoustic window

(6) CMR evaluation of LV/RV function is a valuable alternative in case of poor echogenicity or when data obtained by echo are inconclusive

(7) CCT evaluation of LV/RV function is a valuable alternative in case of poor echogenicity/data obtained by echo are inconclusive and CMR is not available or contraindicated

(8) Qualitative assessment of LV/RV function is not advised

(9) Left atrial volume is the best parameter to assess its size

Aortic regurgitation

AR is a common valvular disease. Non-invasive imaging plays a key role in the assessment and management of patients with AR.[1,2]

Anatomy and function of the aortic valve

The aortic valve consists of a composite of structures surrounding the aortic orifice along the outflow tract of the left ventricle.[28] Typically, the valve has three leaflets or cusps, which are semi-lunar in shape (*Figure 5*). The cusps are inserted into a fibrous connective tissue sleeve, which is attached to the aorta media above (the Valsalva sinuses and the sino-tubular junction). Below, the cusps are attached to the myocardium of the LV outflow tract (LVOT) and to the anterior mitral leaflet (virtual basal ring), below the anatomic ventriculo-aortic junction. Hence, the true anatomic aortic annulus is not actually the ring projected at the most basal leaflet insertion—as usually defined and measured with various imaging techniques—but a crown-like 3D structure. Of note, the size of aortic annulus and root is influenced by inner pressure and changes dynamically during the cardiac cycle. Each cusp is attached to the aorta along its curved edge, and the cusps meet at three commissures that are equally spaced along the circumference of the sleeve at the supra-aortic ridge. In normal aortic valve, the cusps are symmetrical, mobile, and free at the commissures, with equal overlap on closure. The cusps are named left, right, and non-coronary cusps based on the location of the coronary ostia.

Aetiology and mechanisms of AR

AR results from disease of either the aortic leaflets or the aortic root that distorts the leaflets and prevents their correct apposition. Common causes of leaflet abnormalities that result in AR include senile leaflet calcifications, bicuspid aortic valve, infective endocarditis, and rheumatic fever. Aortic causes of AR include annulo-aortic ectasia (idiopathic root dilatation), Marfan's syndrome, aortic dissection, collagen vascular disease, and syphilis. The Carpentier's classification is also commonly used to describe the mechanism of AR (*Figure 6*; *Table 6*).[29]

> **Key point: In patients with AR, careful assessment of the aortic valve, aortic annulus, and aortic root is mandatory. The imaging report should include information about the aetiology, the lesion process, and the type of dysfunction. The likelihood of valve repair should also be discussed in case of pure AR.**

Imaging evaluation in AR

Imaging findings in AR

Information about the cusp pathology (redundancy, restriction, cusp height to indicate likely adequacy of coaptation, mobility/pliability, thickness, and integrity), commissure variations (fusion, splaying,

Table 5 Multimodality imaging for the assessment of the patients with valvular regurgitation

	Echocardiography (TTE/TOE)		CMR	CCT
	2D/colour Doppler/PW and CW Doppler	3D/colour Doppler		
Qualitative				
Valve morphology	+++	+++	++	++
Regurgitant jet	+++	+++	++	-
Flow reversal into aorta/pulmonary arteries	+++	+	+++	-
Flow reversal into veins	+++	+	++	-
Regurgitant jet morphology	++	+++	++	-
Semi-quantitative				
Vena contracta width	+++	+++	++	-
Vena contracta area	-	+++	++	-
Quantitative				
Anatomic ROA	-	+	++	+++
EROA	++ (PISA)	+ (PISA)	-	-
R Vol	++ (PISA)	++ (PISA)	+++	-
RF	+	+	+++	-
Heart chamber size				
Annular dimensions	++	+++	+++	+++
Volumes	++	+++	+++	+++
Ejection fraction	++	+++	+++	+++
Vena cava diameter	+++ (proximal only)	+++	+++	+++
Vascular assessment	+	+	+++	+++
Calcification burden	++	++	+	+++

+, Somewhat useful; ++, useful; +++, very useful; -, not useful; EROA, effective regurgitant orifice area; RF, regurgitant fraction; R Vol, regurgitant volume; VC, vena contracta.
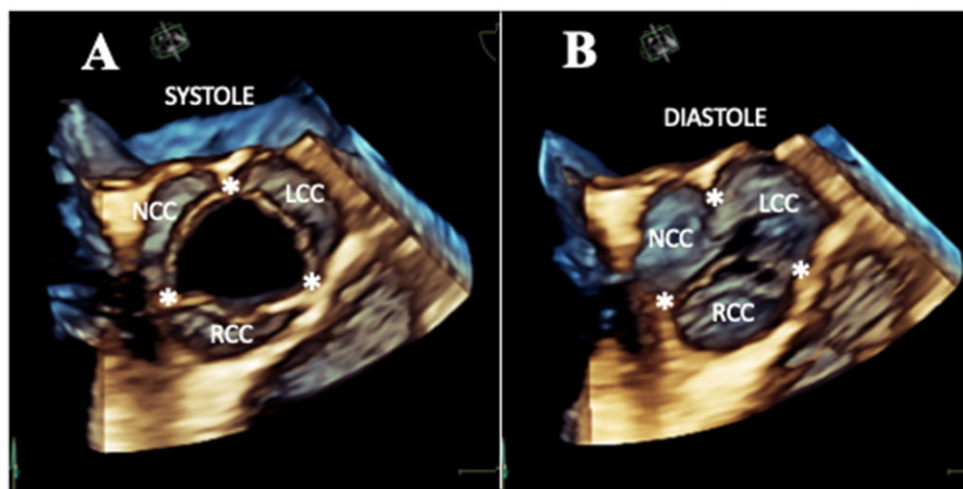
Figure 5 Transesophageal 3D images of normal aortic valves (AV) in systole (*A*) and diastole (*B*) as seen from the aorta. Each valve has three semilunar cusps and three commissures (asterisk)*. LCC, left coronary cusp; NCC, non-coronary cusp; RCC, right coronary cusp.

attachment site, and alignment), and root morphology (septal hypertrophy, annular size, sinus and sino-tubular junction dimension, and ascending aorta dimension) should be provided. The presence of a flail valve is specific for severe AR.

Echocardiography usually provides all this information as the first line imaging approach. The parasternal long-axis view is classically used to measure the LVOT, the aortic annulus, and the aortic sinuses dimensions. Leaflet thickness and morphology can be visualized from

this window as well as from the parasternal short-axis view and the apical five and three-chamber views. However, not uncommonly, 2D TTE does not allow a complete assessment of the anatomy and causes of AR. In this situation, if the acoustic window is optimal, 3D echo could provide better delineation of the aortic valve morphology.[6,28] Three-dimensional TOE is increasingly used for assessing the mechanisms and causes of AR, as well as the aortic root dimensions and morphology.[29] TOE is often used for further detailed examination of the aortic valve and root. Additionally, 2D (reverse doming of the anterior MV leaflet; basal septal hyperechogenic aspect) and M-mode (high frequency fluttering of the anterior mitral leaflet, the MV chordae or the interventricular septum; premature MV closure; premature diastolic opening of the aortic valve) echo findings that can be associated with AR should also be looked for (*Figure 7*).

CMR imaging in AR begins with standard three-chamber and coronal SSFP cine views, which provide a visual assessment of the aortic valve, LV, and LVOT structure and function.[12] It can provide useful information on leaflet morphology and motion. With CCT, multiplanar images can be reconstructed that are analogous to standard echocardiographic views of the aortic valve.

CMR provides limited information on aortic valve leaflets.[30] CCT can also accurately delineate aortic valve anatomy, and it is uniquely useful in evaluating the size of the aortic annulus and the burden of valvular, aortic, and coronary calcifications. Both CMR and CCT, also, allow comprehensive assessment of entire aorta for quantifying aortic dilation or the presence of coarctation in patients with bicuspid aortic valve.[31]

CCT is the preferred imaging modality to assess maximum diameter in patients with dilated aorta and also for sizing the aorta before surgery, while CMR can be used for serial evaluation to limit radiation.[32]

Assessment of AR severity
Semi-quantitative methods

Colour flow Doppler imaging. Using colour flow Doppler, the regurgitant jet into the left ventricle during diastole can be visualized from multiple views. The colour jet area and length are weakly correlated to the degree of AR, are affected by the aortic to LV diastolic pressure gradient and LV compliance, and are often overestimated in the apical views. They are currently considered as not appropriate to quantitate AR severity. Practically, colour flow Doppler serves for detection and initial visual assessment of AR. Central jets are suggestive of rheumatic disease, while eccentric jets are often associated with aortic valve prolapse or perforation. Colour-coded M-mode is suitable for assessing the time-course of flow signals during the heart cycle (*Figure 8*). The diameter and the cross-sectional area of the jet at its origin are semi-quantitative colour Doppler indexes of AR severity. The maximum colour jet diameter (width) is measured in diastole immediately below the aortic valve (at the junction of the LVOT and aortic annulus) in the parasternal long-axis view. The jet width is proportional to the size of the aortic valve defect. However, since it assumes a circular regurgitant orifice, if the orifice shape is irregular, as in bicuspid valve, the colour jet width is less related to the degree of regurgitation. Its accuracy can thus be improved by normalizing the jet width for the LVOT diameter. The cross-sectional area of the jet from the parasternal short-axis view and its ratio to the LVOT
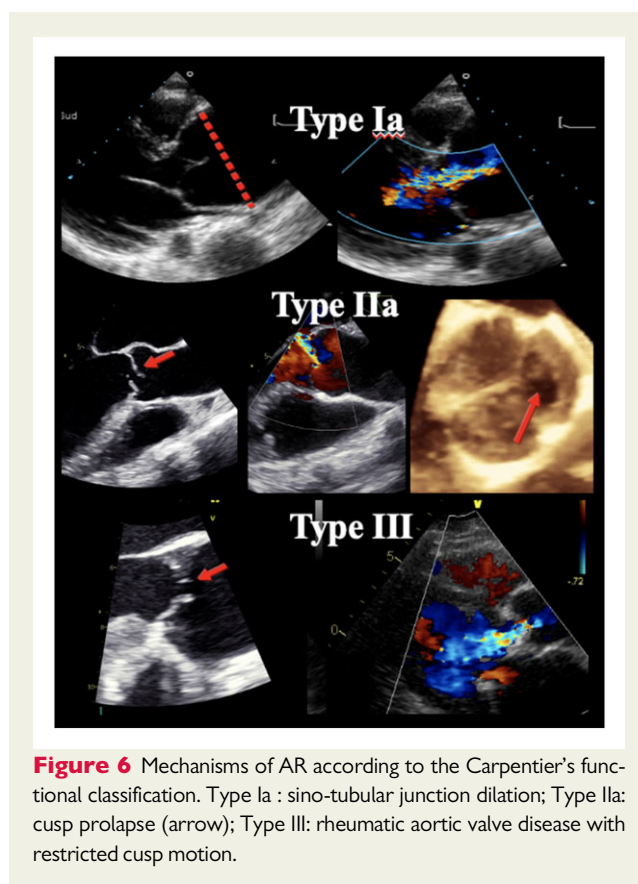
Figure 6 Mechanisms of AR according to the Carpentier's functional classification. Type Ia : sino-tubular junction dilation; Type IIa: cusp prolapse (arrow); Type III: rheumatic aortic valve disease with restricted cusp motion.

area are also semi-quantitative parameters of AR severity. Although these measurements suffer from a high inter-observer variability, a jet width ratio >65% is an argument for severe AR (*Figure 9*).[33]

> **Key point: The colour flow area of the regurgitant jet, as a single parameter, is not appropriate to quantify the severity of AR. The colour jet width and its ratio to the LVOT diameter may be used to semi-quantitate AR severity. A more quantitative approach is required when more than a small central AR jet is observed.**

Vena contracta width. For AR, imaging of the VC—the regurgitant jet as it traverses the aortic orifice or the effective regurgitant area—is obtained from the parasternal long-axis echocardiographic view.[32,34,35] Practically, the VC represents the smallest flow diameter at the level of the aortic valve in the LVOT, immediately below the flow convergence region (*Figure 10*). It provides an estimate of the size of the effective regurgitant orifice area (EROA) and is smaller than the regurgitant jet width in the LVOT (expansion of the jet occurs immediately below the VC). With echo, using a Nyquist limit of 50–60 cm/s, a VC width of less than 3 mm correlates with mild AR, whereas a width >6 mm indicates severe AR. The measurement of the VC is affected by several factors including the presence of multiple jets. In this situation, the respective widths of the VC are not additive. Moreover, the concept of VC is indeed based on the assumption that the regurgitant orifice is almost circular. The orifice is however often elliptic or irregular, which changes the width of the

Table 6   Anatomical and functional classification of AR lesions

Dysfunction	Imaging findings
Type I: normal leaflet motion	• Ia: Sinotubular junction and ascending aorta dilatation • Ib: Sinuses of Valsalva and sinotubular junction dilatation • Ic: Annulus dilatation • Id: Cusp perforation or cusp fenestration without a primary functional aortic annular lesion
Type IIa: excessive leaflet motion due to cusp prolapse with eccentric AR jet	
(1) Cusp flail	(1) Complete eversion of a cusp into the LVOT in long-axis views
(2) Partial cusp prolapse	(2) Distal part of a cusp prolapsing into the LVOT (clear bending of the cusp body on long-axis views and presence of a small circular structure near the cusp free edge on short-axis views)
(3) Whole cusp prolapse	(3) Free edge of a cusp overriding the plane of aortic annulus with billowing of the entire cusp body into the LVOT (presence of a large circular or oval structure immediately beneath the valve on short-axis views)
Type IIb: free edge fenestration with eccentric AR jet	Presence of an eccentric AoR jet without definite evidence of cusp prolapse
Type III: restrictive leaflet motion due to poor cusps quality or quantity	• Thickened and rigid valves with reduced motion • Large calcification deposits/extensive calcifications of all cusps interfering with cusp motion

The degree of calcification of the aortic valve is scored by 2D echocardiography as follows:
- Grade1: no calcification
- Grade 2: isolated small calcification spots
- Grade 3: bigger calcification spots interfering with cusp motion
- Grade 4: extensive calcifications of all cusps with restricted cusp motion
- The degree of calcification can also be quantitated by CT.

VC in different views. In presence of multiple jets, it is suggested to report the VC width of the largest jet, while this metrics may underestimate the overall severity of AR in this context. Three-dimensional colour Doppler echo is useful tool to adequately visualize the shape of the regurgitant orifice with the use of bi-plane imaging to assess the VC in simultaneous orthogonal views (the largest diameter is reported) or 3D zoom colour flow Doppler.[35] The VC area can then be measured by manual planimetry. For both 2D and 3D VC measurements, 2D and, respectively, 3D gain should be reduced and colour priority increased to improve visualisation of the colour flow.

> **Key point: When feasible, the measurement of the VC width is very useful to quantify AR. Intermediate VC values (3–6 mm) need confirmation by a more quantitative method, when feasible. The VC can often be obtained even in eccentric jets. In case of multiple jets, the respective values of VC width are not additive. The assessment of the cross-sectional area of VC by 3D echo can be helpful to better delineate the regurgitant orifice morphology and quantitate AR severity.**

Diastolic flow reversal in the descending aorta (or peripheral arteries). AR can lead to diastolic flow reversal in the aorta. The flow reversal is best imaged in the upper descending aorta at the aortic isthmus level from a suprasternal view by using pulse wave (PW) Doppler.

With echo, the sample volume is placed just distal to the origin of the left subclavian artery and it is aligned as much as possible along the major axis of the aorta. The Doppler filter is decreased to its lowest setting to allow detection of low velocities (<10 cm/s). With milder degrees of regurgitation, there is a brief reversal of flow limited to early diastole. As the degree of the regurgitation increases, the duration and the velocity of the reversal flow during diastole increase. It becomes sustained throughout diastole at velocities exceeding 20 cm/s in severe AR (end-diastolic velocity measured at peak R wave) (*Figure 11*). This cut-off value has been validated in the proximal descending aorta just beneath the aortic isthmus.[36] Significant holodiastolic reversal in the abdominal aorta is also a very specific sign of severe AR. With CMR, cine images of the aorta can visualized flow reversal in the descending aorta. Additionally, velocity-encoded imaging is used to assess holodiastolic flow reversal at the level of the mid-descending aorta (highly specific for severe AR).[21]

> **Key point: The measurement of the diastolic flow reversal in the descending and abdominal aorta must systemically be performed, when assessable. It should be considered as the strongest additional parameter for evaluating the severity of AR.**

Continuous wave Doppler of the AR jet. Continuous wave (CW) Doppler of the AR jet is classically best obtained from the apical five-

chamber view (*Figure 12*). However, effort should be made to obtain correct Doppler angle in order to minimize errors related to possible ultrasound beam misalignment. For eccentric jets, better signals may be obtained from the right parasternal window. While faint spectral display is compatible with trace or mild AR, significant overlap between moderate and severe AR exists in more dense jet tracings. Practically, the CW density does not provide useful information about the severity of AR. The grading by this method is qualitative. The rate of deceleration of the diastolic regurgitant jet and the derived pressure-half time reflect both the degree of regurgitation and the ventricular end-diastolic pressures. As the degree of AR increases, the aortic diastolic pressure decreases and the LV end-diastolic pressure increases.[37,38] The late diastolic jet velocity is thus reduced and the pressure half-time shortened. A pressure half-time of <200 ms is consistent with severe AR, whereas a value >500 ms suggests mild AR. Of note, the pressure half-time is however influenced by LV and aortic compliance, the acuteness of AR (i.e. in severe acute AR, the pressure half-time is almost always short) and the aorto-ventricular pressure gradient.

> **Key point: The CW Doppler density of the AR jet does not provide useful information about the severity of AR. The assessment of the pressure-half time requires good Doppler beam alignment. A careful probe angulation is often needed. Because of the influences by LV and aortic chamber compliance and pressures, pressure half-time can only serve as a complementary finding for the assessment of AR severity.**

Quantitative assessment

Anatomic orifice area. The anatomic ROA may be measured directly by planimetry using 2D/3D echocardiography, CCT, or CMR. Using an 'en face view' of the aortic valve, the smallest diastolic ROA in mid-diastole is traced. Cut-offs of severity are, however, less well defined than for EROA and its clinical use is still limited. With CMR, an anatomic ROA $\geq$48 mm^2 is consistent with severe AR.[39]

The proximal isovelocity surface area method. With echocardiography, the assessment of the flow convergence zone has been less extensively studied in AR than in mitral regurgitation.[40,41] Imaging of the flow convergence zone is obtained from the apical three- or five-chamber or parasternal long-axis or upper right parasternal views. The radius of the PISA is measured at diastole using the first aliasing. R Vol and EROA are obtained using the standard formulas (*Figures 13 and 14*). The flow convergence or PISA method has several limitations. Firstly, it is not feasible in a significant percentage of patients with AR due to interposition of valve tissue and difficulty in correctly identifying the flow convergence zone. Non-planar or confined flow convergence zones that invalidate the hemispheric assumption are potential causes of either under- or over-estimation of AR severity by the PISA method. Accordingly, caution should be exercised when using the PISA method in patients with obtuse flow convergence angles, such as those with aneurysmal dilation of the ascending aorta or those with confined flow convergence zone such as could occur in patients with cusp perforation or commissural leaks. The use of 3D echocardiography to improve the accuracy of the PISA method and the VC area to quantify AR is promising but requires further validation.[6] The PISA method also allows to measure the R Vol but in addition to the limitations of the PISA method mentioned above for the measurement of the EROA, the CW Doppler signal of AR is often incomplete, especially in eccentric jets. Grading of severity of AR classifies regurgitation as mild, moderate or severe, and sub-classifies the moderate regurgitation class into 'mild-to-moderate' (EROA of 10 to 19 mm or an R Vol of 20–44 mL) and 'moderate-to-severe' (EROA of 20–29 mm^2 or an R Vol of 45–59 mL). An EROA $\geq$30 mm^2 or an R Vol $\geq$60 mL indicates severe AR. A RF [R Vol divided by the LVOT stroke volume] greater than 50% indicates severe AR. A moderate EROA or R Vol may, in fact, correspond to a large RF and thus to a severe AR in patients with depressed LV systolic function and low flow state or in patients with acute AR. In such cases, more weight should be given to the RF to grade AR severity. Hence, patient with an EROA and a R Vol that are in the moderate range but a RF $\geq$50% should be considered as having severe AR.

> **Key point: When feasible, the PISA method is highly suggested to quantify the severity of AR. It can be used in both central and eccentric jets. In eccentric AR jets, the parasternal long-axis view must preferentially be used to evaluate the flow convergence zone. An EROA $\geq$30 mm^2 or a R Vol $\geq$60 mL indicates severe AR. A RF greater than 50% indicates severe AR, even if EROA and R Vol are in the moderate range.**

Doppler volumetric method. PW Doppler method can be used as an alternative method to quantify the AR severity.[1–3] In the absence of significant mitral regurgitation (MR), the mitral inflow is used to calculate the systemic stroke volume (see MR section). The RV outflow tract site can be used in patients with significant MR. The total stroke volume is derived from the LVOT stroke volume. This approach is time consuming and is associated with several drawbacks.

CMR quantification. CMR is the alternative method of choice to quantify the R Vol and RF. In AR, the phase-contrast direct method is the most validated approach with the advantage of not being affected by coexisting valvular regurgitation lesions. Phase-contrast velocity mapping is used to calculate aortic forward and reverse flow per cardiac cycle (*Figure 14*). A through plane phase-contrast imaging slice is positioned at the level of aortic root, often just above the aortic valve and at or below the sinotubular junction. In some cases, velocity-encoded phase-contrast is unreliable as when the area of interest is obscured by artefacts, when flow is complex in a markedly dilated aortic root, or in case of arrhythmias. In these contexts, indirect methods may be used. The RF is calculated by dividing the R Vol by the LV stroke volume. RF is an independent predictor of outcome in patients with AR,[42] and a RF >33% has been shown to predict the likelihood of requiring surgery within 9 years.[43] RF limits that optimize concordance of CMR and echo severity grades are: mild $\leq$15%, moderate 16–25%, moderate–severe 26–48%, and severe >48%.[1,12]

Key point: Although large outcome CMR studies are lacking, CMR is the alternative method of choice for quantitative assessment of AR. The direct approach using the phase-contrast technique is the most reproducible with the advantage of not being affected by coexisting valvular regurgitation lesions. A RF ≥50% indicates severe AR.

### Consequences of AR on LV size and function

The presence of severe AR has significant haemodynamic effects, primarily on the left ventricle. AR imposes additional volume load on the left ventricle. In acute AR, the left ventricle is classically not enlarged, while in the chronic situation, the left ventricle progressively dilates and irreversible LV damage may occur. Hence, dilatation is sensitive for chronic significant (moderate to severe) AR, while normal size almost excludes severe chronic AR. However, dilatation can be observed in other conditions (non-specific) or may be absent in acute severe AR. Three-dimensional echocardiography allows more accurate measurement of LV volumes and EF than 2D echocardiography. LV volumetric data derived by echocardiography (LV end-systolic volume index ≥45 mL/m^2)[43] or CMR (LV end-diastolic volume >246 mL with RF >33%)[42] may be instrumental in the identification of patients at increased risk of clinical progression. Strain imaging (GLS < -19%) may be helpful in identifying subclinical LV dysfunction in the setting of serial echocardiograms and may help for risk stratification.[44] Thresholds recommended in current ESC guidelines[5] for intervention in asymptomatic patients with severe AR are: LVEF ≤ 50%, LV end-systolic diameter >50 mm or >25 mm/m^2. CMR may be used for the detection of myocardial fibrosis, especially in high-risk patients, where it is associated persisting symptoms post-AVR, poor LV recovery, and an adverse prognosis. Further studies are required.[45]

Key point: LV diameters, volumes, and ejection fraction should always be measured and reported in patients with AR. The LV diameters and volumes must be indexed to the body surface area. Three-dimensional echocardiography and CMR imaging allows more accurate evaluation of LV volumes and EF than 2D echocardiography. However, until further data are available current cut-offs for intervention are based on 2D echo results.
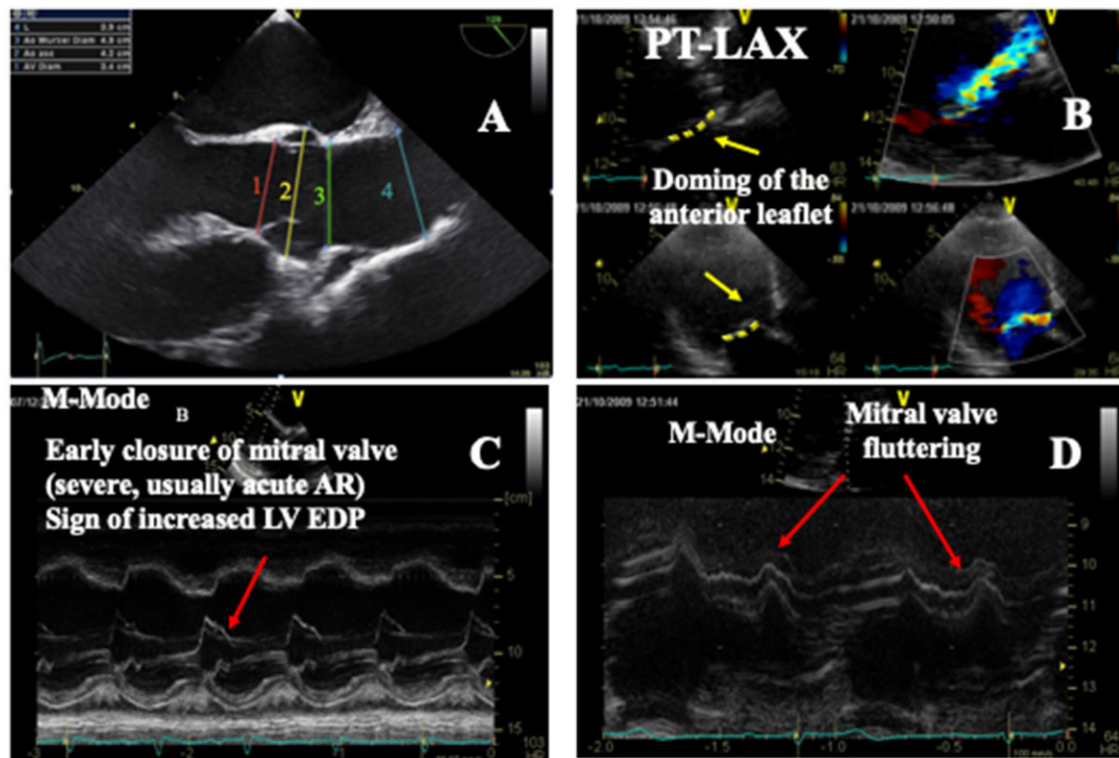
Figure 7 (A) Measurements of the aortic diameters. 1: valve annulus, 2: aortic sinuses, 3: sinotubular junction, 4: proximal ascending aorta; (B) example of AR jet impinging on the anterior mitral valve leaflet with a reverse doming of the anterior mitral valve leaflet; (C) M-mode recording showing early mitral valve closure in a patient with severe AR; (D) M-mode recording showing the fluttering motion of the anterior mitral leaflet in a patient with severe AR.
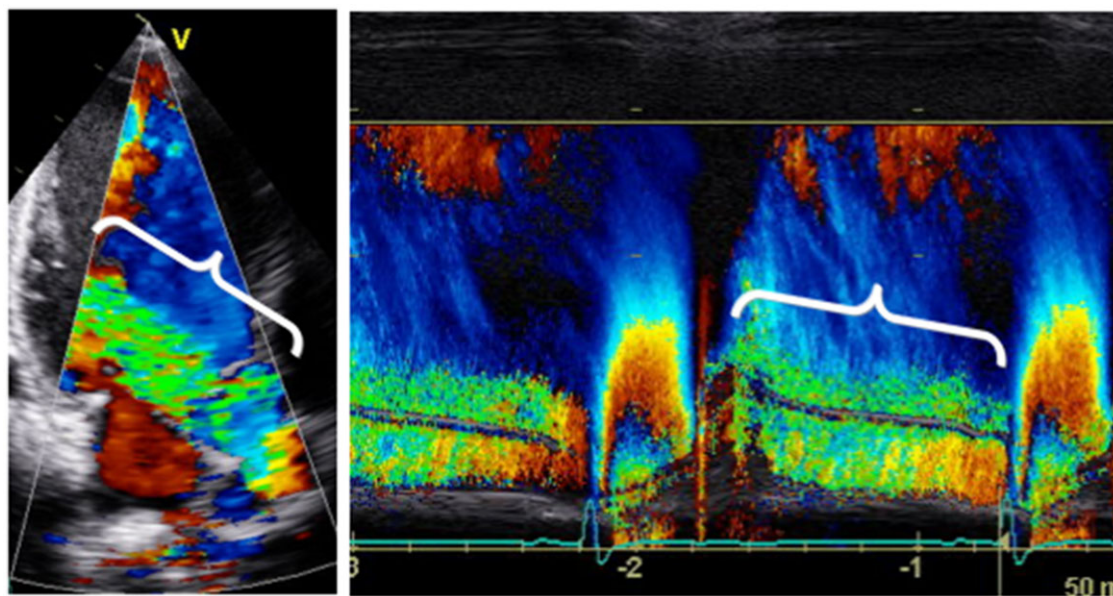
Figure 8 (*A*) Colour Doppler showing a severe AR. (*B*) Colour-coded M-mode depicting the time-dependency of flow signal during the heart cycle.

Role of exercise echocardiography

The development of symptoms during exercise testing is useful in predicting outcome in patients with severe AR who are apparently asymptomatic at rest. The observed magnitude of change in ejection fraction or stroke volume from rest to exercise is related not only to myocardial contractile function but also to severity of volume-overload and exercise-induced changes in preload and peripheral arterial resistance. However, the absence of contractile reserve—decrease in LVEF by 5% at exercise—has been associated with LV decompensation after surgery.[8] As the incremental value of stress echocardiography in predicting outcome of patients with asymptomatic AR is limited by the small number of available studies, this specific application is currently limited to the research arena. In the symptomatic patient with moderate AR, stress echocardiography can be useful to identify factors related to AR or other concomitant conditions that may be responsible for the symptoms, such as significant rise in pulmonary pressure during exercise (>60 mmHg), inducible myocardial ischaemia, or failure to increase LVEF during exercise.[8]

Integrating indices of severity

Echocardiographic assessment of AR should follow a multi-parameter integrative approach that includes data form 2D/3D imaging of the aortic root, aortic valve, and left ventricle as well as Doppler measures of regurgitation severity (*Table 7*) (*Figure 15*). Effort should be made to quantify the degree of regurgitation, except in the presence of mild or less severe AR or when AR is considered severe using specific signs. Both the VC width and the PISA method are the preferred parameters, whenever possible. Adjunctive parameters help to consolidate about the severity of AR. CMR is the alternative method of choice and should be used when the results of echocardiography (TEE and TOE) are
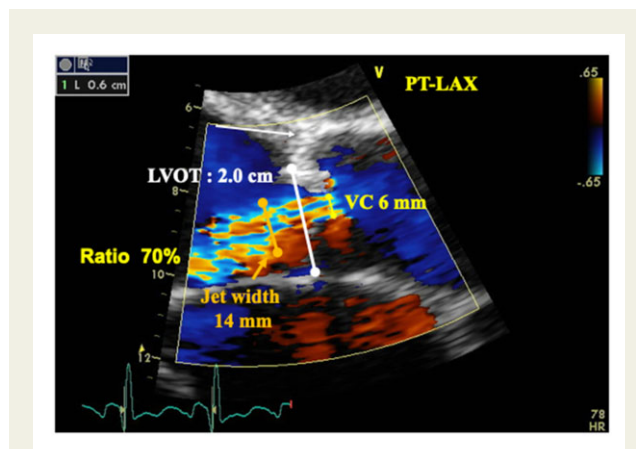
Figure 9 Colour Doppler assessment of the jet width ratio (maximum colour jet diameter divided by LV outflow tract diameter) in a patient with severe AR. VC, vena contracta.

unsatisfactory or inconclusive or when there is discrepancy between AR severity and clinical findings. These parameters should be interpreted according the chronicity of AR and the LV remodelling. CMR may provide additional information about the mechanism of AR, the dimension of aorta, and the presence of local fibrosis. Either echocardiography or CMR is used for serial evaluation of aortic dimension, although the latter gives a more complete assessment of the thoracic aorta. CCT scanning is not routinely used but can be helpful in specific circumstances, especially in the preprocedural intervention planning (presence and extent of aortic valve and root calcifications, annular size assessment, presence of coronary artery disease, and dimension of the aorta).
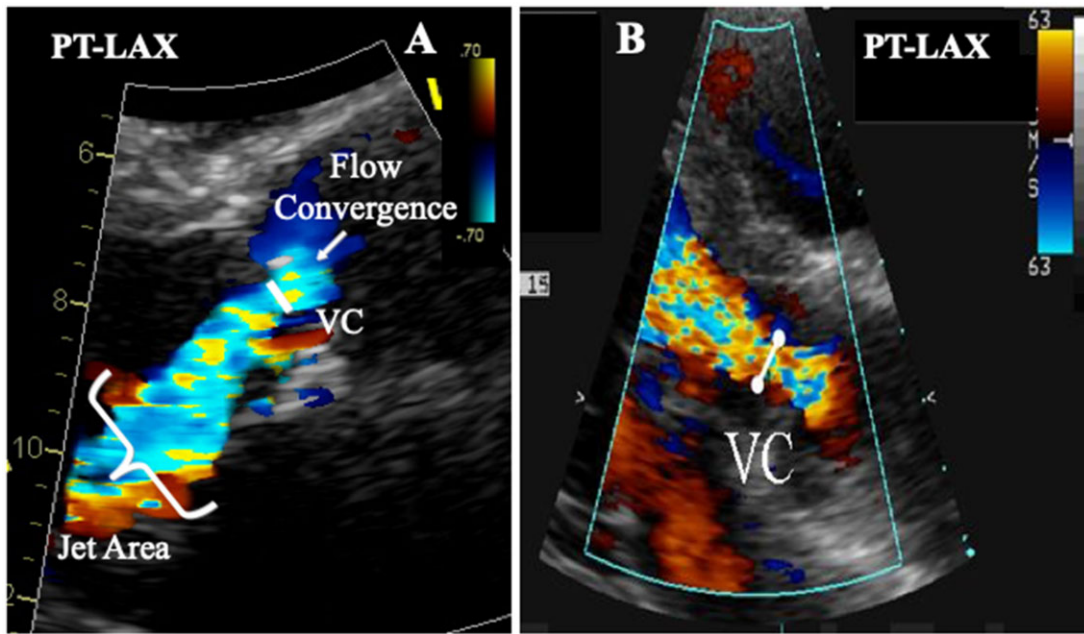
Figure 10 (*A*) Semi-quantitative assessment of AR severity using the vena contracta width (VC). The three components of the regurgitant jet (flow convergence zone, vena contracta, and jet turbulence) are obtained. (*B*) Assessment of the VC in a patient with a AR jet directed towards the septum. PT-LAX, parasternal long-axis view.
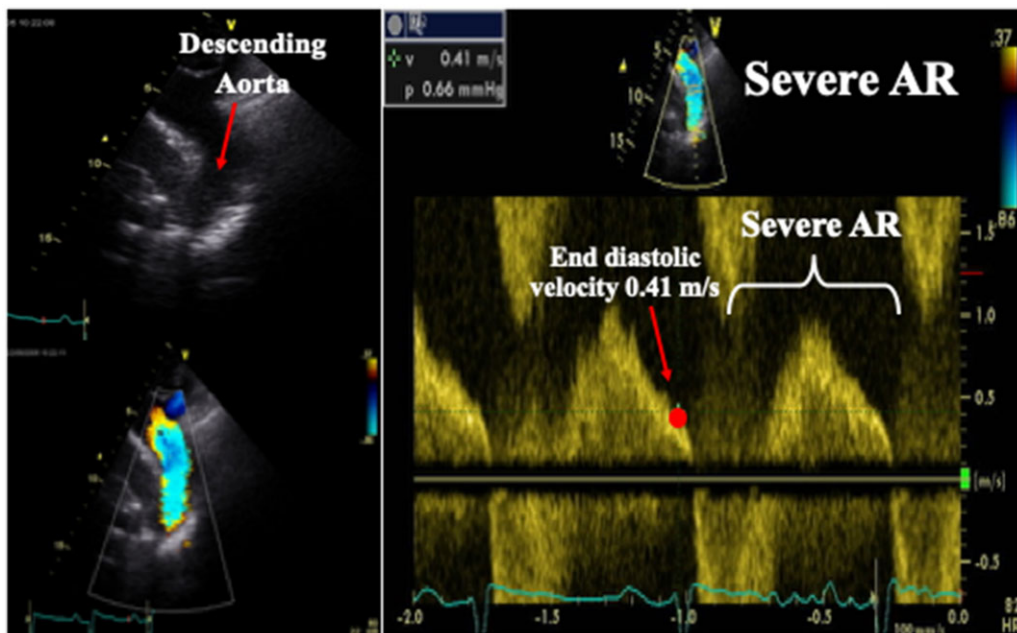
Figure 11 A pulsed Doppler recording within the descending aorta from a patient with severe AR demonstrates flow reversal throughout diastole. An end diastolic flow velocity greater than 20 cm/s is indicative of severe AR.
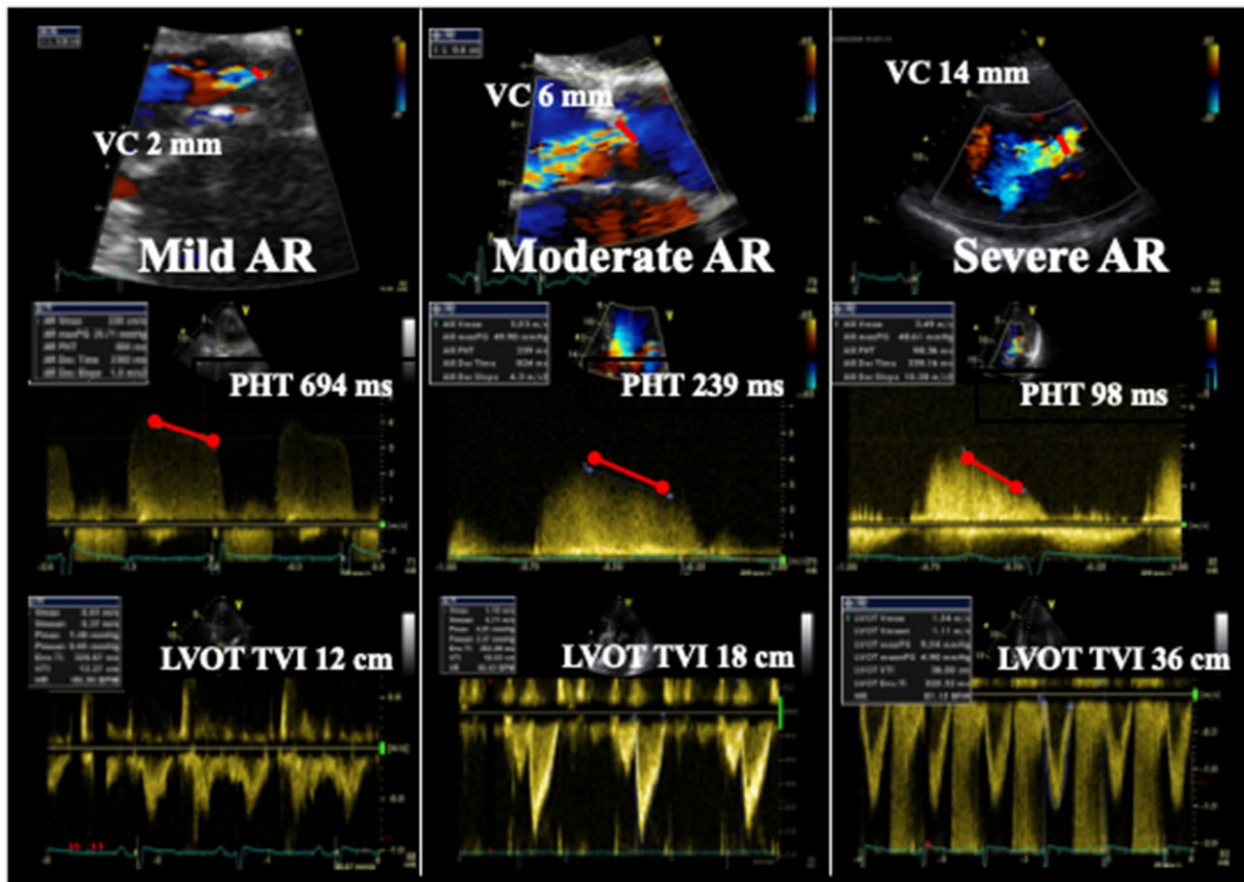
Figure 12 Three examples of AR are provided, all taken from the parasternal long-axis view using colour Doppler (top) and from the apical five-chamber view using continuous wave Doppler (mid). The vena contracta (VC) increases with the severity of AR. The pressure half-time (PHT) decreases with more severe AR whereas the left ventricular outflow time velocity (LVOT TVI) integral increases.

Intervention guidance

The incidence of valve sparing or repair decreases with the severity of dysfunction and is less than 50% in type III dysfunction. The presence and extent aortic calcifications (i.e. porcelain aorta) on CCT may limit the surgical approach by precluding clamping or cannulation. Three-dimensional TOE and CCT, using automated modelling, provide precise measurements of leaflet free edge, height, and coaptation height, which might help estimating the size of the graft during aortic valve surgery. A height <8 mm is predictive of recurrent AR after aortic valve surgery.[46]

Suggested follow-up

Asymptomatic patients with mild AR, no LV dilatation and normal LVEF require echocardiographic evaluation every 2–3 years. In patients with asymptomatic severe AR and normal LV function and size, first echocardiographic monitoring should be performed 3–6 months after the initial diagnosis. After that, follow-up evaluation should be done when symptoms occur, or in asymptomatic patients every 1 year or every 3–6 months when LV size and function are close to thresholds for surgery or in cases of aortic dilatation. If the aorta is not well imaged with echocardiography then a CMR or CCT should be performed, particularly if surgery is being considered. Either echocardiography or CMR are preferred for follow-up assessment of aortic dimension (no radiation exposure). Any increase >3 mm in aortic dimension should be validated by CMR or CCT.[5,47]

Pulmonary regurgitation

A slight amount of PR has been reported in 40–78% of patients with normal pulmonary valves. Acquired mild to moderate PR is most often seen in patients with pulmonary hypertension with dilatation of the pulmonary artery. Severe PR is uncommon and usually observed in patients with anatomic abnormalities of the valve or after valvulotomy.[48] There are very few validated studies owing to the low prevalence rates and difficulties in imaging.

Anatomy and function of the pulmonary valve

The pulmonary valve is a three-leaflet structure, anatomically similar to the aortic valve (*Figure 16*). The pulmonic valve structure is
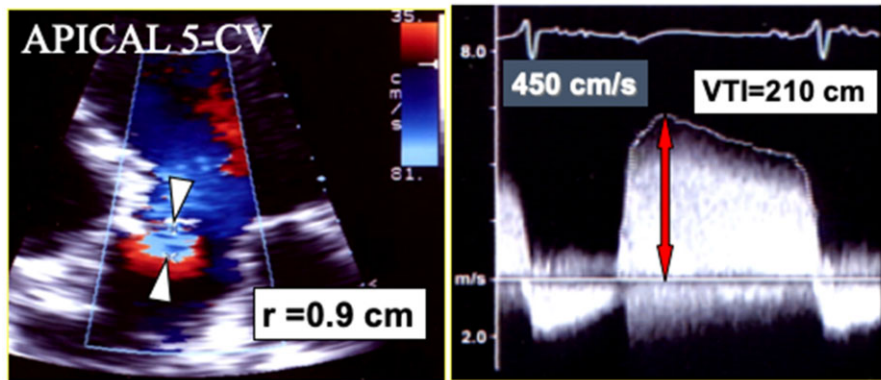
Figure 13 Quantitative assessment of AR severity using the PISA method from the apical five-chamber view (CV). EROA, effective regurgitant orifice area; R Vol, regurgitant volume; TVI, time-velocity integral; Va, aliasing velocity.
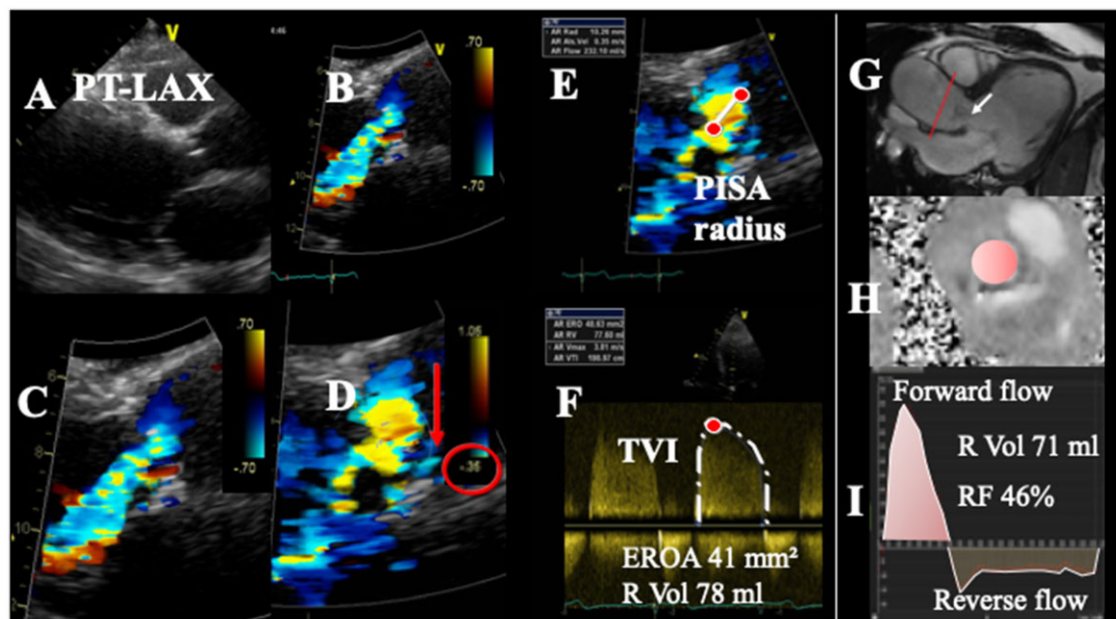
Figure 14 Quantitative assessment of AR severity using the PISA method (*A–F*) and the CMR phase-contrast method (*G–I*). Stepwise analysis of AR. (*A*) Parasternal long-axis view (PT-LAX). (*B*) Colour-flow display. (*C*) Zoom of the selected zone. (*D*) Downward shift of zero baseline to obtain a hemispheric PISA. (*E*) Measure of the PISA radius using the first aliasing. (*F*) Continuous wave Doppler of AR jet allowing calculation the effective regurgitant orifice area (EROA) and regurgitant volume (R Vol). CMR evaluation of AR by direct method (*G–I*). (*G*) Aortic root positioning (white arrow: extent of the signal loss on cine); (*H*) phase-contrast velocity mapping at the aortic root level; and (*I*) flow-time curves computing forward and reverse or backward flows. The reverse flow represents the directly measured volume of AR. TVI, time-velocity integral.

Table 7   Grading the severity of AR

AR severity classes[a]	Mild	Moderate		Severe
AR severity sub-classes[a]	**Mild (Grade 1 or 1+)**	**Mild-to-moderate[a] (Grade 2 or 2+)**	**Moderate-to-severe[a] (Grade 3 or 3+)**	**Severe (Grade 4 or 4+)**
Qualitative parameters				
Aortic valve morphology	Normal/abnormal	Normal/abnormal	Abnormal/prolapse/moderate coaptation defect	Abnormal/**flail/large coaptation defect**
Colour flow AR jet width[b]	Small in central jets	Intermediate	**Large in central jet,** variable in eccentric jets	**Large in central jet,** variable in eccentric jets
Color flow convergence	None or very small	Intermediate	Intermediate	Large
CW signal of AR jet	Incomplete/faint	Dense	Dense	Dense
Diastolic flow reversal in descending aorta[c]	Brief, proto-diastolic flow reversal	Intermediate	Holodiastolic flow reversal (end-diastolic velocity 10 to <20 cm/s)	**Holodiastolic flow reversal** (end-diastolic velocity ≥20 cm/s)
Diastolic flow reversal in abdominal aorta[c]	Absent	Absent	Present	Present
Semi-quantitative parameters				
VC width (mm)	<3	3–6	3–6	**>6**
Jet width/LVOT diameter (%)	<25	25–45	46–64	**≥65**
Jet CSA/LVOT CSA (%)	<5	5–20	21–59	**≥60**
Pressure half-time (ms)[c,d]	>500	Intermediate, 500 to 200	Intermediate, 500 to 200	**<200**
Quantitative parameters				
EROA (mm²)	<10	10–19	20–29	≥30
R Vol (mL)	<30	30–44	45–59	≥60
RF (%)	<30	30–39	40–49	≥50
CMR parameters				
RF (%)	<30	30–39	40–49	≥50
Structural parameters				
LV size[e]	Usually normal	Normal or dilated	Usually dilated	Usually dilated

AR, aortic regurgitation; CSA, cross-sectional area; CW, continuous wave; LA, left atrium; EROA, effective regurgitant orifice area; LV, left ventricle; RF, regurgitant fraction; R Vol, regurgitant volume; VC, vena contracta.

In bold: specific signs for severe AR.

[a] Grading of severity of AR classifies regurgitation as mild, moderate or severe, and sub-classifies the moderate regurgitation group into two subclasses: 'mild-to-moderate' (EROA of 10–19 mm or a R Vol of 20–44 mL) and 'moderate-to-severe' (EROA of 20–29 mm² or a R Vol of 45–59 mL).

[b] At a Nyquist limit of 50–60 cm/s.

[c] These parameters are influenced by LV and aortic compliance. Hence, low transvalvular end-diastolic aorta to LV pressure gradient due to concomitant moderate/severe LV diastolic dysfunction may lead to false positive results. The high dependency of aortic flow reversal on aortic compliance considerably limits the utility of this parameter in the elderly population. These parameters are also influenced by chronotropy.

[d] Pressure half-time is shortened with increasing LV diastolic pressure, vasodilator therapy, and in patients with a dilated compliant aorta or lengthened in chronic AR.

[e] Unless for other reasons, the LV size is usually normal in patients with mild AR. In acute severe AR, the LV size is often normal. *Accepted cut-off values for non-significant LV enlargement:* LV end-diastolic diameter <56 mm, LV end-diastolic volume <82 mL/m², LV end-systolic diameter <40 mm, LV end-systolic volume <30 mL/m².
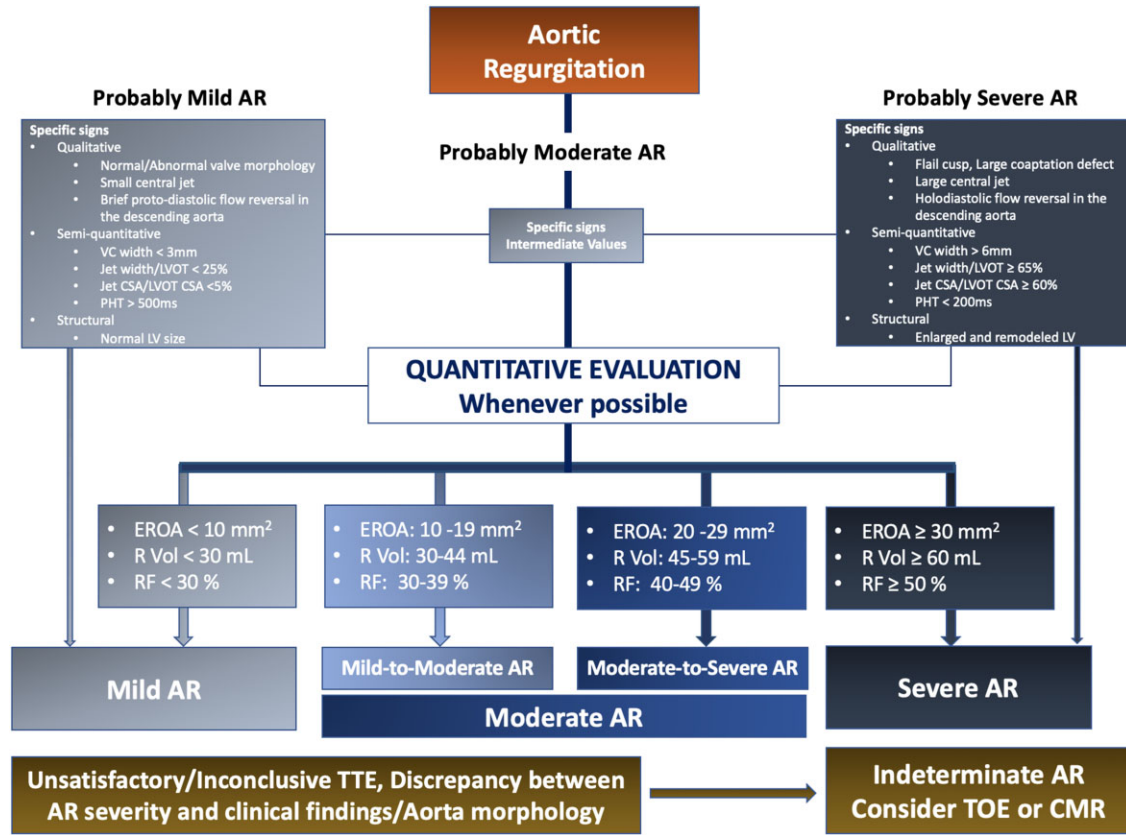
Figure 15 Algorithm for the assessment of AR severity. CSA, cross-sectional area; LVOT, left ventricular outflow tract; PHT, pressure half time; VC, vena contracta.
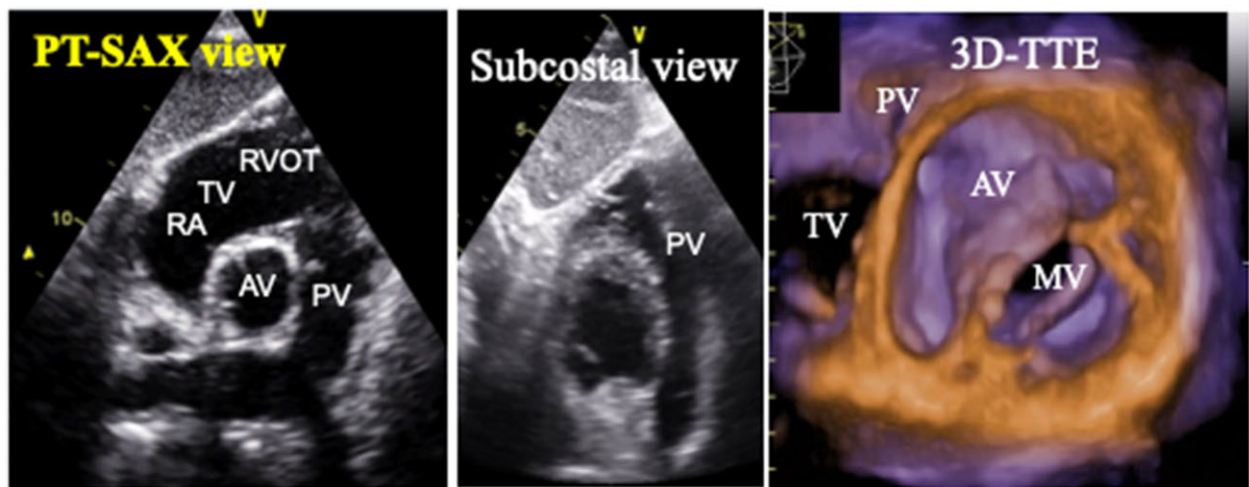
Figure 16 2D and 3D echo recordings of the pulmonic valve. PT-SAX, parasternal short-axis view.
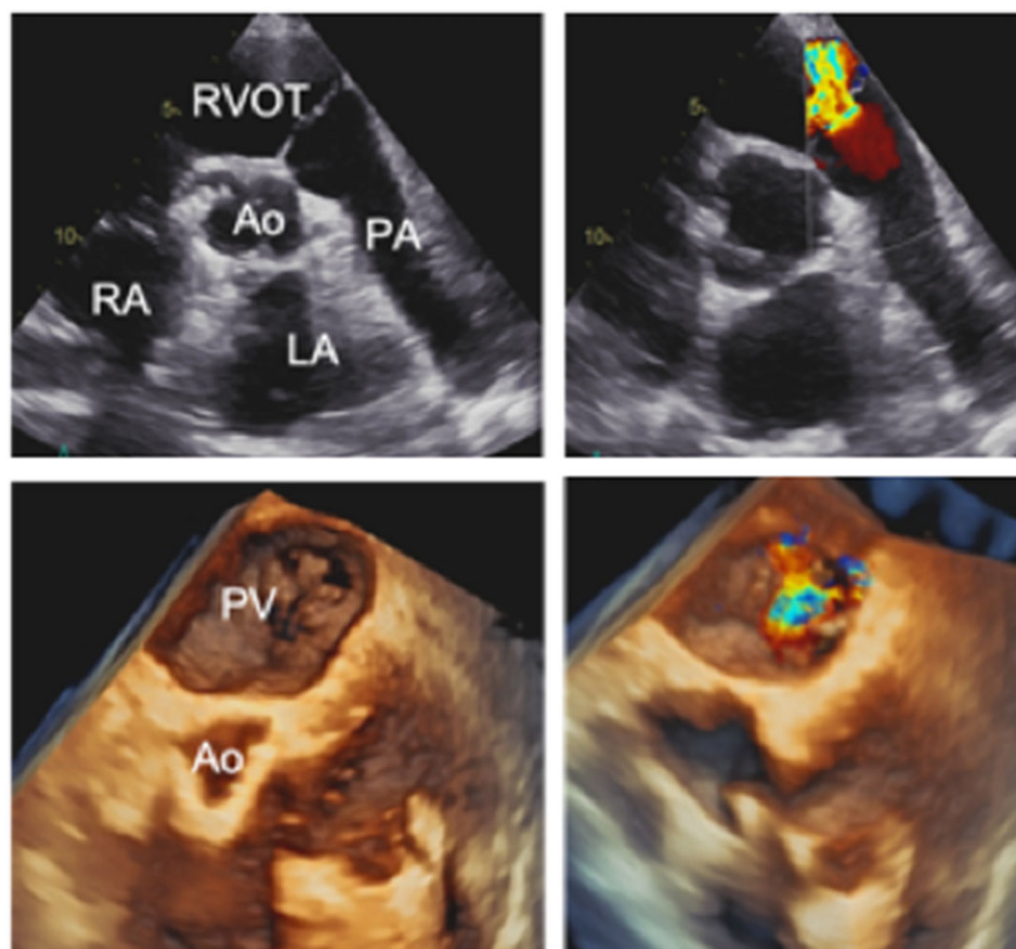
Figure 17 2D and 3D assessment of PR severity by using colour-flow imaging.

however thinner because of the lower pressures in the right than in the left heart.

Aetiology and mechanisms

Primary PR may be caused by congenital anomalies (quadricuspid or bicuspid valves), hypoplasia, post-repair of Tetralogy of Fallot, or prolapse of the pulmonary valve. Other causes include infective endocarditis, carcinoid syndrome, and rheumatic heart disease. Carcinoid syndrome results in shortening and thickening of the pulmonary valve leaflets, similar to the involvement of the TV. Myxomatous valve is rare, resulting in thickening, redundancy, and sagging of the pulmonary valve leaflets. Secondary PR is most common in patients with elevated pulmonary artery pressure. By definition, the pulmonary valve leaflets are normal with secondary PR.

Imaging evaluation in PR

Pulmonary valve morphology

In PR, imaging is key for inspection of the pulmonary valve anatomy, the RV outflow tract, pulmonary annulus, main pulmonary arteries and proximal branches. Two-dimensional/3D TTE and TOE provide

useful information regarding anomalies of cusp number (bicuspid or quadricuspid valves), motion (doming or prolapse), or structure (hypoplasia, dysplasia, and absence of pulmonary valve). Evaluation of the pulmonary valve anatomy is however more difficult than for other valves (limited by poor acoustic access). With 2D echo, typically only one or two leaflets of the pulmonary valve can be simultaneously visualized. On occasion, the pulmonary valve can be seen in a short-axis view. In adults, visualization of the pulmonary valve is obtained from the parasternal short-axis view at the level of the aortic valve or from a subcostal approach. Live TTE 3D echocardiography from the parasternal window can be effective in visualizing en face pulmonary valve short-axis morphology and quantifying cusp number (*Figure 17*).[49] Three-dimensional biplane echo imaging by providing simultaneous 2D orthogonal views allows a better evaluation of the pulmonary valve. Pulmonary annulus diameter derived by 3D TTE in patients with tetralogy of Fallot correlates more closely with surgical measurements, when compared to 2D TTE and cardiac MSCT.[50] The role of TOE in PR is limited since the pulmonary valve is more difficult to image with TOE (far from the probe). The views that maximize visualization of the pulmonary valve include horizontal plane imaging at the level of the short-axis aortic valve ('inflow-
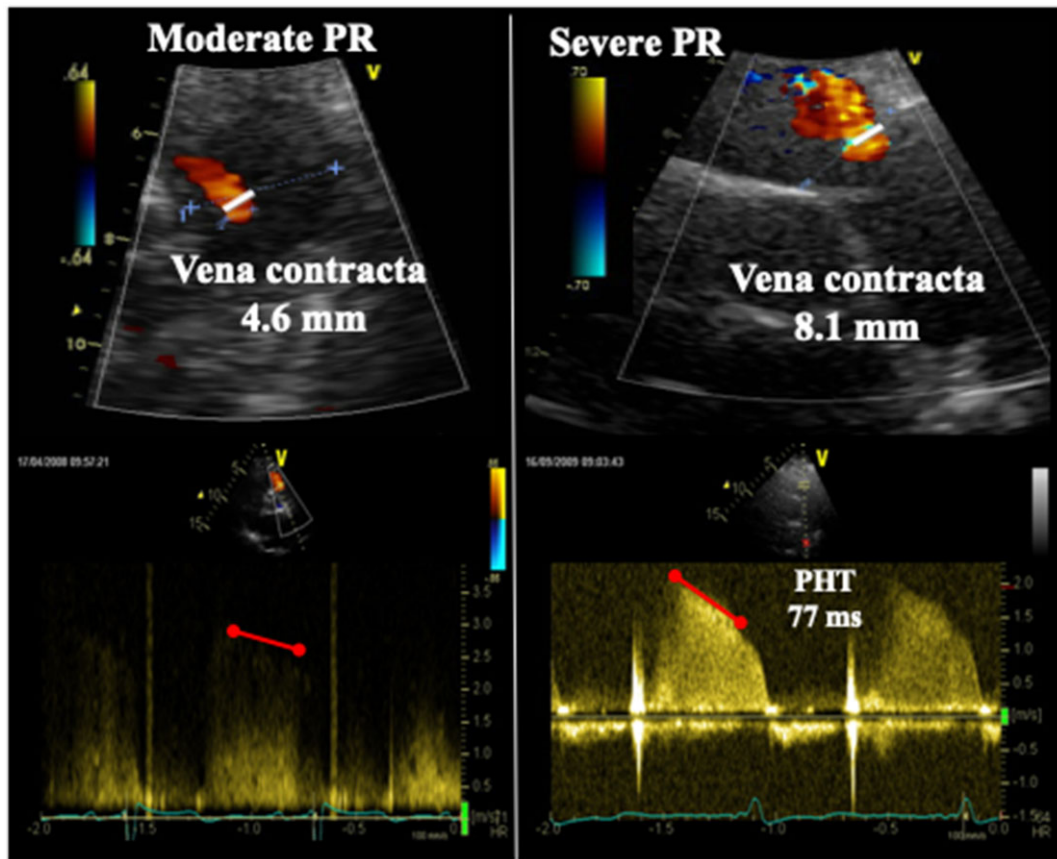
Figure 18 Assessment of PR severity by using colour-flow imaging. *Top*: Measurements of the right ventricular outflow tract dimension (RVOT) and regurgitant jet width in two patients with TR. *Bottom*: continuous wave Doppler recordings.

outflow view') and a deep gastric view in 120° imaging plane (outflow view).

CMR can be used as an alternative tool when echocardiography is suboptimal to assess pulmonary valve morphology. The ability to image in any plane, ensures that the pulmonary valve can be well visualized. Moreover, CMR is excellent for evaluating the anatomy and dimensions of the main pulmonary arteries and its branches, as well as surgically constructed shunts, and is of particular utility in the assessment of congenital pulmonary valve disease.[12,14]

CCT can also delineate pulmonary valve anatomy as well as the size of the pulmonary annulus, the pulmonary arteries dimension and the burden of calcifications. It may be used when echo and CMR assessments are not definitive and to aid preprocedural planning.[26]

Assessment of PR severity

Determination of the PR severity is less well validated than determination of AR severity.

Semi-quantitative methods

Colour flow Doppler Imaging. Detection of PR relies almost exclusively on colour flow imaging. PR is diagnosed by documenting a diastolic jet in the RV outflow tract directed towards the right ventricle.

Pathologic PR is distinguished from physiologic PR by a longer duration of flow (holodiastolic) and a wider jet as the regurgitant jet crosses the pulmonic valve.[51] Functional PR jets are usually very small, central and spindle-shaped. In severe PR, where equalization of diastolic pulmonary artery and RV pressures occurs earlier in diastole, the colour jet area can be brief and inaccurate (dependency on the driving pressure).[52] The assessment of PR severity is usually estimated by the diameter of the jet at its origin.[53] The maximum colour jet diameter (width) is measured in diastole immediately below the pulmonic valve (at the junction of the RV outflow tract and pulmonary annulus) in the parasternal short-axis view or from the subcostal view. Although this measurement suffers from a high inter-observer variability (depending on the cut-plane), a jet width that occupies >65% of the RV outflow tract width measured in the same frame suggests severe PR.[54]

Detection of reversal colour Doppler flow in branch of pulmonary arteries is a very specific (87%) sign of severe PR. This has much greater specificity for CMR-derived severe PR than flow reversal in the main pulmonary arteries (specificity of 39%).[55]

Vena contracta width. Although the VC width is probably a more accurate method than the colour jet width to evaluate PR severity by colour Doppler, it lacks still validation studies (*Figures 18 and 19*). As

for other regurgitations, the same limitations are applicable. A VC/ pulmonary valve annulus ratio ≥50% is an indicator of greater than mild PR. A ratio ≥0.7 is a marker of severe PR. The shape of the VC is complex in most cases. Though, the value of 3D echo has not yet been clearly defined,[56] a 3D VC area > 0.45 cm^2 is in keeping with severe PR.

Pulsed Doppler. Theoretically, PW Doppler assessment of the forward and reverse flows at the pulmonary annulus and in the pulmonary artery can been used to calculate R Vol and RF. The pulmonary annulus should be measured carefully during early ejection (2–3 frames after the R wave on the ECG), just below the valve. This technique is subject to errors in measurement and is not well validated.[57]

Continuous wave Doppler of the PR jet. The density of the CW signal provides a qualitative measure of regurgitation.[58] In mild PR, there is a slow deceleration of the jet velocity. A rapid deceleration rate with termination of flow in mid to late diastole (deceleration time < 260 ms) is not specific but compatible with severe PR. In patients with congenital disease, a pressure half time <100 ms yields good sensitivity and specificity for severe PR.[59] The pressure half time is dependent not only on PR severity but also on diastolic intrapulmonary pressures and on diastolic properties of the right ventricle, with shorter pressure half time when RV physiology is restrictive. A PR index <0.77 (ratio of PR duration by CW Doppler to total diastolic time) is consistent with severe PR, although not specific.[60]

Quantitative assessment
Anatomic orifice area
There is no clinically validated data on direct measurement of the anatomic orifice area.

The proximal isovelocity surface area method. In some patients, the flow convergence zone can be assessed (*Figure 20*). However, no studies have examined the clinical accuracy of this method in quantifying the severity of PR.

Doppler volumetric method. There is no clinically accepted method of quantifying PR using CW Doppler.

CMR quantification. CMR is currently the best method to quantitate PR and serially assess RV remodelling and function in patients with significant PR and congenital heart disease.[61] It should be considered in most patients with suspected substantial PR unless echocardiographic findings are conclusive. Visual assessment of the degree of signal loss due to spin dephasing from the regurgitation can also be used but are less validated and provide only a qualitative assessment of PR severity. Both direct (phase-contrast technique) (*Figure 20*) and indirect methods of quantification can be used to calculate R Vol and RF. The direct method is however the preferred approach, with a co-axial through plane phase-contrast sequence planned just above the pulmonary valve. Quantification of the R Vol by comparing LV and RV stroke volumes is also possible but only valid in the absence of any other concomitant valvular regurgitation. The R Vol can also be calculated from the difference between RV total (using planimetry of short-axis cine images) and forward stroke volume across the aortic

valve (using phase-contrast velocity mapping) in the absence of significant TR. Considered RF threshold for assessing PR severity on CMR are: mild <20%, moderate 20–40%, and severe >40%.[61] When available, CMR is the preferred method to assess the right ventricle due to its high accuracy and reproducibility.

> **Key point: CMR is an accurate tool for quantitative assessment of PR. The direct approach using the phase-contrast technique is the most reproducible with the advantage of not being affected by coexisting valvular regurgitation lesions. A RF >40% indicates severe PR. When available, CMR is the preferred method for assessing RV size.**

Consequences of PR
Evaluation of the size and function of the right ventricle in the absence of pulmonary hypertension provides indirect clues to the severity of PR. Evidence of RV dilatation is however not specific for severe PR, especially if observed in the context of pulmonary hypertension. Nevertheless, its absence suggests milder degree of PR or acute PR. Of note, dilatation can be observed in other conditions (non-specific) or may be absent in acute severe PR. As for TR, the RV function is classically evaluated on echocardiography by the RV volumes and the RV fractional area change. Three-dimensional echocardiography allows more accurate evaluation of RV ejection fraction (RVEF) than 2D. The utility of the other indices deriving from tissue Doppler or strain imaging has not been extensively examined in the context of PR unrelated to congenital heart disease. When available, CMR is the preferred method to assess the right atrium and right ventricle due to its high accuracy and reproducibility. CMR provides larger right atrial (RA)/RV volumes than echocardiography, due to different handling of trabeculations, which are excluded on echocardiography. Conversely, RVEF by 3D echocardiography is comparable to CMR.[6] Indexed RV end-diastolic volume >160 mL/m^2 on CMR has been associated with a low likelihood of RV functional recovery after reintervention for severe residual PR in the context of corrected tetralogy of Fallot.[62]

Role of exercise echocardiography
Latent RV dysfunction and impaired functional response to stress can be unmasked by exercise echocardiography. Except in the setting of congenital heart disease, the value of exercise testing in patients with PR has not been specifically examined.[8]

Integrating indices of severity
Echocardiographic assessment of PR includes integration of data from 2D/3D imaging of the pulmonary valve and right ventricle as well as Doppler measures of regurgitation severity (*Table 8*) (*Figure 21*). In the absence of extensive data on quantitation of PR, the experts strongly suggest to assess the PR severity by integrating information from all different approaches available and to corroborate each other. The simplest and most robust method is PR jet width and VC. CMR is the alternative method of choice and should be used in most cases when there is concern about clinically significant PR (i.e.
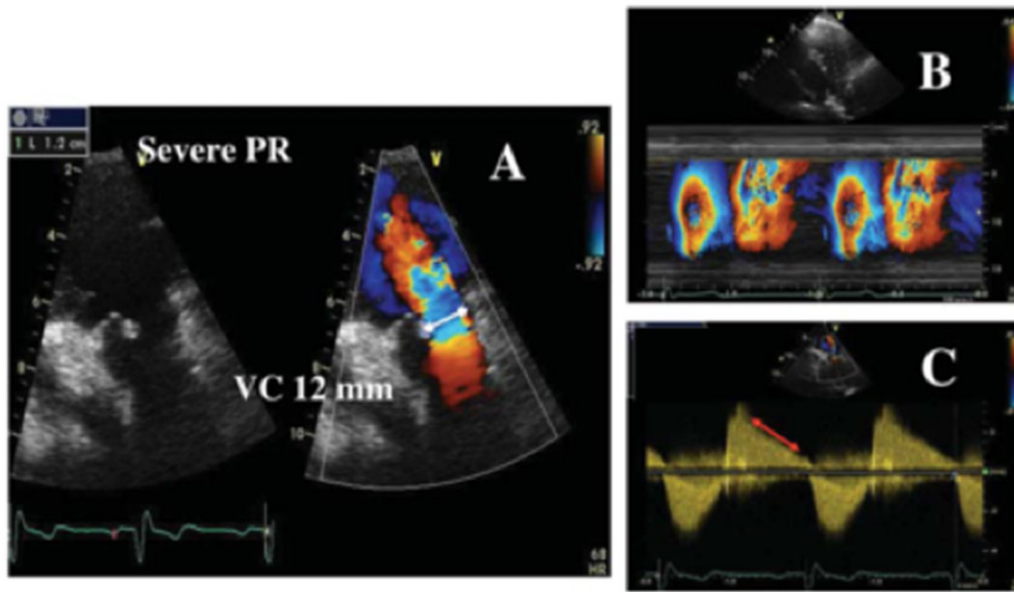
Figure 19 Example of a patient with a severe PR. (*A*) Left, complete lack of valve coaptation and right, measurement of the vena contracta width (VC); (*B*) colour-coded M-mode depicting the time-dependency of flow signal during the heart cycle; and (*C*) Continuous Doppler recording of PR showing a rapid flow deceleration during the diastole (red arrow) and increased systolic flow velocity (not related to concomitant pulmonary stenosis).
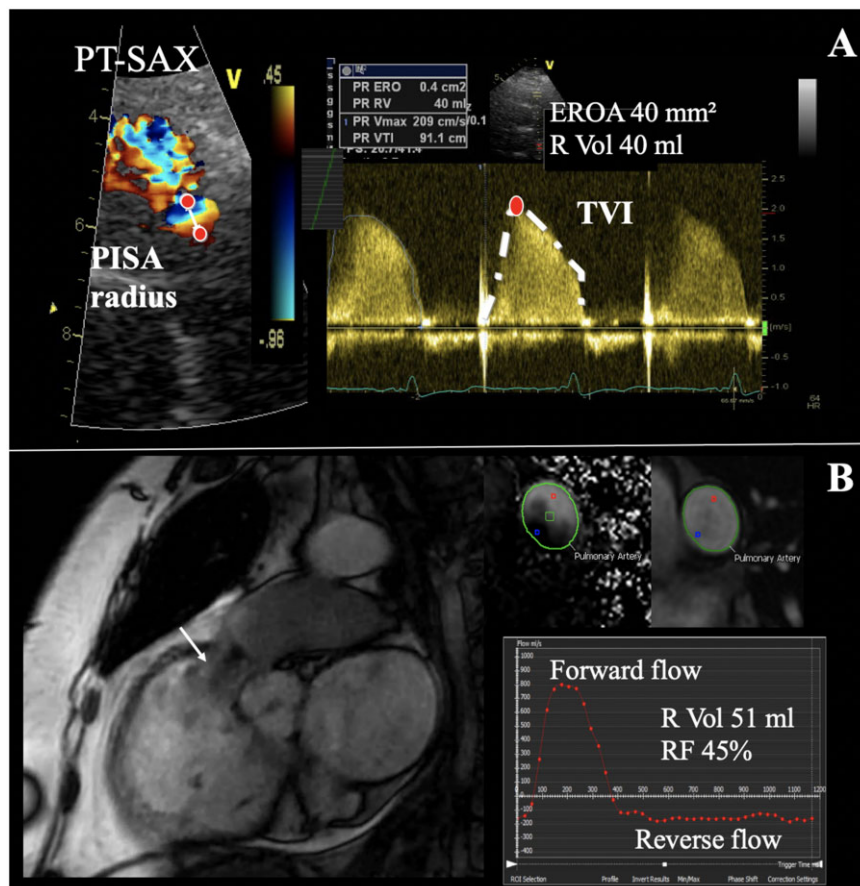
Figure 20 Assessment of PR severity by the PISA method (*A*) and the CMR phase-contrast method (direct method) (*B*). White arrow: extent of the signal loss on cine CMR. Phase-contrast velocity mapping and flow-time curves computing forward and reverse or backward flows. The reverse flow represents the directly measured volume of PR.

Table 8   **Grading the severity of PR**

PR severity classes	Mild	Moderate	Severe
Qualitative parameters			
Pulmonic valve morphology	Normal	Normal/Abnormal	Abnormal
Colour flow PR jet width[a]	Small, usually <10 mm in length with a narrow origin	Intermediate	Large, with a wide origin; may be brief in duration
Reversal flow in pulmonary artery branches	Absent	Absent	**Present**
CW signal of PR jet[b]	Faint/Slow deceleration	Dense/variable	Dense/steep deceleration, **early termination of diastolic flow**
Pulmonic vs. aortic flow by PW	Normal or slightly increased	Intermediate	Greatly increased
Semi-quantitative parameters			
VC width (mm)	Not defined	Not defined	Not defined
Deceleration time of the PR	Not defined	Not defined	<260 ms
Pressure half-time[c]	Not defined	Not defined	**<100 ms**
Jet width/annulus ratio	Not defined	Not defined	**>65**%
PR index[d]	Not defined	Not defined	<0.77
Quantitative parameters			
EROA (mm^2)	Not defined	Not defined	Not defined
R Vol (mL)	Not defined	Not defined	Not defined
RF (%)	<20	20–40	>40
CMR parameters, RF (%)	<20	20–40	>40
Structural parameters, RV size[e]	Usually normal	Normal or dilated	**Usually dilated**

CW, continuous-wave; EROA, effective regurgitant orifice area; PR, pulmonic regurgitation; PW, pulse wave; R Vol, regurgitant volume; RV, right ventricle; VC: vena contracta.
In bold: specific signs for severe PR.
[a]At a Nyquist limit of 50–60 cm/s.
[b]Steep deceleration is not specific for severe PR.
[c]Pressure half time is shortened with increasing RV diastolic pressure.
[d]PR index: ratio of PR duration by CW Doppler to total diastolic time.
[e]Unless for other reasons, the RV size is usually normal in patients with mild PR. In acute severe PR, the RV size is often normal. *Accepted cut-off values for non-significant RV enlargement (measurements obtained from the apical 4-chamber view)*: Mid RV dimension ≤33 mm, RV end-diastolic area ≤28 cm^2, RV end-systolic area ≤16 cm^2, RV fractional area change >32%, maximal.

only moderate PR with dilating RV) unless the echocardiographic findings are conclusive. CCT scan can be helpful in specific circumstances to complement echocardiography, especially in the preprocedural intervention planning.

Intervention guidance

Intervention guidance mainly refer to pulmonary valve replacement either surgically or percutaneously.[63] It should be considered in patients with severe PR and symptoms of evidence of RV decompensation.

Suggested follow-up

As for other valvular regurgitation, the follow-up of patients with PR depends on the aetiology and severity of PR, the size and function of the right ventricle, and the associated diseases. Although information is limited, careful follow-up should be organized in patients with moderate to severe PR.[5]

Mitral regurgitation

MR is increasingly prevalent in Europe despite the reduced incidence of rheumatic disease. Non-invasive imaging plays a key role in the assessment and management of patients with MR.[5]

Anatomy and function of the mitral valve

Normal MV function depends on optimal function of the complex interaction between the mitral leaflets, the subvalvular apparatus (chordae tendineae and papillary muscles), the mitral annulus, the left atrium and the left ventricle. An abnormality in any one of these components can cause the valve to leak.[64] The normal MV has two leaflets; the posterior attached to the two-thirds of the annular plane and the anterior, to the remaining one-third. They are each divided into three scallops: A1, A2, A3 and P1, P2, P3. A1 and P1 correspond to the external, anterolateral portion of their respective leaflet, close to the antero-lateral commissure and the left atrial appendage. On the opposite side, A3 and P3 are internal, close the postero-medial commissure and the tricuspid annulus (*Figure 22*). Normal leaflet

thickness is <5 mm in diastole and the degree of leaflet overlap at the point of coaptation should be >5 mm for a competent valve.

Aetiology and mechanisms of MR

According to aetiology, MR can be classified as primary (i.e. organic/structural: intrinsic abnormalities of the leaflet and/or subvalvular apparatus) or secondary (i.e. functional/non-structural: when MV anatomy is normal but abnormalities of the left ventricle and/or LA disrupt normal valvular function), whereas the mechanism is based on Carpentier's classification of leaflet motion: Type I: normal leaflet motion [primary MR: leaflet perforation or cleft (Ia); secondary MR: annular dilatation either from LA or LV dilatation (Ib)], Type II: excessive motion (leaflet prolapse), and Type III: restrictive motion (A: systolic/diastolic due to rheumatic, post-inflammatory or post-radiotherapy disease and B: systolic due regional/global LV remodelling) (Figure 23). Several types may eventually co-exist in the same patient. Causes of primary MR include most commonly degenerative disease (Barlow, fibroelastic degeneration, Marfan, Ehlers–Danlos, and annular calcification), rheumatic disease, toxic valvulopathy, and endocarditis. Ruptured papillary muscle secondary to myocardial infarction is included as primary ischaemic MR. Rarely, in chronic ischaemic MR, the mechanism of MR is related to fibrosis and elongation of the papillary muscle leading to progressive leaflet prolapse (IIb). The most common causes of mitral regurgitation are outlined below. For the selection of the most appropriate device for MV transcatheter procedures, a pathophysiological classification that accounts for the aetiology of the MV disorder can be used (Table 9).

Degenerative disease (60%), the most common surgical MR cause, covers a large spectrum of lesions (Figures 24 and 25): (i) isolated *billowing* with leaflets tips remaining intra-ventricular to *flail leaflet* with valvular eversion [the leaflet tip is directed towards the left atrium (LA)], (ii) isolated scallop to multi-segment (or generalized) *prolapse* (the leaflet tip is directed towards the left ventricle and the coaptation line is behind the annular plane), and (iii) thin/non-redundant leaflets (fibroelastic deficiency) structure to thick/excess leaflet tissue (Barlow's disease). Calcific degeneration comprises mitral annular calcification that can invade the leaflets and cause retraction with consequent regurgitation of the valve.

Secondary MR (20%) develops despite a structurally normal MV in the context of ischaemic heart disease, dilated cardiomyopathy, or LA remodelling/dilatation.[65,66] It results from an imbalance between the forces acting on the mitral leaflets and the LV-generated closing forces. In patients with LV systolic dysfunction, LV (±LA) remodelling and the resulting tethering of the MV play a major role in the genesis of secondary MR. Chronic secondary ischaemic MR results, in 95% of the cases, from a type IIIb dysfunction. The restrictive motion occurs essentially during systole and is more frequent in patients with previous inferolateral infarction (asymmetric pattern).[66] In this setting, the traction on the anterior leaflet by secondary chordae can induce the so-called « seagull sign » (Figure 26A). In patients with idiopathic dilated cardiomyopathy or with both anterior and inferior infarctions, both leaflets exhibit a reduced systolic motion leading to incomplete coaptation (symmetric pattern) (Figure 26B). Atrial (atriogenic) secondary MR (typically associated with atrial fibrillation, heart failure with preserved LVEF, hypertension, older age) results from significant isolated LA dilatation/remodelling and ensuing annular dilation/deformation with insufficient leaflet expansion as a compensatory

mechanism (Figure 26C).[67] In such case, the leaflet motion is usually normal but there is nonetheless a lack of leaflet coaptation.

Rheumatic MR (15%) is characterized by variable thickening of the leaflets especially at the level of their free edge. Fibrosis of the chordae is frequent, especially of those attached to the posterior valve leaflet explaining the rigidity and reduced motion of the posterior leaflet and in systole (Type IIIa).

In some patients, the posterior leaflet remains in a semi-open position throughout the cardiac cycle and the motion of the anterior leaflet in systole produces a false aspect of prolapse.

Mixed MR is characterized by a combination of both primary and secondary aetiologies, i.e. coexistence of Carpentier Type Ia, II, or IIIa with Ib or IIIb.

Mitral annular disjunction (MAD) is the abnormal atrial displacement of the posterior mitral leaflet hinge-point away from the ventricular myocardium. MAD has been associated with MV prolapse and sudden cardiac death.[68]


> **Key point: In patients with MR, careful analysis of the mitral valve morphology and apparatus is mandatory. The imaging report should include information about the aetiology, the lesion process and the type of dysfunction. The likelihood of valve repair should also be discussed.**
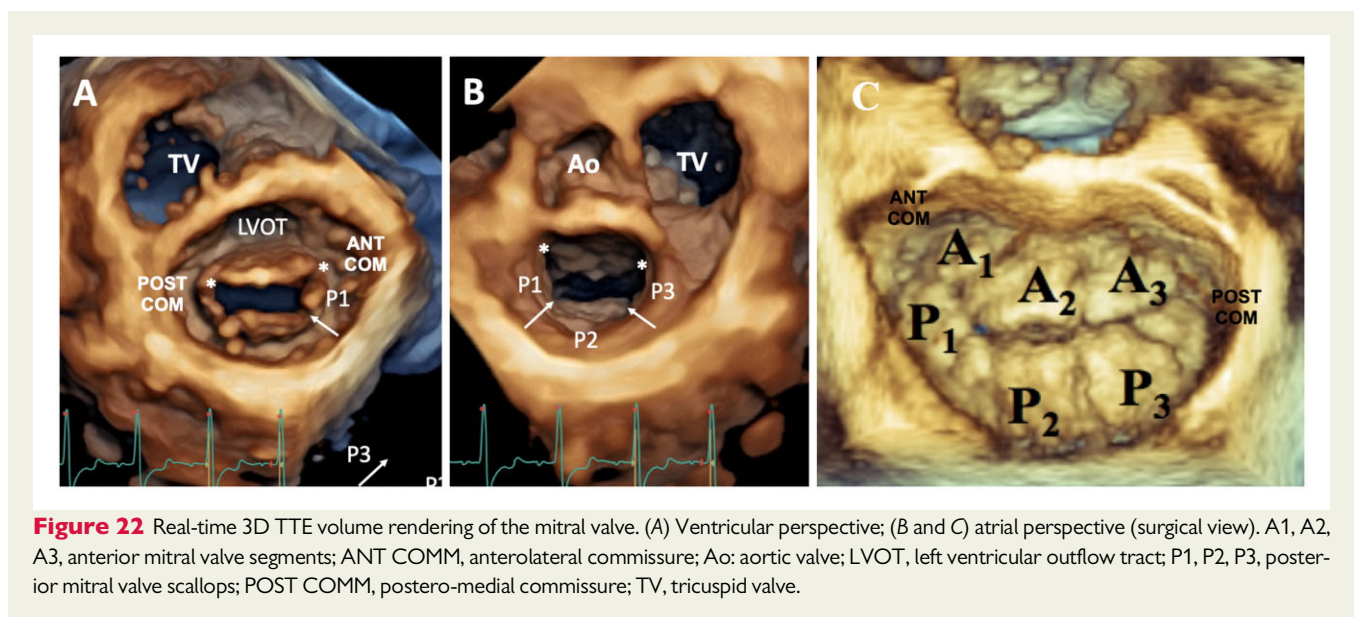

Imaging evaluation in MR

Mitral valve morphology

Two-dimensional TTE and TOE are the primary modalities used to accurately assess the MV morphology (Figures 27 and 28). The TTE *parasternal short-axis* view and the TOE *transgastric view at 0°* permit the assessment of the six scallops and, with colour-Doppler imaging, the localization of the origin of the regurgitant jet may identify prolapsing segments. The TTE *parasternal long-axis* and the TOE *sagittal view at 120°* classically show A2 and P2. With TOE, angulation of the probe towards the aortic valve allows the visualization of A1 and P1 and towards the tricuspid, the visualization of A3 and P3. In *apical 4-chamber view*, appreciation of A3, A2, and P1 (internal to external) is possible. The TTE *2-chamber view* or the TOE *view at 40° to 60°* with TOE displays P3, A2, and P1 (left to right, bi-commissural view). The precise location of the involved leaflets/scallops, the description of the presence and extent of calcifications and the extent of anatomic changes are fundamental parameters to be provided. A flail leaflet, a ruptured papillary muscle or a large coaptation defect is specific for severe MR.

Of note, with 2D TTE, the diagnosis of prolapse should be made in the parasternal or apical long-axis views, but not in the apical four-chamber view, because the saddle shaped annulus may lead to false positive diagnosis. Using the *parasternal long-axis TTE view (or TOE 135°)*, annular dilatation is identified when the ratio annulus diameter/anterior leaflet length is >1.3 (in diastole) or when the antero-posterior annulus diameter is >35 mm.[69] Commissural diameter can be measured in TTE apical two-chamber view or in TOE at 50°. The normal contraction of the mitral annulus (decrease in annular area in systole) is 25%.[66]
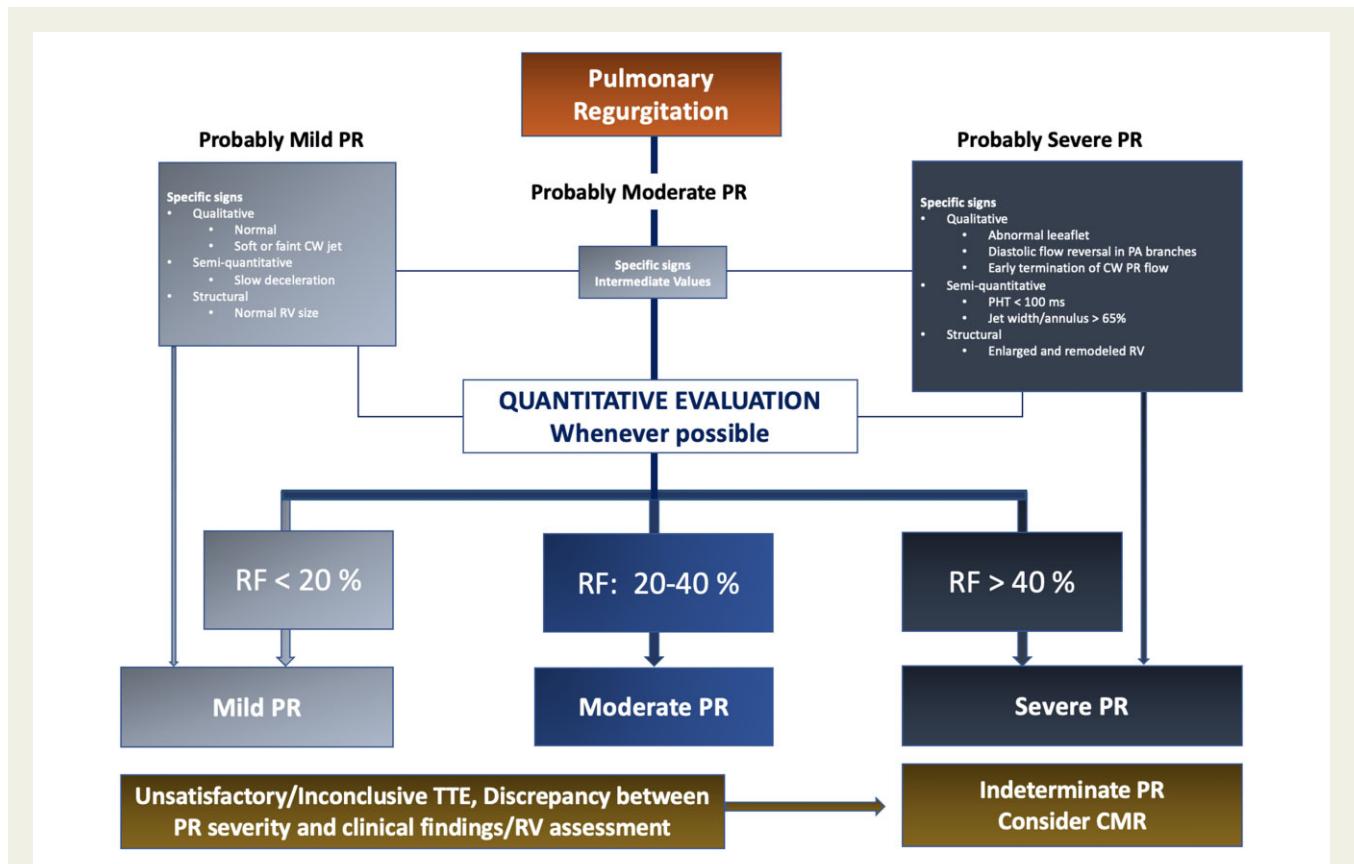
Figure 21 Algorithm for the assessment of PR severity. CW, continuous wave; pressure half time.

Figure 22 Real-time 3D TTE volume rendering of the mitral valve. (*A*) Ventricular perspective; (*B and C*) atrial perspective (surgical view). A1, A2, A3, anterior mitral valve segments; ANT COMM, anterolateral commissure; Ao: aortic valve; LVOT, left ventricular outflow tract; P1, P2, P3, posterior mitral valve scallops; POST COMM, postero-medial commissure; TV, tricuspid valve.

Volumetric datasets acquired during 3D imaging provide visualization of the valve from any angle or in any plane (*Figures 22, 27, and 28*). The TTE MV datasets can be acquired in either the parasternal or apical views. The 'en face' view of the valve from the atrial perspective is identical to the surgical view in the operating room.[2,3,6] In this view, by displaying the aortic valve at the
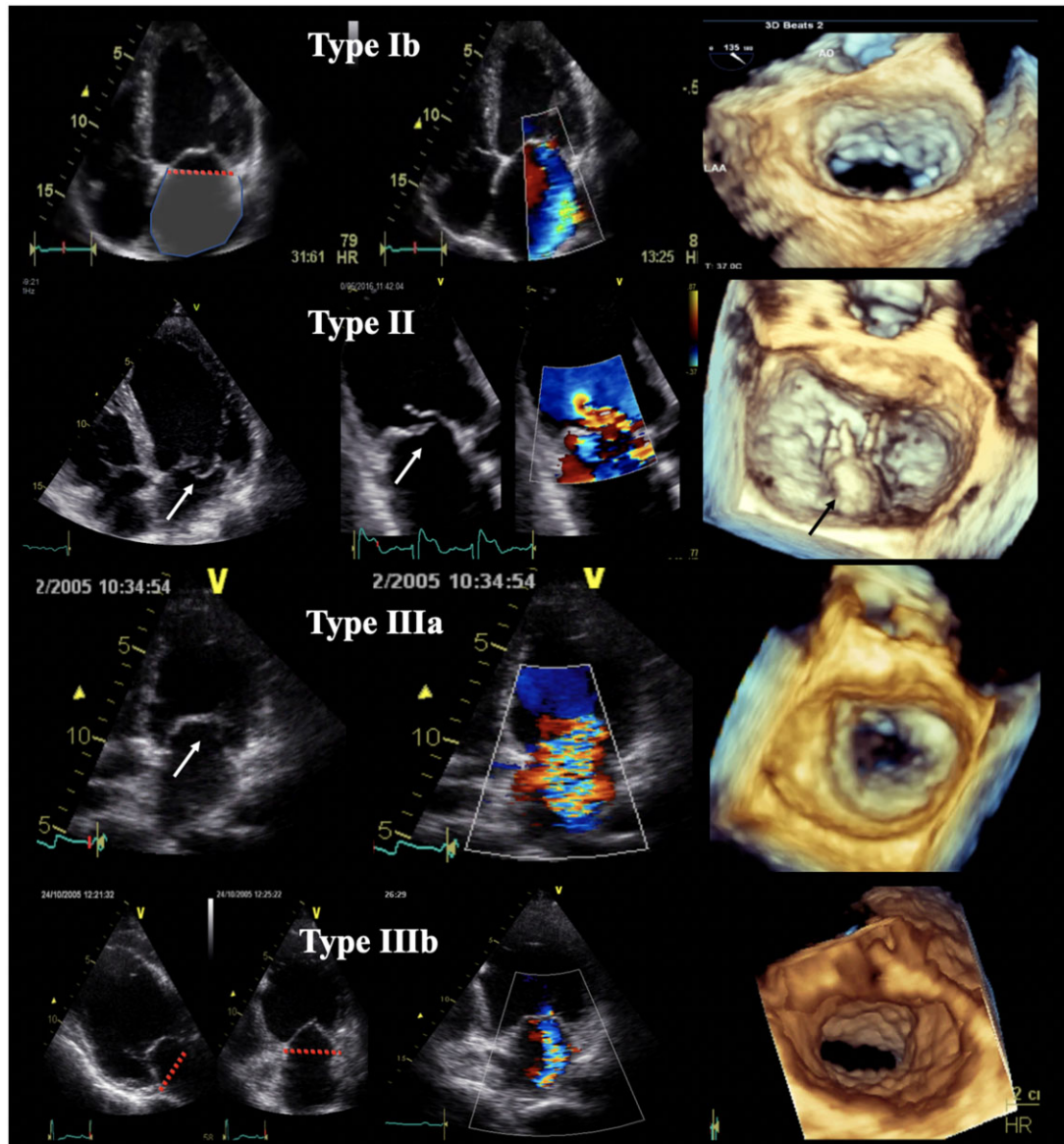
Figure 23 Mechanisms of mitral regurgitation according to the Carpentier's functional classification.

top centre of the image (12 o'clock) and the left atrial appendage to the left (9 o'clock), scallops 1 to 3 are seen from left to right. Simultaneous multi-plane imaging (such as Xplane or Multi-D) allows visualization of the MV through from the lateral to the medial aspect of the coaptation line. Practically, 3D imaging provides a comprehensive evaluation of the MV morphology (*Figure 22*) and should be used when available (TTE or TOE if necessary). This technique is superior for describing mitral pathology, especially for anterior leaflet defects and commissural involvement in degenerative disease and commissural fusion in rheumatic process.

CMR can be used as an alternative tool when TTE images are suboptimal, and TOE is not possible to assess MV morphology. MV anatomy can be imaged by acquisition of standard short-axis, two-, three-, and four-chamber long-axis views in combination with oblique long-axis cines orthogonal to the line of coaptation.[6,27] Whilst the spatial resolution of CMR is less than echo, it can still readily identify morphologic abnormalities of the mitral apparatus such as billowing, prolapse or flail segments.[69]

CCT may also be helpful in assessing MV anatomy but it is major role in is the planning of intervention where it provides accurate assessment of the mitral annulus size, the presence and extent of calcification of the leaflets and subvalvular apparatus, the angle between the anterior MV and LVOT and the presence of coronary artery disease in younger patients.[26]

Assessment of MR severity

Semi-quantitative methods

Colour flow Doppler imaging. Colour flow imaging is the most common way to assess MR severity.[70] The general assumption is that as the severity of the MR increases, the size and the extent of the jet into the LA also increases. Theoretically, larger colour jets that extend deep into the LA represent more MR than smaller thin jets that appear just beyond the mitral leaflets. However, the relation between jet size and MR severity presents a large range of variability because, in addition to regurgitation severity, the colour flow display depends on many technical and haemodynamic factors (*Figure 29*). For a similar severity, patients with increased LA pressure or with eccentric jets that hug the LA wall or in whom the LA is enlarged may exhibit smaller jets area than those with normal LA pressure and size or with central jets (*Figure 30*).[71] In acute MR, even centrally directed jets may be misleadingly small. Furthermore, as this method is a source of many errors, it must be avoided to assess MR severity. Nevertheless, the detection of a large eccentric jet adhering, swirling and reaching the posterior wall of the LA is in favour of severe MR. Conversely, small thin jets that appear just beyond the mitral leaflets usually indicate mild MR.

> **Key point: The colour flow area of the regurgitant jet has to be avoided for quantifying the severity of MR. Colour flow imaging should only be used for detecting MR. A more quantitative approach is required when more than a small central MR jet is visualized.**

Vena contracta width. The VC is the area of the jet as it leaves the regurgitant orifice; it thus reflects the ROA.[72,73] The VC is typically imaged in a view perpendicular to the commissural line (*Figure 31*). Averaging measurements over at least two–three beats and using two orthogonal planes whenever possible is a must. A VC width <3 mm indicates mild MR, while a width ≥7 mm defines severe MR.

The concept of VC assumes that the regurgitant orifice is quasi-circular. The orifice is roughly circular in primary MR; while in secondary MR, it appears to be non-circular and rather elongated along the mitral coaptation line.[74,75] Thus, the VC could appear narrow in the four-chamber view and broad in the two-chamber view. Moreover, conventional 2D colour Doppler imaging does not provide appropriate orientation of 2D scan planes to obtain an accurate cross-sectional view of the VC. If available, use of 3D echo formats such as biplane imaging to assess the VC in simultaneous orthogonal views or 3D zoom colour flow Doppler can aid in better identifying the regurgitant orifice morphology. The VC area can then be measured by manual planimetry. In case of multiple MR jets, the respective widths of the multiple VC are not additive. Such characteristics may be better appreciated and measured by 3D echocardiography. In secondary MR, an average of VC widths (four- and two-chamber views) has been shown to be better correlated with the 3D VC area. An average value ≥8 mm on 2D echo (*Figure 32*) has been reported to define severe MR for all aetiologies of MR including secondary MR.[76,77] Although prognostic data is lacking, 3D VC cross-sectional area is increasingly used with a suggested threshold for severe MR of ≥40 mm^2.[78]

> **Key point: When feasible, the measurement of VC is the best parameter to quantify MR. Intermediate VC values (3–6 mm) need confirmation by a other quantitative method, when feasible. The VC can often be obtained in eccentric jet. In case of multiple jets, the respective values of the VC width are not additive. The assessment of the VC by 3D echo can be helpful to better delineate the regurgitant orifice morphology.**

Anterograde velocity of mitral inflow—mitral to aortic VTI ratio. In the absence of mitral stenosis, the increase in transmitral flow that occurs with increasing MR severity can be detected as higher flow velocities during early diastolic filling (increased E velocity). In the absence of mitral stenosis, a peak *E* velocity >1.2 m/s suggests severe MR. Conversely, a dominant A wave (atrial contraction) basically excludes severe MR. These patterns are more applicable in patients older than 50 years or in conditions of impaired myocardial relaxation. The pulsed Doppler mitral to LVOT VTI ratio (or Doppler velocity index) is also used as an easily measured index for the quantification of isolated pure organic MR. Mitral inflow Doppler tracings are obtained at the mitral leaflet tips and LVOT just below the aortic annulus in the apical four-chamber view. A VTI ratio >1.4 suggests severe MR whereas a VTI ratio <1 is in favour of mild MR (*Figure 33*).[79]

Pulmonary venous flow. Pulsed Doppler evaluation of pulmonary venous flow pattern is another aid for grading the severity of MR (*Figure 33*).[80] In normal individuals, a positive systolic wave (S) followed by a smaller diastolic wave (D) is classically seen in the absence of diastolic dysfunction. With increasing severity of MR, there is a decrease of the S wave velocity. In severe MR, the S wave becomes frankly reversed. As unilateral pulmonary flow reversal can occur at the site of eccentric MR jets if the jet is directed into the sampled vein, sampling through all pulmonary veins is required, especially during TOE. Although evaluation of right upper pulmonary flow can often be obtained using TTE, evaluation is best performed using TOE with the pulsed Doppler sample placed about 1 cm deep into the pulmonary vein. Atrial fibrillation and elevated LA pressure from any cause can blunt forward systolic pulmonary vein flow. Therefore, blunting of pulmonary venous flow lacks of specificity for the diagnosis of severe MR, while systolic pulmonary flow reversal is specific for severe MR.[1–3]

> **Key point: Both the pulsed Doppler mitral to aortic VTI ratio and the systolic pulmonary flow reversal are specific for severe MR. They represent the strongest corroborating parameters for evaluating MR severity.**

Continuous wave Doppler of MR jet

Peak MR jet velocities by CW Doppler typically range between 4 and 6 m/s. This reflects the high systolic pressure gradient between the left ventricle and left atrium. The velocity itself does not provide useful information about the severity of MR. Conversely, the signal

Table 9   Pathophysiological classification of MR

|	Leaflet structure	Pathophysiology	Aetiology	Imaging	Transcatheter treatment
Primary	• Abnormal	• Lack of leaflet coaptation due to intrinsic changes, excessive mobility, or perforation	• Myxomatous disease • Rheumatic • Endocarditis • Congenital • Toxic • Ischaemic papillary muscle fibrosis/ellongation	• According to the aetiology • Description of the aetiology, lesions and dysfunction	• Leaflet devices • Percutaneous TV replacement
Secondary A. **Atrial**	• Normal	LA enlargement and dysfunction leading to significant isolated annulus dilation; LV often normal	• Atrial fibrillation/flutter	• Severe LA dilatation/remodelling • LV basal diameter may appear abnormal, despite normal LV volume • Leaflet tethering is absent or minimal	
B. **Ventricular**	• Considered normal	Global LV enlargement/dysfunction leading to significant leaflet tethering and annulus dilation	Previous large anterior myocardial scar or multiple infarction	• Mostly symmetric tethering, LV global remodelling/dysfunction, annular dilation/dysfunction	• Leaflet devices • Percutaneous TV replacement
		Regional LV enlargement/dysfunction leading to significant leaflet tethering and annulus dilation	• Non-ischaemic dilated cardiomyopathy	• Mostly symmetric tethering, annular dilation/dysfunction	
		Conduction disorders (left bundle branch block/pacemaker-induced dyssynchrony)	Previous infero-posterior myocardial infarction	• Asymmetric tethering due to local/regional LV remodelling, and some degree of annular dilation/dysfunction	• Leaflet devices • Percutaneous TV replacement
			Papillary muscles dyssynchrony	• Dyssynchrony between papillary muscles and wall motion	• Cardiac resynchronisation therapy
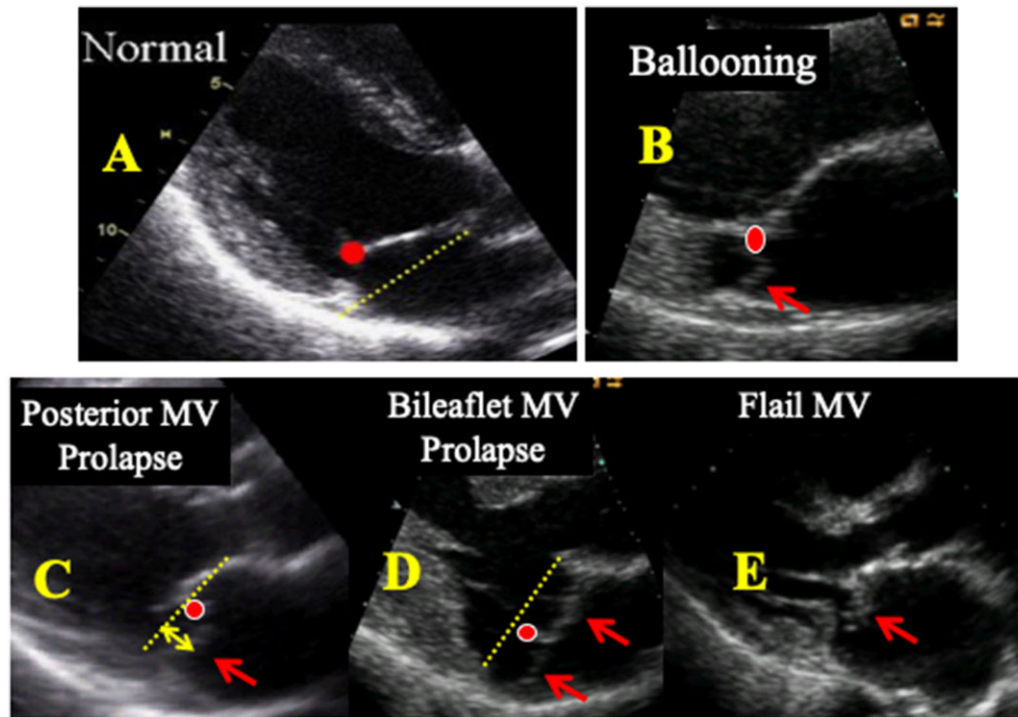
Figure 24 (*A*) In normal mitral valve, the coaptation (red point) occurs beyond the mitral annular plane (line). (*B*) Billowing mitral valve is observed when a part of the mitral valve body protrudes into the left atrium (arrow). (*C* and *D*) Mitral valve prolapse is defined as abnormal systolic displacement of 1 (*C*: posterior prolapse) or both leaflets into the left atrium below the annular (*D*: bileaflet prolapse). (*E*) Flail of the anterior leaflet (arrow).
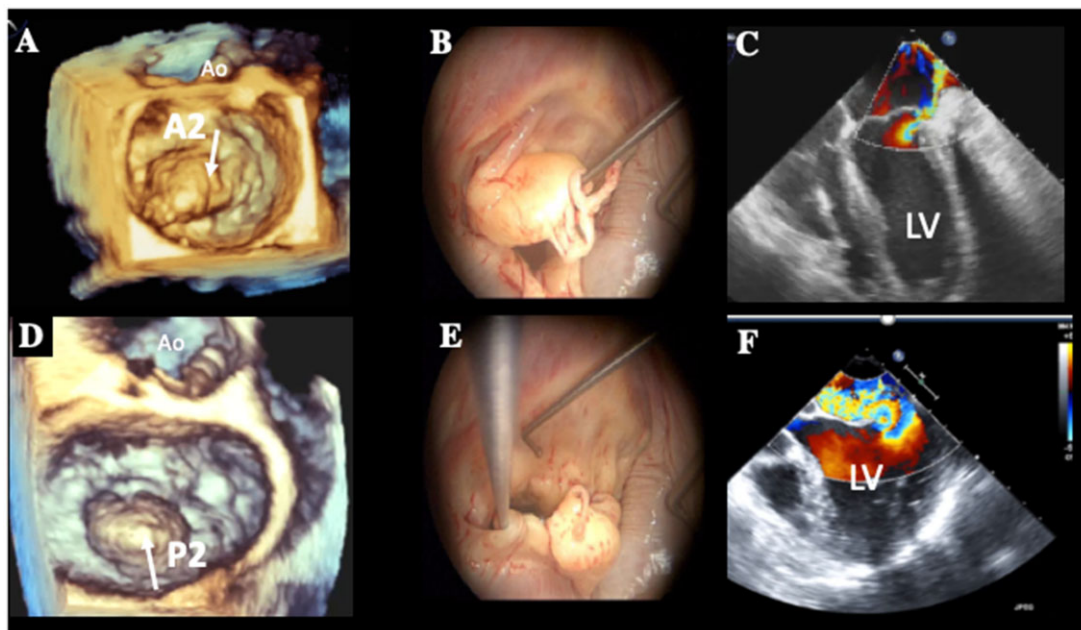
Figure 25 Examples of anterior (top panels) and posterior prolapses (bottom panels). (*A*) Flail of A2 (arrow) with (*B*) the corresponding intraoperative image and (*C*) the colour Doppler showing the direction of the jet towards the lateral wall of the left atrium. (*D*) Flail of P2 (arrow) with (*E*) the corresponding intraoperative image and (*F*) the colour Doppler showing the direction of the jet towards the interatrial septum.

intensity (jet density) of the CW envelope of the MR jet can be a qualitative guide to MR severity. A dense MR signal with a full envelope indicates more severe MR than a faint signal (*Figure 33*). The CW Doppler envelope may be truncated (notched) with a triangular contour and an early peak velocity (blunt). This indicates elevated LA pressure or a prominent regurgitant pressure wave in the LA due to severe MR. In eccentric MR, it may be difficult to record the full CW envelope of the jet because of its eccentricity, while the signal intensity shows dense features.[1–3]

> **Key point: The CW Doppler density of the MR jet is a qualitative parameter of MR severity.**

Quantitative assessment

Anatomic regurgitant orifice area. The AROA may be measured directly by planimetry using 2D/3D echocardiography, CT or CMR. Cutoffs of severity are, however, less well defined than for EROA and its clinical use remains limited.

The proximal isovelocity surface area method. The flow convergence method is the most valuable quantitative approach whenever feasible[81] (*Figure 34*). The apical four-chamber view is classically used for optimal visualization of the PISA. However, the parasternal long- or short-axis view is often useful for visualization of the PISA in case of anterior MV prolapse. The area of interest is optimized by lowering imaging depth and reducing the Nyquist limit to approximately 15–40 cm/s. The radius of the PISA is measured at mid-systole using the first aliasing from a single-frame image. R Vol and EROA are obtained using the standard formulas (*Figure 35*). Qualitatively, the presence of flow convergence at a Nyquist limit of 50–60 cm/s should alert to the presence of severe MR.[1–3]

The PISA method faces several advantages and limitations (*Figures 36–39*).[1–3,81] Colour M-mode is important to assess the variation of MR flow and the related PISA during systole (*Figure 36*). The PISA radius is most frequently constant in patients with rheumatic MR. It frequently increases progressively with a maximum during the second half of systole in patients with MV prolapse. In the presence of secondary MR, there is a dynamic variation of ROA with early and late systolic peaks and a mid-systolic decrease. These changes reflect the phasic variation in transmitral pressure that acts to close the mitral leaflets more effectively when pressure reaches its peak in mid-systole.[82] The PISA method assumes hemispheric symmetry of the velocity distribution proximal to the circular regurgitant lesion, which may not hold for eccentric jets, multiple jets, or complex or elliptical regurgitant orifices. Practically, the geometry of the PISA varies, depending on the shape of the orifice and MV leaflets surrounding the orifice. In secondary MR, the PISA might look like an ellipsoidal shape and two separate MR jets originating from the medial and lateral sides of the coaptation line can be observed on 2D echo. When the shape of the flow convergence zone is not a hemisphere, the PISA method may underestimate the degree of secondary MR, particularly when the ratio of long-axis length to short-axis length of the 3D regurgitant orifice is >1.5.[83] When the EROA is calculated with the hemispheric assumption (using the vertical PISA), the horizontal length of PISA is ignored. In primary MR, the shape of the PISA is rounder, which
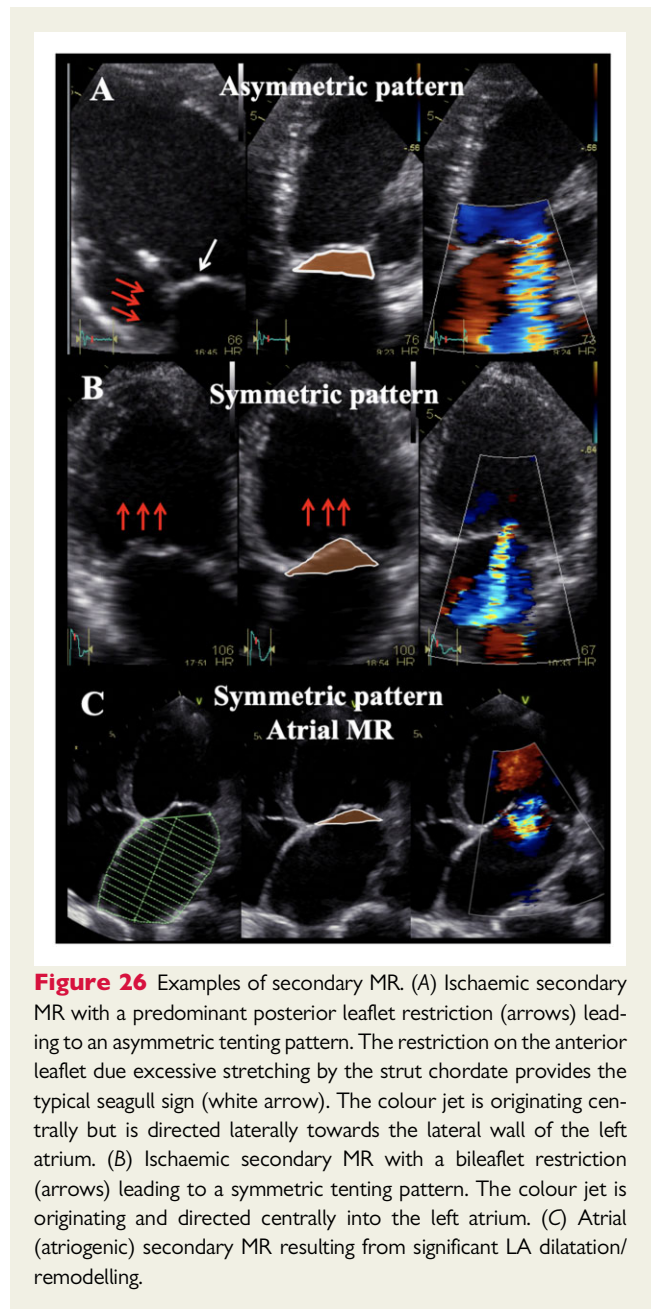
Figure 26 Examples of secondary MR. (*A*) Ischaemic secondary MR with a predominant posterior leaflet restriction (arrows) leading to an asymmetric tenting pattern. The restriction on the anterior leaflet due excessive stretching by the strut chordate provides the typical seagull sign (white arrow). The colour jet is originating centrally but is directed laterally towards the lateral wall of the left atrium. (*B*) Ischaemic secondary MR with a bileaflet restriction (arrows) leading to a symmetric tenting pattern. The colour jet is originating and directed centrally into the left atrium. (*C*) Atrial (atriogenic) secondary MR resulting from significant LA dilatation/remodelling.

minimizes the risk of EROA underestimation (*Figure 39A*). These findings could, in part, explain why the threshold used to define a severe secondary MR is inferior to that used for primary MR. EROA is the most robust parameter as it represents a marker of lesion severity. A large EROA can lead to a large regurgitant kinetic energy (large RVol) but also to more potential energy with low RVol in case of high LA pressure. The R Vol may also be lower in low flow states, which is often present in patients with secondary MR. In such conditions, a moderate R Vol may correspond to a severe RF.

In secondary MR, the EROA is expected to increase in proportion to increasing LV size as a result of leaflet tethering and annular dilatation. In proportionate MR, the estimated degree of MR is proportionate to the size of the left ventricle. In disproportionate MR, the degree of MR is unexpectedly large compared with the LV size, and

so the symptoms are driven by MR and the outcome is improved after transcatheter MV repair.[84–86] Grading the severity of secondary MR should be performed under optimal medical therapy.

Grading of severity of MR using semi-quantitative and quantitative parameters classifies regurgitation in three main classes: mild, moderate, or severe, and sub-classifies the moderate regurgitation class into 'mild-to-moderate' (EROA of 20–29 mm or a R Vol of 30–44 mL) and 'moderate-to-severe' (EROA of 30–39 mm^2 or a R Vol of 45–59 mL). The mild-to-moderate sub-class is also labelled as 'Moderate' or 'Grade 2' or '2+' and the moderate-to-severe sub-class also labelled as 'moderately severe' or 'Grade 3' or '3+' in grading schemes of other medical societies or group of experts.[1–3,5] Quantitatively, MR is considered severe if EROA is ≥40 mm^2 and/or R Vol ≥60 mL. The cut-off values of EROA and R Vol at which MR has a significant impact on outcomes may be lower in secondary MR, especially in case of an elliptical regurgitant orifice or in low flow conditions (EROA ≥30 mm^2 and/or R Vol ≥45 mL). In secondary MR, even lower thresholds may be associated with poor prognosis (EROA ≥20 mm^2 and/or R Vol ≥30 mL)[87,88] but these criteria are not sufficient to refer patients for MV intervention.[84–86] In such conditions it is preferable to put more weight on the RF than of EROA or R Vol to grade MR severity. The RF is calculated by diving the R Vol by the total LV stroke volume. The total stroke volume can be calculated as the difference between LV end-diastolic volume minus LV end-systolic volume measured by 2D echocardiography or preferably by 3D echocardiography. The total LV stroke volume can also be calculated as the sum of R Vol and systemic stroke volume [obtained by multiplying the LVOT area - $\pi d^2/4 = 0.785\ d^2$, where d is the LVOT diameter—by LVOT time-velocity integral (TVI)]. A RF ≥50% indicates severe MR, regardless of the EROA or R Vol.

> **Key point: When feasible, the PISA method is highly valuable to quantitate the severity of MR. It can be used in both central and eccentric jets. An EROA ≥40 mm^2 and/or a R Vol ≥60 mL indicates severe MR. In secondary MR, the cut-offs of EROA and R Vol, beyond which MR portends a significant impact on outcomes and thus requires intervention, may be lower (EROA ≥30 mm^2 and/or R Vol ≥45 mL; i.e. consistent with moderate-to-severe MR but with generally RF ≥ 50%, consistent with severe MR), especially in case of an elliptical regurgitant orifice and/or in low flow conditions.**

Doppler volumetric method. Quantitative PW Doppler method can be used as an additive or alternative method, especially when the PISA and the VC are not accurate or not applicable (*Figure 40*). This approach is time consuming and is associated with several drawbacks.[1–4] Briefly, mitral R Vol is obtained by calculating the difference between the total stroke volume (product of mitral annulus area—$\pi d^2/4 = 0.785\ d^2$, where d is the mitral annulus diameter—and mitral inflow TVI) and systemic stroke volume (obtained by multiplying the LVOT area—$\pi d^2/4 = 0.785\ d^2$, where d is the LVOT diameter—by LVOT TVI). This calculation is inaccurate and so should not be applied in the presence of significant AR.

> **Key point: The Doppler volumetric method is a time-consuming approach and should not considered as a first line method to quantify MR severity. This method can however be used when PISA is not feasible or uncertain.**

CMR quantification. CMR is the alternative method of choice to quantify the R Vol and RF. The preferred approach relies on the indirect calculation of the R Vol from the difference between LV total (using planimetry of short-axis cine images) and forward stroke volume across the aortic valve (using phase-contrast velocity mapping) (*Figure 34*). The RF is calculated by dividing the R Vol by the LV stroke volume. This method is highly reproducible and considered robust as it is not affected by the direction or eccentricity of the regurgitant jet, is not affected by the presence of AR and makes no haemodynamic or LV geometry assumptions. As a second choice, quantification of the R Vol can be obtained by comparing LV and RV stroke volumes. The phase-contrast technique with direct assessment of flow at the level of the MV is less accurate and rarely used for this purpose due to the significant motion of the MV plane during systole.[1,89] The RF is calculated by dividing the R Vol by the LV stroke volume for the two first methods and by the mitral inflow stroke volume for the direct approach. Reference ranges for MR quantification are yet to be as firmly established as those for echocardiography. A threshold of R Vol >55 mL or RF >40% was found to be associated with progression to symptoms and need for MV surgery in patients with primary MR.[90] There are few comparative studies between echocardiography and CMR. The majority of them showed modest agreement in assessing the severity of MR, particularly in secondary MR.[91] Compared to CMR, echocardiographic grading of MR severity tends to be higher and 2D-PISA-derived R Vol larger.[92] This is because CMR calculates mitral regurgitation across systole whereas echo considers a single time point. A significant discrepancy is seen in 10–20% of patients, which requires further assessment by TOE or invasive means.[92] We propose that a CMR RF of ≥50% is considered as severe MR, with further work required to validate severity thresholds.[90]

> **Key point: Although there is only modest agreement between MR severity by CMR versus quantitative echocardiography and that large studies on prognostic value of CMR-quantitated MR are lacking, CMR is the alternative or corroborating method of choice for quantitative assessment of MR. The indirect approach by comparing ventricular stroke volume to aortic forward flow is the most reproducible with the advantage of not being affected by coexisting AR, and the direction or eccentricity of the regurgitant jet. A RF ≥50% indicates severe MR.**

Consequences of MR

The presence of severe primary MR has significant haemodynamic effects, primarily on the left ventricle and LA.[5] In acute primary MR, the left ventricle is classically not enlarged while the LVEF usually increases in response to the increased preload. In the chronic compensated phase (the patient could be asymptomatic), the forward
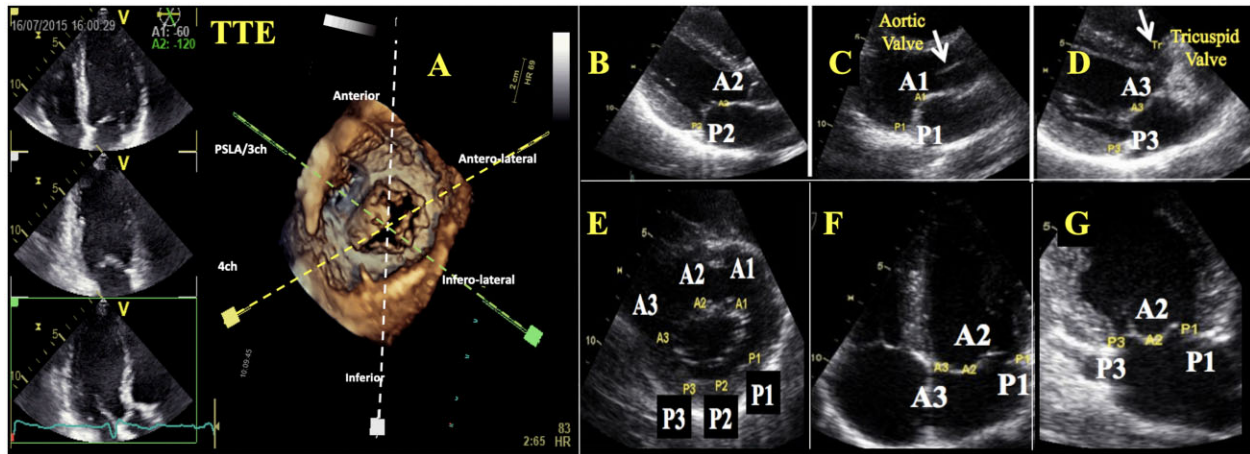
Figure 27 Mitral valvular segmentation analysis with 2D TTE. (*A*) 3D TTE cut planes across the mitral valve. (*B*) 2D TTE parasternal long-axis view depicting A2 and P2; (*C*) A1 and P1 (tilting of the probe towards the aortic valve); (*D*) A3 and P3 [tilting of the probe towards the tricuspid (Tr) valve]; (*E*) 2D TTE parasternal short-axis view depicting each scallop; (*F*) four-chamber view depicting A3, A2, and P1; (*G*) bicommissural view.
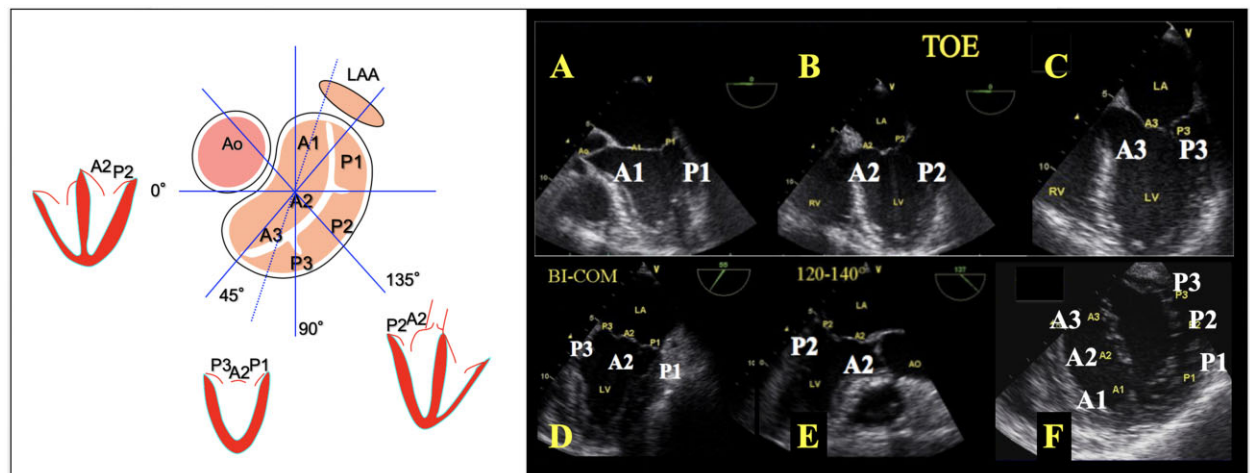

Figure 28 Mitral valvular segmentation analysis with 2D TOE. (*A–C*) Views obtained at O°: (*A*) five-chamber view depicting A1 and P1, four-chamber view depicting A2 and P2; downward four-chamber view depicting A3 and P3; (*D*) bicommissural view; (*E*) view at 120° visualizing A2 and P2; and (*F*) transgastric view at 0° depicting each scallop.

stroke volume is maintained through an increase in LVEF. Such patients typically have LVEF >65%. In this phase, the LA remodels and dilates but the LA pressure is often normal. In the chronic de-compensated phase (the patients could still be asymptomatic or may fail to recognize deterioration in their clinical status), the forward stroke volume decreases and the LA pressure increases significantly. The LV contractility can thus decrease silently and irreversibly. However, the LVEF may still be in the low normal range despite the presence of significant myocardial dysfunction. Hence, dilatation is sensitive for chronic significant MR, while normal size almost excludes severe chronic MR. However, dilatation can be observed in other conditions or may be absent in acute severe MR and is,

therefore, a non-specific finding. Three-dimensional echocardiog-raphy and CMR allows more accurate evaluation of LV volumes and EF than 2D. Strain imaging (GLS < -18%) may be helpful in identifying subclinical LV dysfunction in the setting of serial echocardiograms and may help determine appropriate follow-up intervals or timing for intervention.[93] The excess regurgitant blood entering the LA may in-duce a progressive LA remodelling, a rise in pulmonary arterial pres-sure and a significant tricuspid annular dilatation. Secondary MR has a different physiology, as it is the consequence of an initial ventricular/annular disease. The LV and LA dilatation are in excess to the degree of MR. The LA pressure is often elevated despite lower R Vol than in primary MR. Therefore, the assessment of LV size and systolic
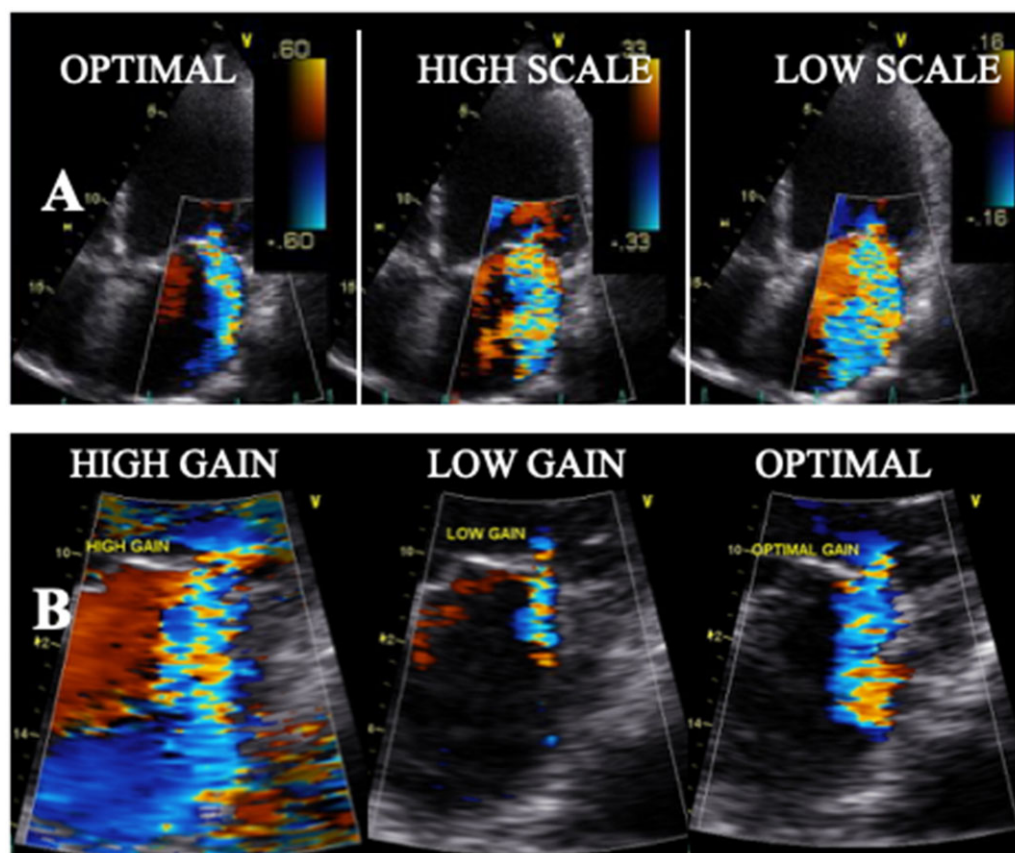
Figure 29 Effect of colour scale (*A*) and gain setting (*B*) on mitral regurgitant jet size.

function, of LA size, and pulmonary arterial pressure help identify the optimum timing of intervention. Current cut-off values used for defining the timing of intervention are based on echo results.[5] Although CMR provides the most accurate assessment of LA and LV size and function, thresholds for intervention are not yet clearly defined.

> **Key point: When MR is more than mild MR, providing the LV diameters, volumes and ejection fraction as well as the LA dimensions (preferably LA volume) and the pulmonary arterial systolic pressure in the final echocardiographic report is mandatory. Three-dimensional echocardiography and CMR allows more accurate evaluation of LV volumes and EF than 2D but further work to validate appropriate thresholds are required. Current cut-offs for intervention remain based on 2D echo results.**

Role of exercise echocardiography

In patients with primary MR, exercise echocardiography may provoke symptoms, and be useful to assess the SPAP response and stratify risk. Although there is less evidence, the test is also reasonable in

symptomatic patients with at least moderate MR. The increase in MR severity (≥ 1 grade), dynamic pulmonary hypertension (SPAP $\geq$ 60 mmHg),[8] the absence of contractile reserve (< 5% increase in EF or < 2% increment in GLS), and a limited RV contractile recruitment [quantified by tricuspid annular plane systolic excursion (TAPSE) <18 mm] are all parameters of poor prognosis. When MR is not severe at rest, the dataset should include colour flow Doppler (to allow off-line quantification of severity by PISA method and VC of the regurgitant jet), MR CW Doppler for quantification of severity by PISA method, TR CW Doppler for estimation of the SPAP, and LV views for global and regional systolic function evaluation. Assessment of TR velocity should also be made early during exercise since early increases in SPAP are indicators of more significant disease.

In secondary MR, exercise stress echocardiography may provide helpful information in patients with the following clinical context: when resting LV systolic function and degree of MR are disproportionate to the degree of symptoms; following recurrent and unexplained episodes of pulmonary oedema; to assess moderate MR prior already planned coronary artery bypass grafting (to identify those who may benefit from combined revascularization and MV repair); persistent PH after MV repair. Increase in MR severity (increase in EROA ≥ 13 mm^2) and dynamic pulmonary hypertension (SPAP $\geq$ 60 mmHg) are predictors of worse prognosis.[8]
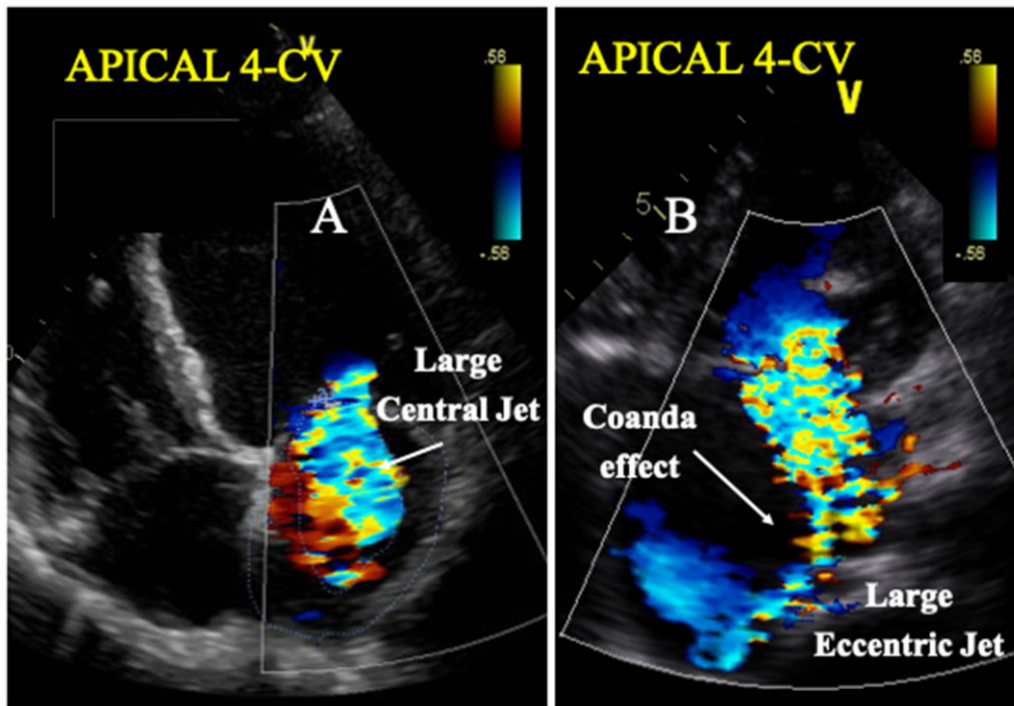
Figure 30 Visual assessment of mitral regurgitant jet using colour-flow imaging. Examples of two patients with severe mitral regurgitation (*A*) large central jet and (*B*) large eccentric jet with a clear Coanda effect. CV, four-chamber view.
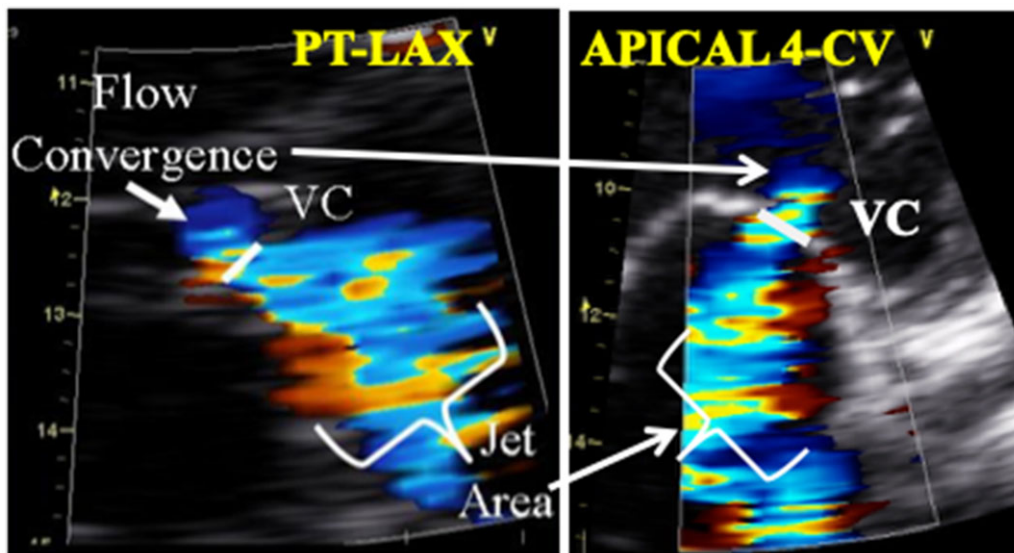
Figure 31 Semi-quantitative assessment of MR severity using the vena contracta width (VC). The three components of the regurgitant jet (flow convergence zone, vena contracta, jet turbulence) are obtained. CV, chamber view; PT-LAX, parasternal long-axis view.

Integrating indices of severity

Echocardiographic assessment of MR includes integration of data from 2D/3D imaging of the valve and ventricle as well as Doppler measures of regurgitation severity (*Table 10*; *Figure 41*). Effort should be made to quantify the degree of regurgitation, except in the presence of mild or obviously severe MR using specific signs. Both the VC
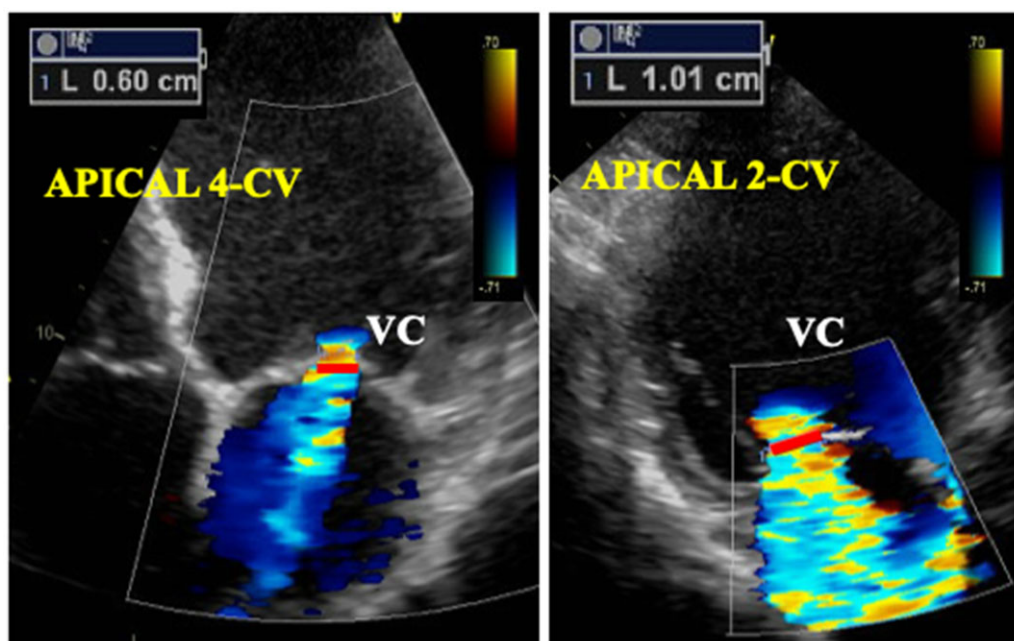
Figure 32 Semi-quantitative assessment of MR severity using the vena contracta width (VC) obtained from the apical four-chamber and two-chamber views (CV) in a patient with ischaemic functional MR. The mean vena contracta is calculated (6 + 10/2 = 8 mm).
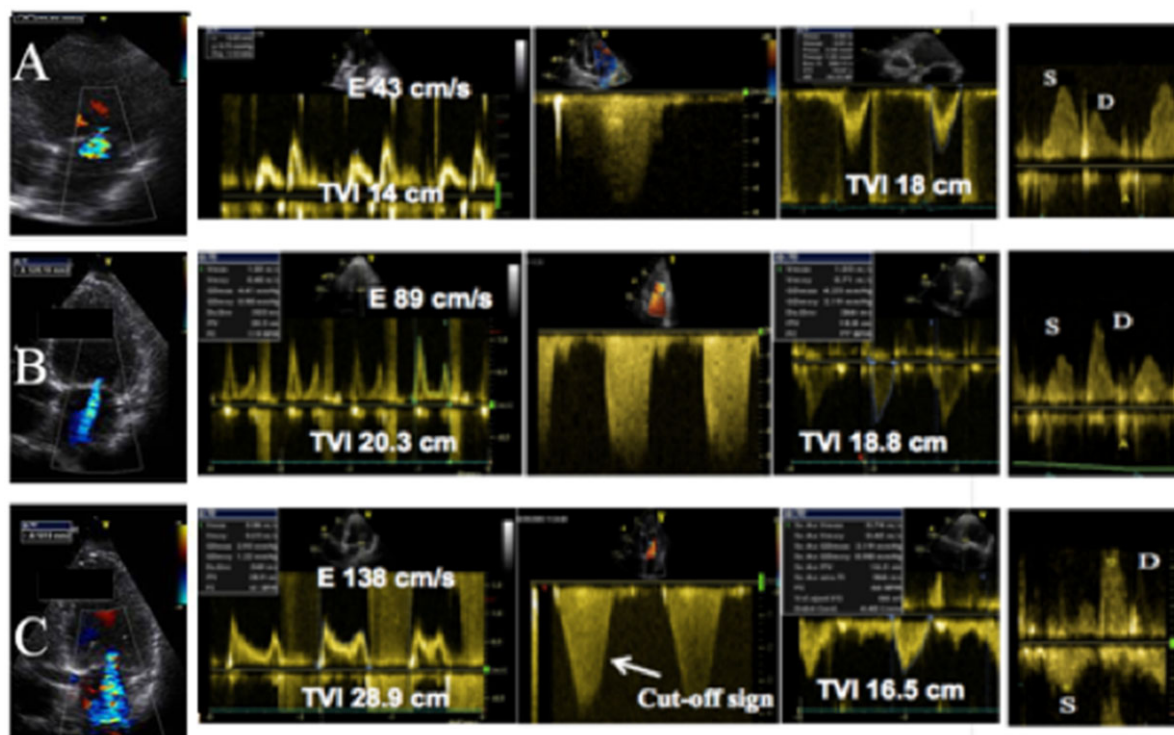
Figure 33 Three examples of various degrees of MR, mild (*A*), moderate (*B*), and severe (*C*) are provided. The regurgitant jet area (RJA) as well as the mitral E wave velocity increase with the severity of MR. In severe MR, the continuous wave Doppler signal of the regurgitant jet is truncated, tri-angular and intense. Notching of the continuous wave envelope (cut-off sign) can occur in severe MR. D, diastolic wave; Mild MR, normal pulmonary vein flow pattern; Moderate MR, blunt forward systolic pulmonary vein flow in a patient with moderate MR; S, systolic wave; Severe MR, reversed systolic pulmonary flow in a patient with severe MR; TVI, time-velocity integral.
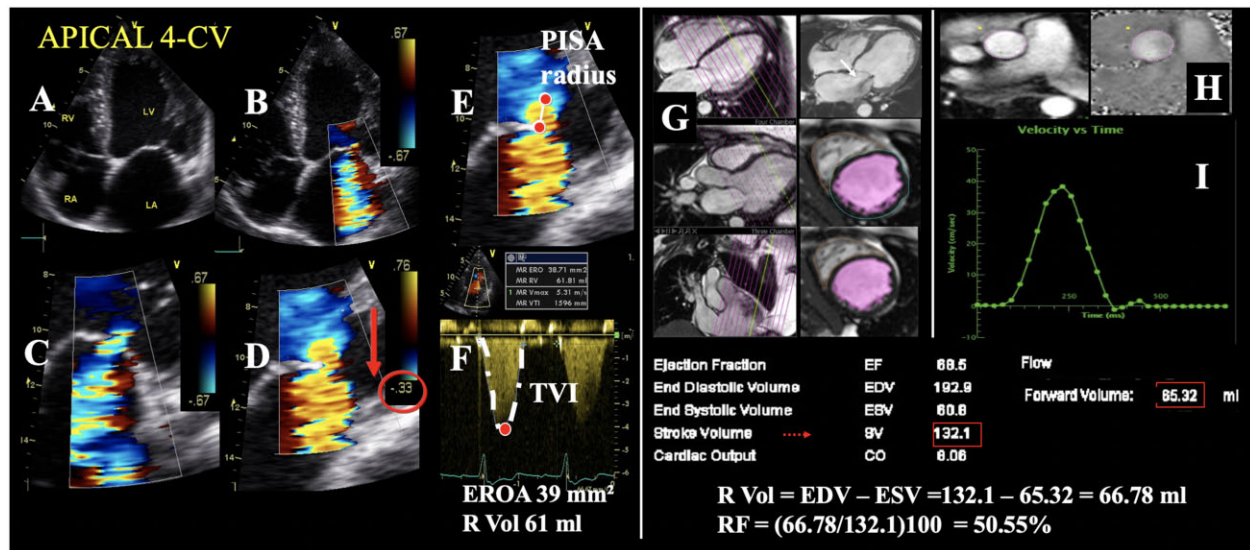
Figure 34 Quantitative assessment of MR severity using the PISA method (*A–F*) and the indirect CMR method (*G–I*). Stepwise analysis of MR. (*A*) Apical four-chamber view (CV). (*B*) Colour-flow display. (*C*) Zoom of the selected zone. (*D*) Downward shift of zero baseline to obtain a hemispheric PISA. (*E*) Measure of the PISA radius using the first aliasing. (*F*) Continuous wave Doppler of MR jet allowing calculation the effective regurgitant orifice area (EROA) and regurgitant volume (R Vol). TVI, time-velocity integral. *CMR*: White arrow: extent of the signal loss on cine CMR. (*G*) Assessment of LV volumes using cine images; (*H*) phase-contrast velocity mapping at the aortic root level; and (*I*) flow-time curves computing forward aortic flow.

width and the PISA method are valuable. Adjunctive parameters help to consolidate about the severity of MR. CMR is the alternative method of choice and should be largely used when the results of echocardiography (TEE and TOE) are unsatisfactory or inconclusive or when there is discrepancy between MR severity and clinical findings. These parameters should be interpreted according the chronicity of MR and the LV remodelling. CMR may provide additional information about the mechanism of MR, myocardial viability, and the presence underlying cardiomyopathic disease. CCT scan can be helpful in specific circumstances to complement echocardiography, especially in the preprocedural intervention planning (presence and extent of MV calcifications, mitral annular size assessment, and presence of coronary artery disease).

Intervention guidance

Several echocardiographic parameters can help to identify patients at risk of treatment failure. In primary MR, some predictors of unsuccessful repair have been reported: the presence of a large central regurgitant jet, severe annular dilatation (>50 mm), involvement of ≥3 scallops especially if the anterior leaflet is involved, and extensive valve calcification (*Table 11*).[94] Moreover, lack of valve tissue is also an important predictor of unsuccessful repair both in rheumatic valve disease and in patients who have had infective endocarditis with large valve perforation. The development of systolic anterior motion (SAM) of the MV with LVOT obstruction after MV repair can lead to severe haemodynamic instability. Factors predisposing patients to SAM are the presence of a myxomatous MV with redundant leaflets (excessive anterior leaflet tissue), a non-dilated hyperdynamic LV,

and a short distance between the MV coaptation point and the ventricular septum after repair.

In secondary ischaemic MR, patients with a mitral diastolic annulus diameter ≥37 mm, a systolic tenting area ≥1.6 cm^2 and a severe functional ischaemic MR could have a 50% probability of recurrence of regurgitation after MV repair.[95] Pre-operatively (TTE), several parameters are associated with an increased risk of MV repair failure (*Table 12*)[82] (*Figure 42*).

In case of transcatheter MV edge-to-edge-repair several unfavourable morphological characteristics can be identified by echocardiography (*Table 13*).[5,96]

> **Key point: Imaging report should provide information regarding the likelihood of surgical or transcatheter MV repair.**

Suggested follow-up for MR

Moderate primary MR requires clinical examination every year and an echocardiogram every 1–2 years. In patients with severe primary MR, clinical and echocardiographic assessment is needed every 6 months. Progression of MR severity is frequent with important individual differences in the progression rate. The average yearly increase in R Vol is 7.5 mL and 5.9 mm^2 in EROA.[81] In addition, the progression of other parameters needs to be assessed: the increase in annular size, the development of a flail leaflet, the evolution of LV end-systolic dimension, LVEF, LA area or volume, pulmonary systolic
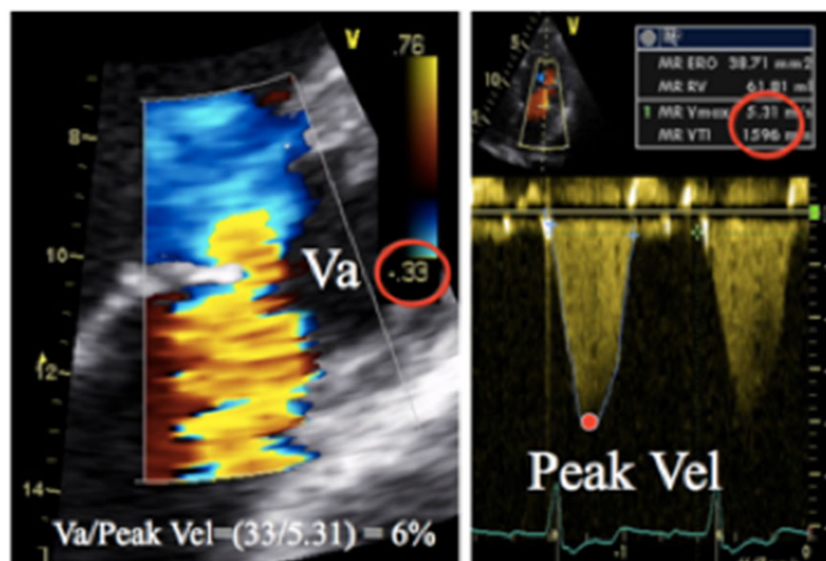
$$EROA = Flow/Peak\ velocity$$
$$EROA = (2\pi r^2 \times Va)/Peak\ velocity$$

$$EROA = (2 \times 3.14 \times 1 \times 33)/531$$
$$EROA = 207/531 = 0.39\ cm^2$$

$$R\ Vol = EROA \times TVI$$
$$R\ Vol = 0.39\ cm^2 \times 158\ cm = 61mL$$

Figure 35 Quantification of MR using the PISA method. To avoid the underestimation of the regurgitant volume the ratio of the aliasing velocity (Va) to peak orifice velocity (vel) is maintained less than 10%.

arterial pressure, exercise capacity, and occurrence of atrial arrhythmias.

Tricuspid regurgitation

TR is a common finding.[97] Since it is mostly asymptomatic and not easily audible on physical examination, it is frequently only diagnosed by echocardiography performed for other indications. Although a mild degree of TR is frequent and benign, moderate and severe TR are associated with poor prognosis.[98,99] It should be stressed that TR is most often seen in patients with multiple valvular disease, especially aortic or MV disease.

Anatomy and function of the tricuspid valve

The TV complex is similar to the MV but has greater variability.[100] It consists of the annulus, leaflets, RV, papillary muscles, and chordae tendinae. The TV is located between the right atrium and the right ventricle and is placed in a slightly more apical position than the MV.[101] The TV has three leaflets of unequal size: the anterior leaflet is usually the largest and extends from the infundibular region anteriorly to the inferolateral wall posteriorly; the septal leaflet extends from the interventricular septum to the posterior ventricular border; the posterior leaflet attaches along the posterior margin of the annulus from the septum to the inferolateral wall. The insertion of the septal leaflet of the TV is characteristically apical relative to the septal insertion of the anterior mitral leaflet. Normal leaflet thickness is <1 mm in diastole and the degree of leaflet overlap at the point of coaptation should be >5 mm for a competent valve.[100]

Aetiology and mechanisms

The most common cause of TR is not a primary TV disease (organic TR) but rather impaired valve coaptation (secondary or functional TR) caused by dilatation of the right ventricle and/or of the tricuspid annulus due to left-sided heart valve diseases, pulmonary hypertension, congenital heart defects, atrial fibrillation and cardiomyopathy.[102] *Mixed TR* is characterized by a combination of both primary and secondary aetiologies.

The Carpentier's classification remains the most common used functional classification in TR: Type I: (i) primary (Ia): leaflet perforation (infective endocarditis, trauma caused by catheter or lead) or
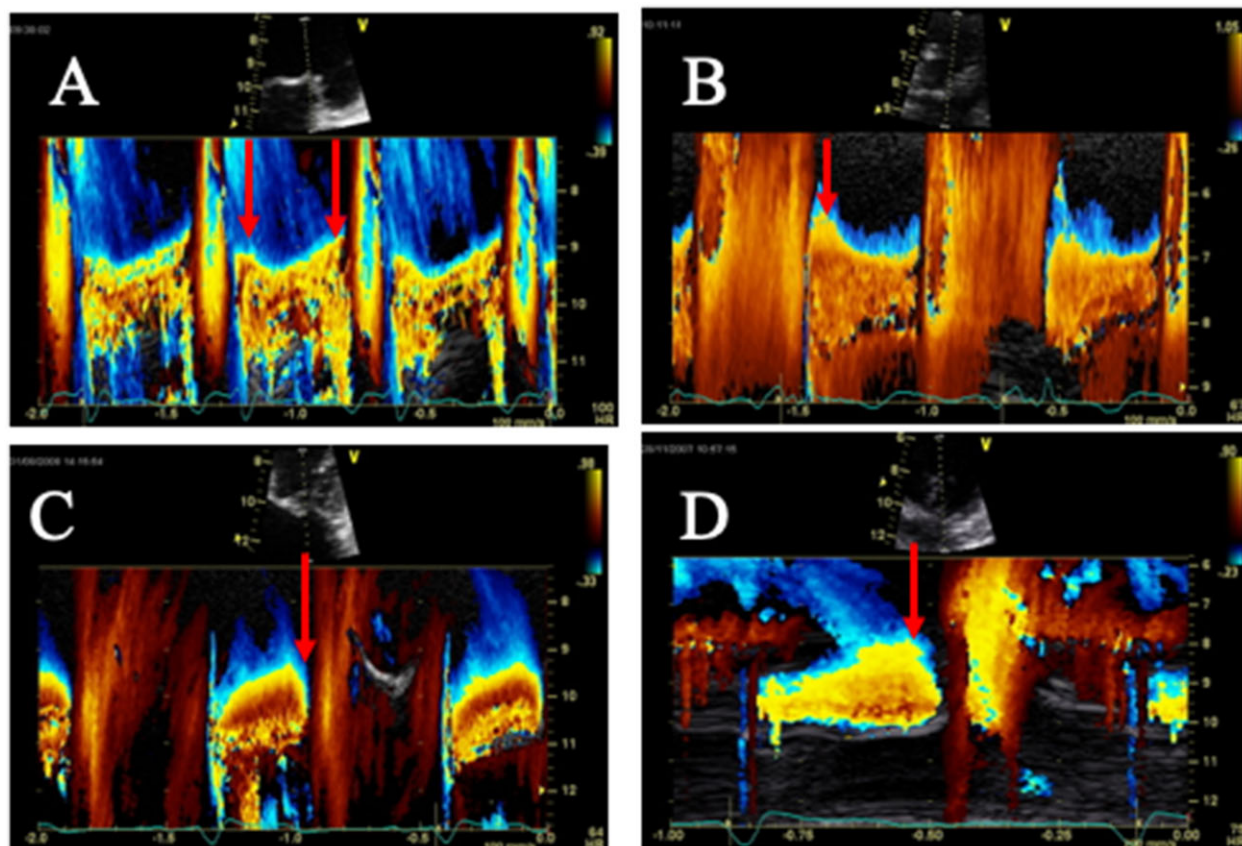
Figure 36 Four examples of flow convergence zone changes during systole using colour M-Mode. (*A* and *B*) Functional MR (*A*: early and late peaks and mid-systolic decreases; *B*: early systolic peak), *C*: rheumatic MR with an end-systolic decrease in flow convergence zone, and *D*: M mitral valve prolaspe (late systolic enhancement).

(ii) atrial secondary (Ib) caused by tricuspid annular dilatation; Type II (primary): prolapse of one or more leaflets (TV prolapse); and Type III: restricted motion in diastole/systole (IIIa, primary) as the consequence of rheumatic disease, significant calcifications, toxic valvulopathy, or in systole (IIIb) as in ventricular secondary TR (*Figure 43*). Types Ib and IIIb are, by far, the most frequent aetiologies of TR. For the selection of the most appropriate device for TV transcatheter procedures, a pathophysiological classification that accounts for the aetiology of the TV disorder can be used (*Table 14*).

A variety of primary disease processes can affect the TV complex directly and lead to valve incompetence: infective endocarditis, congenital disease like Ebstein anomaly or atrioventricular canal, rheumatic fever (commissural fusion, shortening and retraction of one or more leaflets and of the chordae tendinea), carcinoid syndrome (lack of commissural fusion, thickened valve with markedly restricted motion during cardiac cycle), endomyocardial fibrosis, myxomatous degeneration of the TV leading to prolapse or flail TV, penetrating and non-penetrating trauma, and iatrogenic damages during cardiac surgery, biopsies, and catheter/pacemaker placement in right heart chambers.[103]

Tricuspid annular disjunction is the abnormal atrial displacement of the hinge points of the TV away from the ventricular myocardium, which may cause TR.[104]

In 'ventricular' secondary TR (Carpentier), the progressive remodelling of the RV cavity leads to tricuspid annular dilatation, papillary muscle displacement, and tethering of the leaflets, resulting in secondary TR. Atrial (atriogenic) secondary TR, typically associated with atrial fibrillation (but can also be seen in its absence, namely idiopathic atrial TR), results from significant isolated RA dilatation/remodelling associated with progressive lack of TV coaptation.[105] Here, the right ventricle may be non-dilated, with normal papillary muscle geometry and no evidence of leaflet tethering or tenting.[106] As for secondary MR, secondary TR begets TR. Indeed, TR itself leads to further RV dilation and dysfunction, right atrial enlargement, more tricuspid annular dilatation and tethering, and worsening TR. With increasing TR, the RV dilates and eventually fails, causing increased RV diastolic pressure and, in advanced situations a shift of the inter-ventricular septum towards the left ventricle. Such ventricular interdependence might reduce the LV cavity size (pure compression), causing restricted LV filling and increased LV diastolic and pulmonary artery pressure. The tricuspid annular dilatation, the loss of its contraction and the increased tethering are probably the most important factors in the development of TR. Indeed, the tricuspid annulus is not saddle-shaped anymore; it becomes flat, planar, and distorted.[107]

Leads of cardiac implantable electronic device can interfere with the TV apparatus by impinging upon a leaflet, adhering to a leaflet,
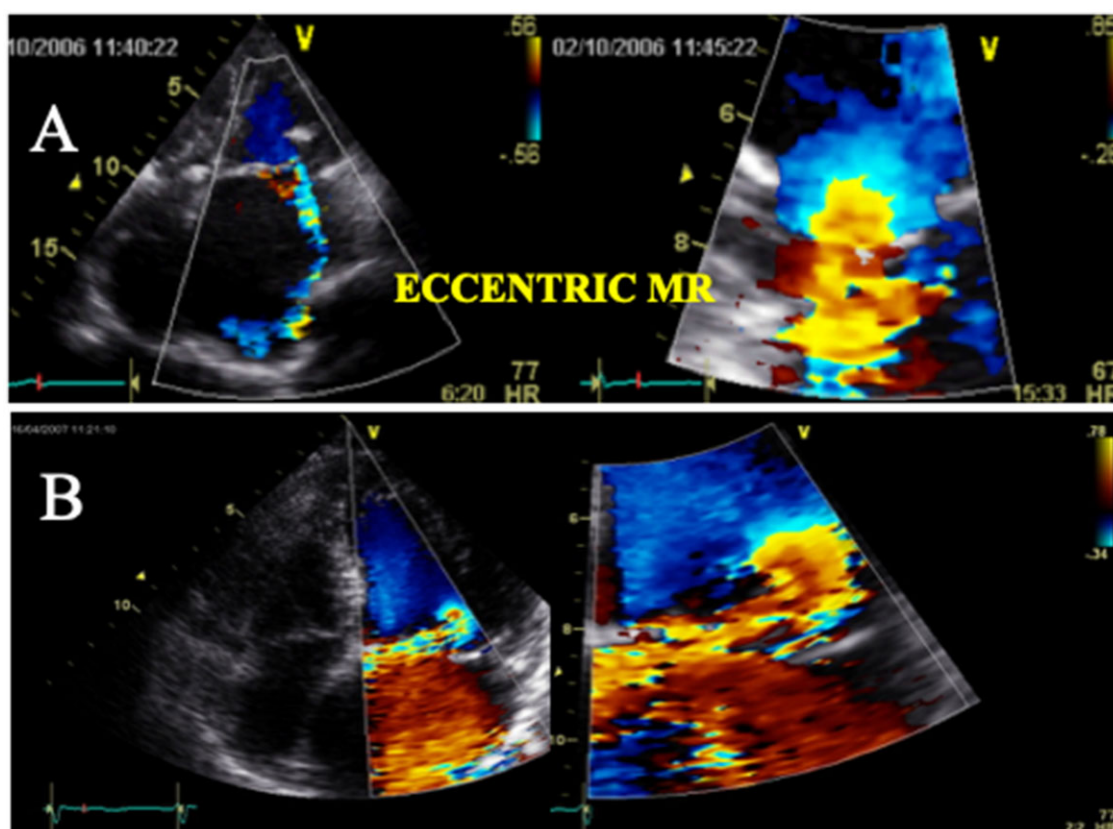
Figure 37 Examples of eccentric MR that can still be perfectly assessed by using the PISA method.

interfering with the subvalvular apparatus, perforating/lacerating a leaflet, and avulsion of a leaflet, which may uncommonly happen during lead extraction (*Figure 44*).[108]

Imaging evaluation in TR

Tricuspid valve morphology

Echocardiography is the first line imaging to assess the TV morphology, the presence, severity and mechanism of TR and its consequences on right ventricle. The four main TTE views allowing the TV visualization are the parasternal (long-axis view of RV inflow, short-axis view at the level of the aortic valve), the apical four-chamber and the subcostal views (*Figure 45*). RV focused apical four-chamber view is preferable for TV and RV dimension assessment. TOE for the TV is typically more difficult than for the MV. TOE is possible with the four-chamber view at 0° in the basal transoesophageal and oesogastric junction planes. TOE is of interest for the diagnosis of endocarditis, venous catheters, and pacemakers lead infection, and visualization of traumatic rupture of the TV. However, it is rarely possible to visualize by 2D echo the three leaflets simultaneously (usually from a modified subcostal view). Therefore, the designation of individual leaflets of the TV should be done with caution unless a simultaneous view of all three cusps is obtained.[109,110] On short-axis, the leaflet adjacent to the aorta is either the septal or anterior leaflet, and the leaflet adjacent to the RV free wall is usually the posterior leaflet. In the

apical four-chamber view, there is more certainty, with the anterior leaflet on the free wall and the septal leaflet adjacent to the septum.

Three-dimensional echo has become an essential tool to evaluate TV morphology; it allows simultaneous visualization of the three leaflets moving during the cardiac cycle, their commissures and their attachment to the tricuspid annulus[103,107,110] (*Figure 45*). Multi-slice and/or transversal cut planes using volume rendering display are used to ensure that the whole TV and annulus are included in the dataset throughout the cardiac cycle. Transversal cut planes from the RV or the RA perspective are used to assess the anatomy of the leaflets and the TVA, whilst longitudinal cut planes are used to assess the papillary muscles and the chordae. A standardized imaging display of the transversal cut planes is preferred, with the LVOT and septal leaflet at 12 o'clock. With the 'en face view', 3D echo allows precise localization of defects such as prolapse, vegetation and perforation. Three-dimensional echo is superior to 2D echo for the assessment of the tricuspid annulus dimension, since the latter makes the geometric assumption that the annulus is circular, and thus systematically underestimates tricuspid annulus dimensions.[111]

CMR can be used as an alternative tool when echocardiography is suboptimal to assess TV morphology. Despite its lower spatial resolution than echocardiography, CMR can image in any planes and can effectively assess the morphology of TV in most patients.[12,14]

CCT may also be helpful in assessing TV anatomy, particularly in evaluating the size of the tricuspid annulus and the presence and

extent of calcification of the TV and subvalvular apparatus to aid pre-procedural planning.[26]

In secondary TR, a tenting area, measured in mid-systole from the apical four-chamber view, >1 cm^2 has been shown to be associated with severe TR.[112] The tricuspid annulus forms a non-planar structure with an elliptical saddle-shaped pattern, having two high points (oriented superiorly towards the right atrium) and two low points (oriented inferiorly towards the right ventricle that is best seen in mid-systole).[113] Normal TV annulus diameter in adults is 28 ± 5 mm in the four-chamber view. Significant tricuspid annular dilatation is defined by a diastolic diameter of ≥21 mm/m^2 (≥40 mm). The normal contraction (decrease in annular area in systole) of the tricuspid annulus is 25%. These cut-offs are still derived from 2D echocardiography.

Assessment of TR severity

Semi-quantitative methods

Colour flow Doppler imaging. Grading the severity of TR is in principle similar to MR. However, because standards for determining the TR severity are less robust than for MR, the algorithms for relating colour flow-derived parameters to TR severity are less well developed. Colour-flow imaging is useful to recognize small jets, but the assessment of larger TR jets has important limitations.[114] Indeed, flow jets that are directed centrally into the right atrium generally appear larger than eccentric wall-impinging jets with similar or worse severity. Basically, multiple windows (apical four-chamber, parasternal long and short-axis views, and sub-costal view) are required to assess TR severity by colour-flow analysis. The general assumption is that larger colour jets that extend deep into the RA represent more TR than smaller thin jets that are seen just beyond the tricuspid leaflets. As for MR, this method is a source of many errors and is limited by several technical and haemodynamic factors[1–4,115] and on that basis colour flow imaging is not appropriate for assessing TR severity (*Figure 46*). Nevertheless, the detection of a large eccentric jet adhering, swirling and reaching the posterior wall of the right atrium is in favour of severe TR. Conversely, small thin central jets usually indicate mild TR.

> **Key point: The colour flow area of the regurgitant jet is not appropriate to quantify the severity of TR. Colour flow imaging should only be used for diagnosing TR. A more quantitative approach is required when more than a small central TR jet is observed.**

Vena contracta width. The VC width of the TR is typically imaged in the apical four-chamber view using the same settings as for MR (*Figure 47*). Averaging measurements over at least two–three beats needs to be performed. A VC width >7 mm is in favour of severe while a width <6 mm may be either mild or moderate TR.[57] The geometry of the regurgitant orifice of secondary TR is usually more complex than for MR and rarely circular or ovale, given its trileaflet anatomy.[116] If available, use of 3D echo formats such as biplane imaging to assess the VC in simultaneous orthogonal views or 3D zoom colour flow Doppler can aid in better identifying the regurgitant orifice morphology. The VC area can then be measured by manual planimetry. A poor correlation exists between the 2D VC width and the 3D VC area, the latter being well correlated with EROA. The maximal VC diameter by 3D echocardiography is usually greater than the 2D measurement. This could underline the poor accuracy of the 2D VC width in eccentric jets. Although prognostic data is still lacking, 3D VC area is increasingly used with a suggested threshold for severe TR of >40 mm^2.[117]

> **Key point: When feasible, the measurement of the VC is the best method to quantify TR. A VC width >7 mm defines severe TR. Lower values are difficult to interpret. In case of multiple jets, the respective values of the VC width are not additive. The assessment of the VC by 3D echo can be helpful to better delineate the regurgitant orifice morphology and grade the TR severity.**

Anterograde velocity of tricuspid inflow. Similar to MR, the severity of TR will affect the early tricuspid diastolic filling (E velocity). In the absence of tricuspid stenosis, the peak E velocity increases in proportion to the degree of TR. Tricuspid inflow Doppler tracings are obtained at the tricuspid leaflet tips. A peak *E* velocity >1 m/s suggests severe TR (*Figure 48*).[1,2,4]

Hepatic vein flow. Pulsed Doppler evaluation of hepatic venous flow pattern is another aid for grading TR. In normal individuals, the pattern of flow velocity consists of anterograde systolic, transient flow reversal as the TV annulus recoils at the end of systole, anterograde diastolic and a retrograde A wave caused by atrial contraction. Such hepatic flow patterns are affected by respiration. With increasing severity of TR, there is a decrease in hepatic vein systolic velocity. In severe TR, systolic flow reversal occurs (*Figure 49*). The sensitivity of flow reversal for severe TR is 80%.[114] Thus, the absence of systolic flow reversal does not rule out severe TR. Blunted systolic hepatic vein flow can be observed in case of abnormal right atrial and RV compliance, atrial fibrillation and elevated right atrial pressure from any cause.[118] Blunting of hepatic flow may thus lack of specificity. Retrograde systolic flow can also be seen with colour flow Doppler. It can be associated with phasic spontaneous appearance of some contrast in the hepatic vein.

> **Key point: The systolic hepatic flow reversal is specific for severe TR. It represents the strongest additional parameter for evaluating the severity of TR.**

Continuous wave Doppler of the TR jet. As for MR, the CW envelope of the TR jet can be a guide to TR severity. A dense TR signal with a full envelope indicates more severe TR than a faint signal. The CW Doppler envelope may be truncated (notched) with a triangular contour and an early peak velocity (blunt), which is indicative of elevated right atrial pressure or a prominent regurgitant pressure wave in the right atrium due to severe TR.[1,2,4] Marked respiratory variation (decreased TR velocity with inspiration) suggests an elevated RA pressure (Kussmaul's sign on physical examination). The TR jet can be used to determine RV or pulmonary artery systolic pressure. This
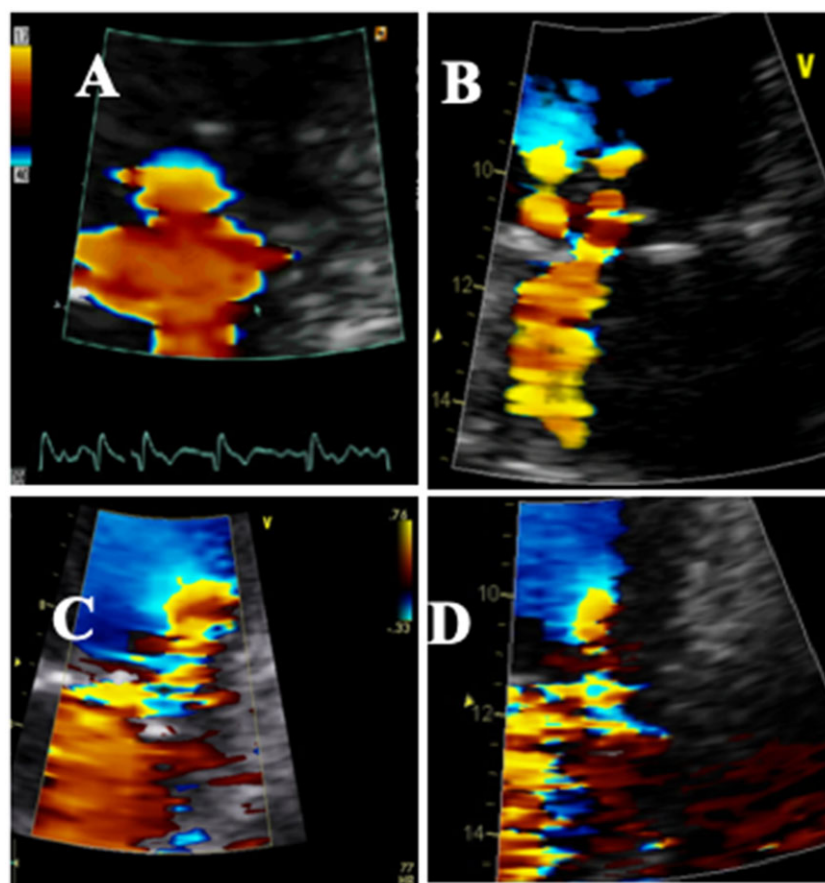
Figure 38 (*A*) Example of a flat flow convergence zone; (*B*) presence of 2 jets; and (*C* and *D*) distorted and constrained flow convergence zone by the lateral myocardial wall.

is done by calculating the RV to RA pressure gradient using the modified Bernoulli equation and then adding an assumed RA pressure. Of note, the velocity of the TR jet by itself does not provide useful information about the severity of TR. For instance, massive/torrential TR is often associated with a low jet velocity (<2 m/s) as there is near equalization of RV and RA pressures.[119] In some case, a high-velocity jet that represents only mild TR may be present when severe pulmonary hypertension is present.

Quantitative assessment

Anatomic orifice area. The AROA may be measured directly by planimetry using 2D/3D echocardiography (*Figure 50*), CT or CMR. Cut-offs of severity are, however, less well defined than for EROA and its clinical use is still limited.[120]

The proximal isovelocity surface area method. Although providing quantitative assessment, the flow convergence method is rarely applied for TR assessment in clinical practice (*Figure 51*), partly because one of the basic assumptions (circularity of regurgitant orifice) for its application is rarely met in secondary TR. This approach has been validated in small studies.[115,121,122] The apical four-chamber view and the parasternal long- and short-axis views are classically required for

optimal visualization of the PISA. The area of interest is optimized by lowering imaging depth and the Nyquist limit to approximately 15–40 cm/s. The radius of the PISA is measured at mid-systole using the first aliasing (*Figures 51 and 52*). Qualitatively, a TR PISA radius >9 mm at a Nyquist limit of 28 cm/s alerts to the presence of severe TR whereas a radius <5 mm suggests mild TR.[121] An EROA $\geq$ 40 mm^2 or a R Vol of $\geq$45 mL (due to lower TR velocity than in MR) indicates severe TR.[1,2,4] The PISA method faces several advantages and limitations.[1,122] It could underestimate the severity of TR by up to 30%.[123] This method is also less accurate in eccentric jets. Of note, the number of studies having evaluated the value of the flow convergence method in TR remains limited. When severe, TR can be subcategorized into severe, massive and torrential, which is of clinical interest in patients referred for transcatheter intervention.[124–126]

> **Key point: When feasible, the PISA method is the best to quantify the TR severity. A TR PISA radius >9 mm at a Nyquist limit of 28 cm/s indicates severe TR. An EROA $\geq$40 mm^2 and/or a R Vol $\geq$45 mL indicates severe TR. When severe, TR can be subcategorized into severe, massive and torrential, which is of clinical interest in patients referred for transcatheter intervention.**
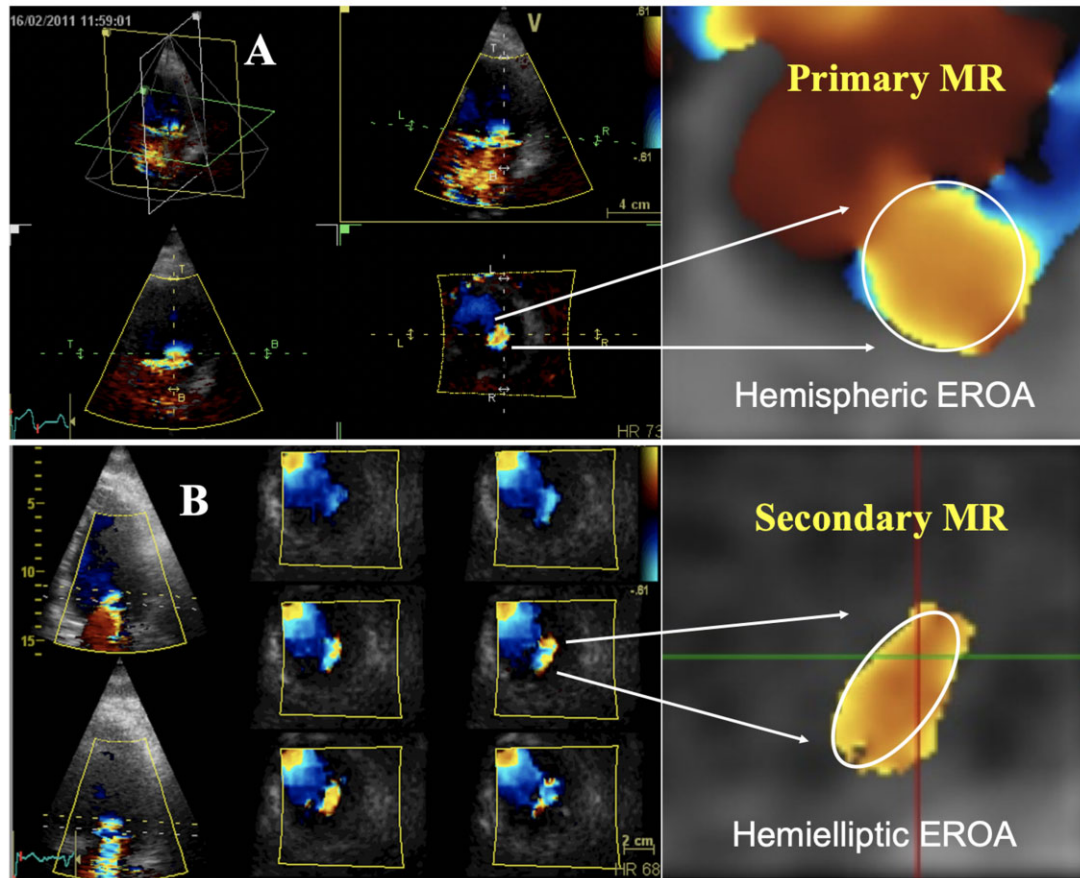
Figure 39 3D shape of the flow convergence in functional (*A*) (hemielliptic) and organic MR (*B*) (hemispheric).

Pulsed Doppler

Doppler volumetric method. Quantitative PW Doppler method has not been validated to quantify the TR severity. This approach is useless.[1,2,4]

CMR quantification

CMR evaluation of TR is feasible, but less established than that of other regurgitant valvular lesions. Indirect methods include calculation of the R Vol from the difference between RV total (using planimetry of short-axis cine images) and forward stroke volume across the pulmonary valve (using phase-contrast velocity mapping) (*Figure 52*).[14] The RF is calculated by dividing the R Vol by the RV stroke volume. A recent study demonstrated that a RF of >50% and a R Vol of >45 ml identified patients at increased risk of death.[61] Indeed, TR quantified by CMR was independently associated with mortality after adjustment for clinical and imaging covariates including RVEF, MR severity and pulmonary artery pressures.[127] Another study demonstrated that CMR RVEF assessments performed preoperatively provided important long-term prognostic information in patients undergoing corrective surgery for severe functional TR.[128] As another choice, in the absence of other regurgitant lesions, quantification of the RVol can be obtained by comparing LV and RV stroke volumes. Direct measurement using phase-contrast images position

at the level of the TV are of limited value due to substantial through-plane motion of the TV. Further studies are required to validate the CMR thresholds for severe TR but we would currently advocate using a RF cut off >50%.[1,4,61]

> **Key point: Although less validated, CMR may be used to assess TR severity using direct phase-contrast assessments.**

Consequences of TR

Signs of severe TR include RA and RV dilatation, a dilated and pulsatile inferior vena cava and hepatic vein, a dilated coronary sinus and systolic bowing of the interatrial septum towards the LA. The shape of the septum differs according to the TR aetiology (D-shaped LV predominantly in diastole in RV volume overload; septal flattening throughout the cardiac cycle in pulmonary hypertension). Although not specific, a rapid anterior motion of the interventricular septum at the onset of systole (isovolumic contraction) (paradoxical ventricular septal motion) represents a qualitative sign of RV volume overload due to severe TR. An end-systolic RV eccentricity index >2—obtained by dividing the longest right lateral distance by the distance connecting the ventricular septum and the RV free wall—is in favour
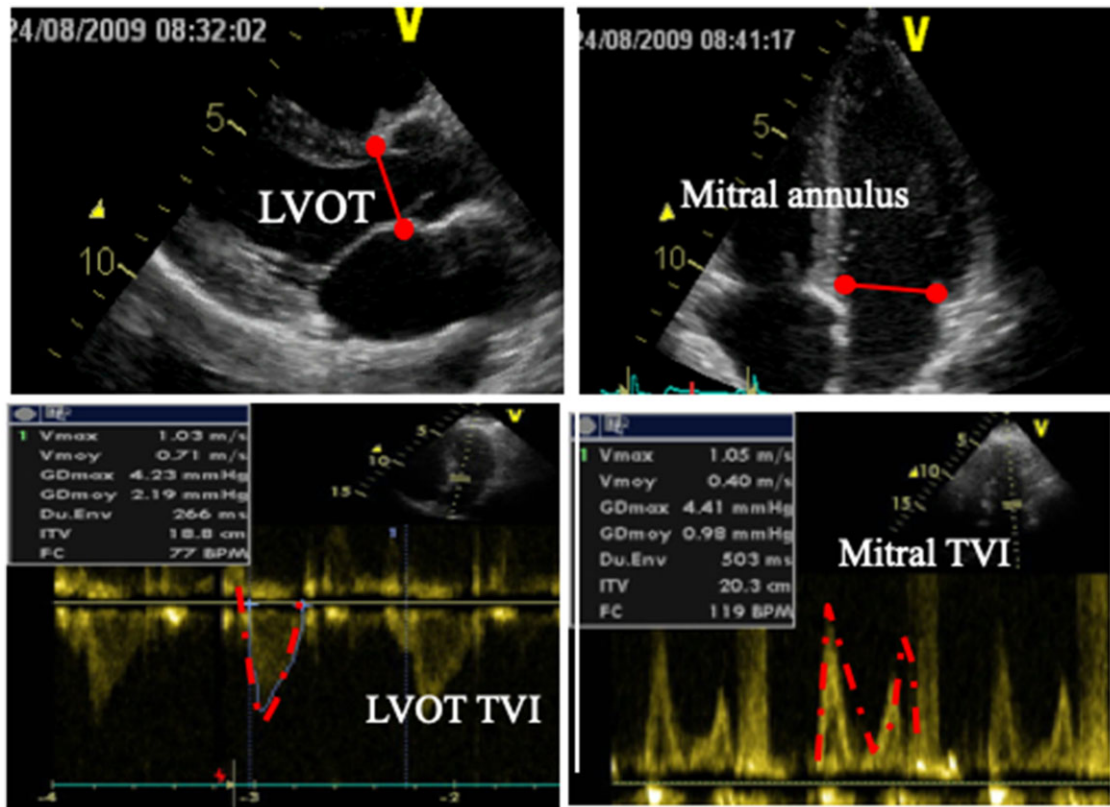
Figure 40 The quantitative assessment of MR severity by the Doppler volumetric method requires the measurement of the left ventricular outflow tract diameter (LVOT), the mitral annulus diameter and of two pulse wave velocity profiles (outflow tract and mitral inflow velocities). TVI, time-velocity integral.

of severe TR (sensitivity of 79%).[112] Three-dimensional echocardiography allows more accurate evaluation of RV volumes and EF than 2D and should be used as much as possible.[6,110] Although evidence of right heart dilatation is not specific for TR and can be noted in other conditions (pulmonary valve regurgitation, left-to-right atrial shunt, and anomalous venous return), its absence suggests milder degree of TR. As for the left ventricle, the RVEF is a crude estimate of RV function. It is dependent on loading conditions, ventricular interaction as well as myocardial structure. Other parameters such as TAPSE, systolic myocardial velocities, and GLS are currently available for a better assessment of RV function.[129] Imaging the vena cava and its respiratory variation also provides an evaluation of RA pressure. Thresholds for RV dysfunction are: RV fractional area change <35%, TAPSE <17 mm, systolic myocardial velocity <9.5 cm/s, and Free-wall longitudinal strain <20%.[27] A tricuspid annulus dimension ≥40 mm or ≥21 mm/m^2 represents the threshold used for intervention in patients with mild or moderate TR undergoing left-sided valvular intervention.[5]

When available, CMR is the preferred method to assess the right atrium and right ventricle due to its high accuracy and reproducibility. CMR provides larger RA/RV volumes than echocardiography, due to different handling of trabeculations, which are excluded on echocardiography. Conversely, RVEF by 3D echocardiography is comparable to CMR.[130,131] Indexed RV end-diastolic volume >164 mL/m^2 on CMR has been associated with a low likelihood of RV functional recovery after re-intervention for severe residual TR in the context of previous left-sided valve surgery.[128]

> **Key point: When TR is more than mild, the evaluation of RV dimensions and function, RA volume, inferior vena cava diameter and the pulmonary arterial systolic pressure is mandatory.[1] Three-dimensional echocardiography allows more accurate evaluation of RV volumes and EF than 2D. The assessment of RV systolic function using TAPSE, systolic myocardial velocities, or GLS is useful to look for RV dysfunction. When available, CMR is the preferred method for assessing RA and RV size. CMR values are not interchangeable with echo derived-data.**

Role of exercise echocardiography

As for MR, the goal of exercise echocardiography is to examine the RV functional reserve and to evaluate the changes in pulmonary artery systolic pressure. No data are currently available on patients with isolated TR.[8]

Table 10 Grading the severity of MR

MR severity classes	Mild	Moderate		Severe
MR Severity sub-classes[j]	Mild (Grade 1 or 1+)	Mild-to-moderate (Grade 2 or 2+)	Moderate-to-severe (Grade 3 or 3+)	Severe (Grade 4 or 4+)
Qualitative parameters				
MV morphology	None or mild leaflet abnormality or minimal tenting	Moderate leaflet abnormality or moderate tenting	Moderate leaflet abnormality or moderate tenting	**Flail leaflet/large coaptation defect/severe tenting**
Colour flow MR jet	Small, central (usually <4 cm² or <20% of LA area)	Intermediate (usually 4–6 cm² or 20–30% of LA area)	Intermediate (usually 6–8 cm² or 30–40% of LA area)	**Large central jet** (usually >8 cm² or >50% of LA area) or eccentric jet swirling and reaching the posterior wall of the LA
Flow convergence zone[a] CW signal of MR jet	No or small faint/parabolic	Dense, partial or parabolic	Dense, parabolic or triangular	• **Large throughout systole** • Holosystolic/dense/triangular
Semi-quantitative parameters				
VC width (mm)	<3	3 to <5	5 to <7	**≥7 (≥8 for biplane)**[b]
Pulmonary vein flow	Systolic dominance[e]	Normal or systolic blunting	Systolic blunting	Minimal to no systolic flow/**systolic flow reversal**[d]
Mitral inflow	A wave dominant[b]	Variable	E-wave dominant (Peak E > 1.2 m/s)[f]	E wave dominant (Peak E > 1.2 m/s)[f]
VTI mitral/VTI LVOT	<1	Intermediate	>1.2[f]	**>1.4**[f]
Quantitative parameters[h,j,k]				
EROA (mm²)	<20	20–29	30–39	**≥40**
R Vol (mL)[i]	<30	30–44	45–59	**≥60**
RF (%)	<30	30–39	40–49	**≥50**
CMR parameters				
RF (%)	<30	30–39	40–49	**≥50**
Structural parameters				
LV and LA size[g]	Usually normal	Normal or dilated	Usually dilated	**Usually dilated**
PA pressures[g]	Usually normal	Normal or elevated	Normal or elevated	**Usually elevated**

CW, continuous-wave; EROA, effective regurgitant orifice area; LA, left atrium; LV, left ventricle; MR, mitral regurgitation; PA, pulmonary arterial; R Vol, regurgitant volume; RF, regurgitant fraction; VC, vena contracta.

In bold: specific signs for severe MR.

[a]At a Nyquist limit of 50–60 cm/s.

[b]For average between apical four- and two-chamber views.

[d]Unless other reasons of systolic blunting (atrial fibrillation, elevated LA pressure).

[e]Usually after 50 years of age.

[f]In the absence of other causes of elevated LA pressure and/or of mitral stenosis.

[g]Unless for other reasons, the LA and LV size and the pulmonary pressure are usually normal in patients with mild MR. In acute severe MR, the pulmonary pressures are usually elevated while the LV size is still often normal. In chronic severe MR, the LV is classically dilated. *Accepted cut-off values for non-significant left-sided chambers enlargement:* LA volume <36 mL/m², LV end-diastolic diameter <56 mm, LV end-diastolic volume <82 mL/m², LV end-systolic diameter <40 mm, LV end-systolic volume <30 mL/m², LA diameter <39 mm, LA volume <29 mL/m².

[h]The measurement of the PISA by 2D TTE in patients with secondary MR may underestimate the true ERO because of the crescentic shape of the proximal convergence.

[i]MR regurgitant volume may be lower in low flow conditions but correspond to a larger RF.

[j]Grading of severity of MR classifies regurgitation as mild, moderate or severe, and sub-classifies the moderate regurgitation group into 'mild-to-moderate' and 'moderate-to-severe'. In secondary MR, an EROA ≥30 mm² and/or a R Vol >45 mL can define severe MR.

[k]Discrepancies between EROA, R Vol, and RF may be seen in case of low or high flow states.
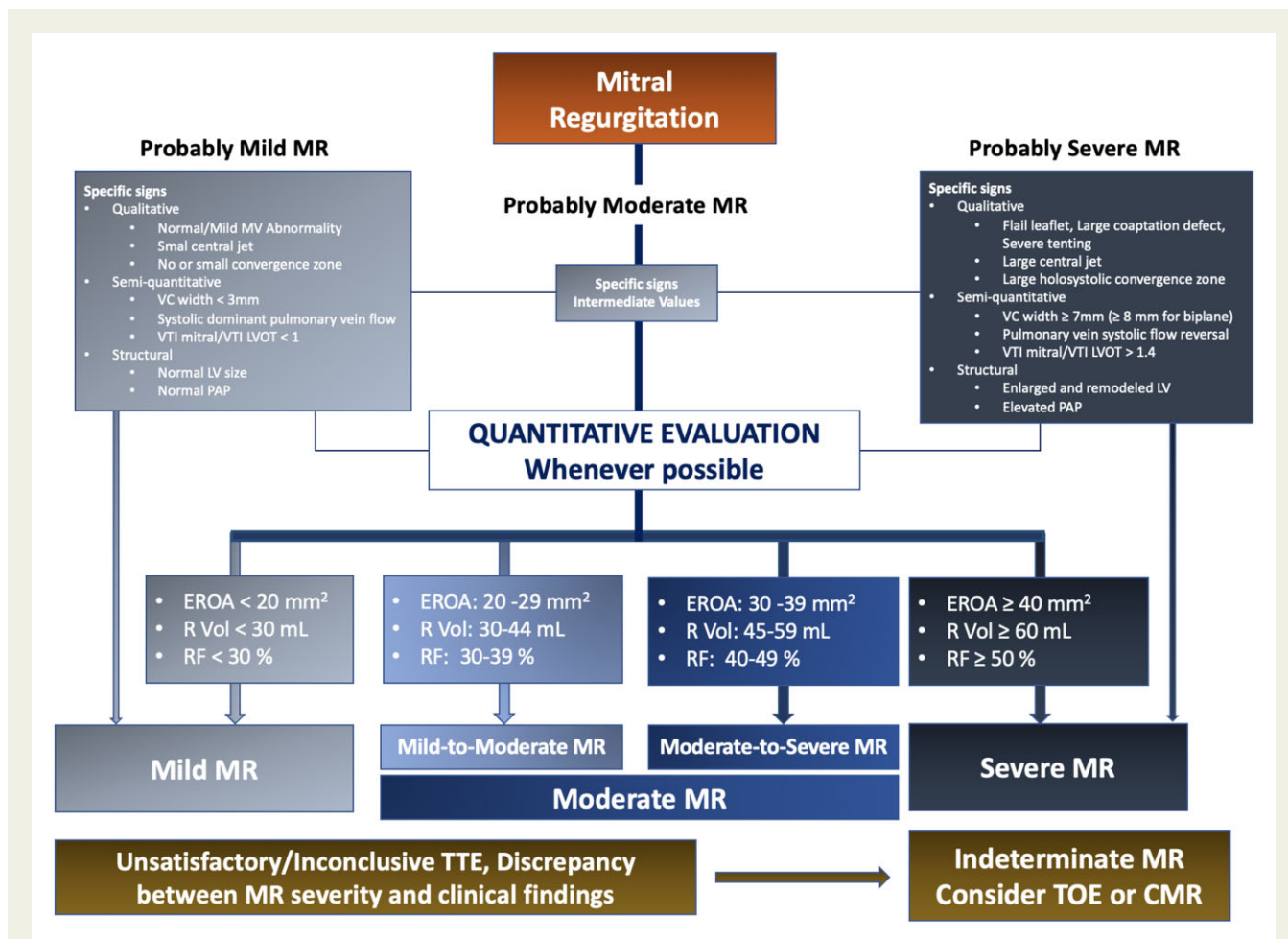
Figure 41 Algorithm for the assessment of MR severity. PAP, pulmonary arterial pressure.

Table 11   **Probability of successful surgical mitral valve repair in MR based on echo findings**

Aetiology	Dysfunction	Calcification	Mitral annulus dilatation	Probability of repair
Degenerative	II: Localized prolapse (P2 and/or A2)	No/localized	Mild/moderate	**Feasible**
Secondary	I or IIIb	No	Moderate	**Feasible**
Barlow	II: Extensive prolapse (≥3 scallops, posterior commissure)	Localized (annulus)	Moderate	**Difficult**
Rheumatic	IIIa but pliable anterior leaflet	Localized	Moderate	**Difficult**
Severe Barlow	II: Extensive prolapse (≥ 3 scallops, anterior commissure)	Extensive (annulus + leaflets)	Severe	**Unlikely**
Endocarditis	II: Prolapse but destructive lesions	No	No/mild	**Unlikely**
Rheumatic	IIIa but stiff anterior leaflet	Extensive (annulus + leaflets)	Moderate/severe	**Unlikely**
Secondary	IIIb but severe valvular deformation	No	No or severe	**Unlikely**

Integrating indices of severity

Echocardiographic assessment of TR includes integration of data from 2D/3D imaging of the valve, right heart chambers, septal motion and inferior vena cava as well as Doppler measures of regurgitant severity (*Figures 53 and 54*; *Table 15*). Colour-flow Doppler should be examined in multiple windows. The consensus of the expert is to advocate grading the severity of TR by using the VC width and the PISA radius, except in the presence of mild or trivial TR or when TR is considered severe using specific signs. When severe, TR can be subcategorized into severe, massive and torrential, which is of clinical interest in patients referred for transcatheter intervention (*Table 16*). CMR may be useful when the results of echocardiography are unsatisfactory or inconclusive. CCT scan can be helpful in preprocedural intervention planning.

Intervention guidance

Persistent or recurrent TR has been reported in up to 20–50% of patients undergoing MV surgery.[132] In secondary TR, this has been related to the extent of tricuspid leaflet restriction and to the severity of tricuspid annular dilatation.[100] Both the severity of pre-operative

Table 12 Unfavourable Imaging characteristics for surgical mitral valve repair in secondary MR[82]

- **Mitral valve deformation**
  - Coaptation distance (leaflet tenting height) ≥1 cm
  - Leaflet tenting area >2.5–3 cm^2
  - Complex jets originating centrally and postero-medially
  - Postero-lateral angle >45° (severe posterior leaflet tethering)
- **Local LV remodelling**
  - Interpapillary muscle distance >20 mm
  - Posterior papillary-fibrosa distance >40 mm
  - Lateral wall motion abnormality
- **Global LV remodelling**
  - LV EDD >65 mm, LV ESD >51 mm (LV ESV >140 mL) (low likelihood of reverse LV remodelling after repair and poor long-term outcome)
 - Systolic sphericity index >0.7

EDD, end-diastolic diameter; ESD, end-systolic diameter; ESV, end-systolic volume; LV, left ventricle.

TR and RV dysfunction contributes to residual post-operative TR. Similarly, severe TV tethering predicts residual TR after TV annuloplasty. A tenting area >1.63 cm^2 and a tethering (coaptation) distance >0.76 cm are good predictors of residual TR after TV surgery (*Figure 55*).[133] Exclusion criteria for transcatheter TriClip therapy are: a systolic pulmonary arterial pressure >60 mm Hg, a severe coaptation defect (>2 cm) of the tricuspid leaflets, leaflet calcification in the grasping area, a TV orifice of ≤1 cm^2 and/or mean gradient ≥5 mmHg, or the presence of Ebstein anomaly.[134]

> **Key point: Imaging report should provide information on the likelihood of successful surgical or transcatheter tricuspid valve repair.**

Suggested follow-up for TR

As for other valvular regurgitation, the follow-up of patients with TR depends on the aetiology and severity of TR, the RV size and function and the associated diseases. Usually, the follow-up will be dictated by the severity of left-sided valve disease. Although data are limited, careful follow-up should be organized in patients with moderate to severe TR.[5]
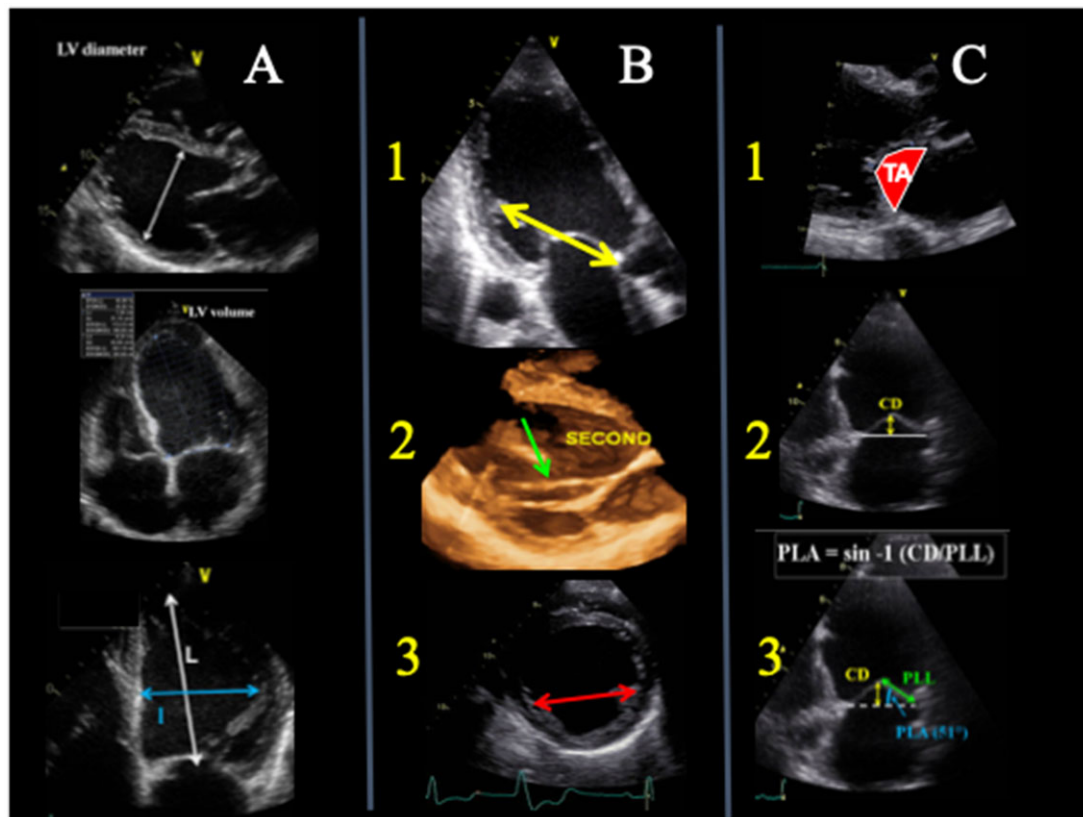
Figure 42 Echo morphologic parameters that are measured in secondary MR. (*A*) Global LV remodelling [diameter, LV volumes, sphericity index (SI = L/l; L: major axis, l: minor axis)]. (*B*) Local LV remodelling (1: apical displacement of the postero-medial papillary muscle; 2: second order chordate; and 3: interpapillary muscle distance). (*C*) Mitral valve deformation [1: systolic tenting area (TA); 2: coaptation distance (CD); and 3: postero-lateral angle (PLA)].

Table 13 Unfavourable parameters for percutaneous mitral valve repair with MitraClip[5,96]

Primary MR	Secondary MR
Leaflet perforation/large cleft	Severe tenting (coaptation depth > 11 mm)
Rheumatic MR	Coaptation length <2 mm, large coaptation gap
Large flail gap >10 mm	Posterior leaflet length <7 mm
Large flail width >15 mm	LVEDD >70 mm; LVEDV >200 mL or LVEDV index >96 mL/m^2
Mitral valve opening area ≤3 cm^2	
Leaflet calcification in the grasping area	
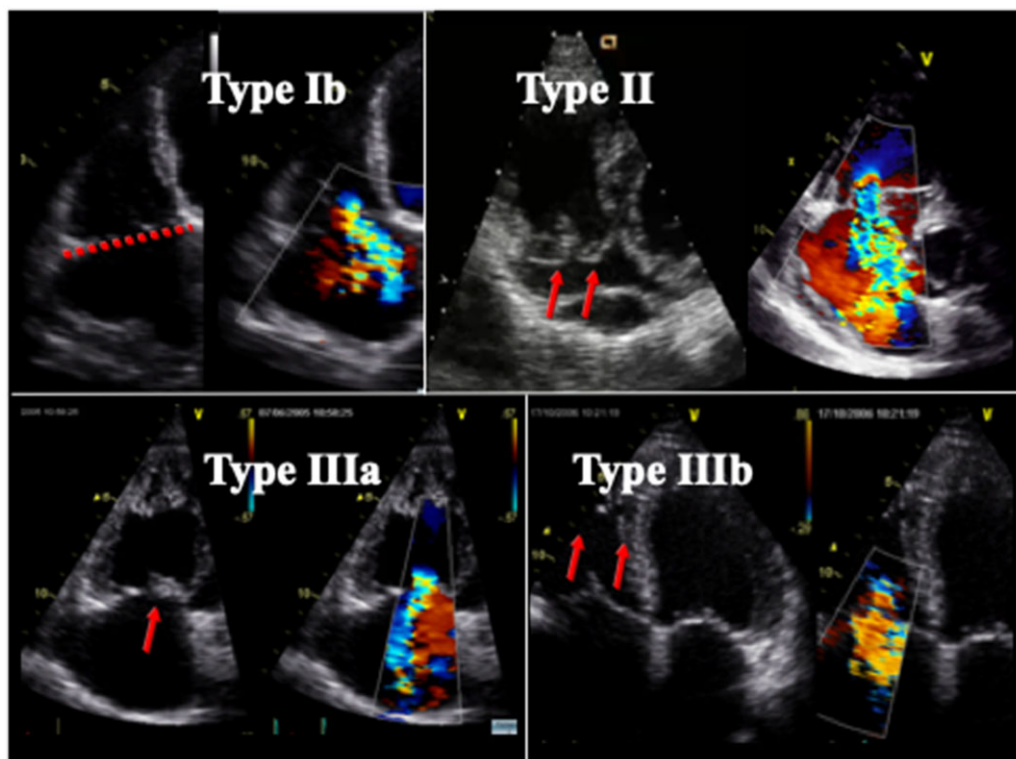
Figure 43 Mechanisms of TR according to the Carpentier's functional classification.

Table 14   Pathophysiological classification of tricuspid regurgitation

|	Leaflet morphology	Pathophysiology	Aetiology	Imaging	Treatment
Primary	Abnormal	Loss of leaflet coaptation due to intrinsic changes, excessive mobility or perforation	• Myxomatous disease • Endocarditis • Trauma • Carcinoid • Rheumatic • Iatrogenic (biopsy) • Congenital	• According to the etiology • Description of the etiology, lesions and dysfunction	• Surgical annuloplasty±leaflet repair/extension • Surgical valve replacement • Transcatheter leaflet devices±annular devices • Transcatheter valve replacement
Secondary					
A. Atrial	Normal	RA enlargement and dysfunction leading to TA dilation, conical remodeling of the RV	Atrial fibrillation	• Severe RA remodeling • RV basale diameter may be enlarged despite usually normal RV volume • Leaflet tethering is absent or limited	• Surgical annuloplasty • Surgical valve replacement • Transcatheter leaflet devices±annular devices • Transcatheter valve replacement
B. Ventricular	Considered normal	RV enlargement and/or dysfunction leading to significant leaflet tethering and TA dilation	• Pulmonary hypertension • RV cardiomyopathy • RV infarction	Dominant mechanism is leaflet tethering ± TA dilation	• Surgical annuloplasty±leaflet repair/extension • Surgical valve replacement • Transcatheter leaflet devices • Transcatheter valve replacement
C. CIED-related					
i. *Primary*	Abnormal	• Leaflet impingement • Leaflet/chordal entanglement • Leaflet adherence • Leaflet laceration/perforation • Leaflet avulsion (post lead extraction)	• Pacemaker • Implantable cardiac defibrillator • Cardiac resynchronization therapy	3D echocardiograhy (±color) is mandatory for reliable diagnosis	• Lead reposition/extraction • Surgical valve replacement • Transcatheter leaflet devices • Transcatheter valve replacement
ii. *Secondary*	Normal	RV enlargement and/or dyssynchrony/dysfunction due to pace-maker stimulation and leading to significant leaflet tethering and TA dilation	Pacemaker rhythm	Dominant mechanism is leaflet tethering ± TA dilation	• Surgical annuloplasty±leaflet repair/extension • Surgical valve replacement • Transcatheter leaflet devices • Transcatheter valve replacement
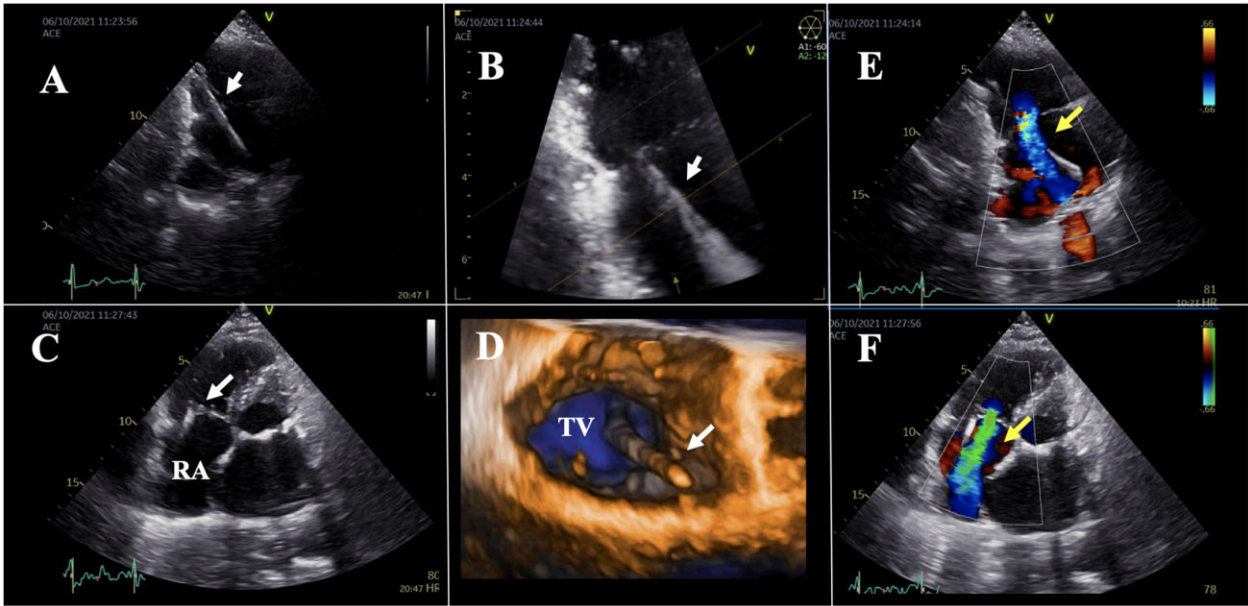
Figure 44 Pacemaker lead-associated TR. (*A–D*) An RV pacing lead can be seen crossing the TV (white arrow). (*D*) 3D TOE live zoom image of the right atrium (RA) en face view of the TV showing the position of the pacing lead close to the posterior leaflet, with resultant severe TR (*E* and *F*). TV, tricuspid valve.
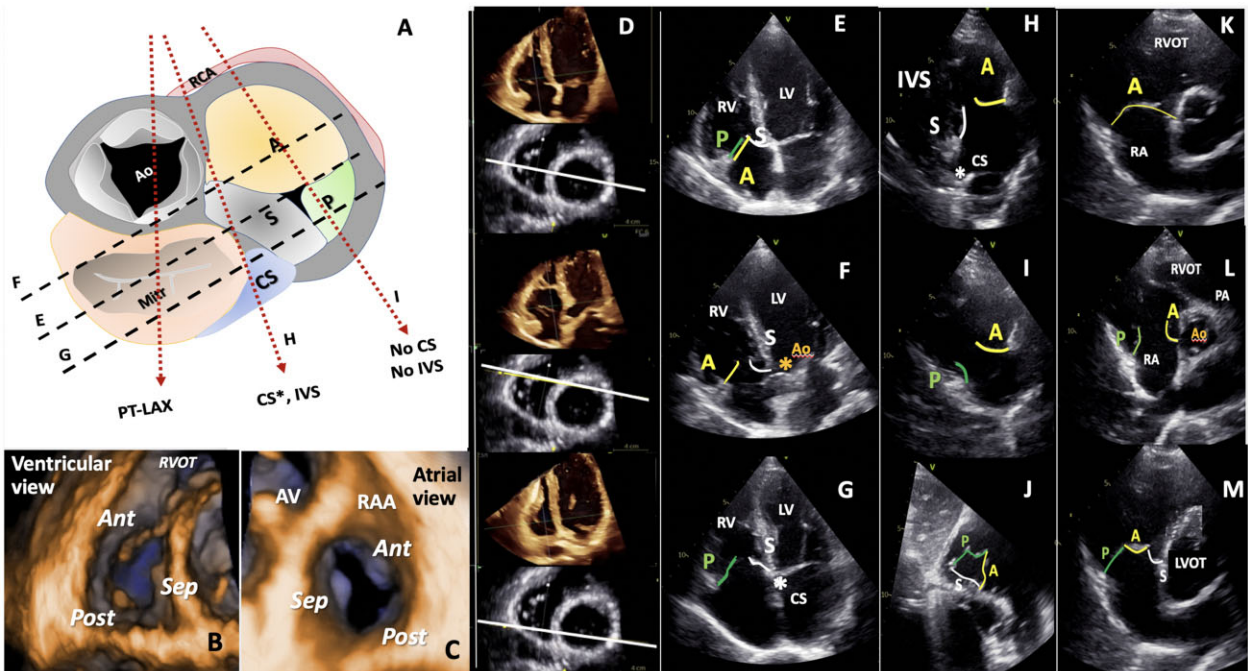
Figure 45 (*A*) Drawing of the TV. (*B* and *C*) 3D TTE volume rendering of the normal TV. (*B*) Ventricular perspective. (*C*) Atrial perspective (surgical view). (*D*) 3D cut planes trough the TV. (*E–M*) 2D echo recordings of the TV. (*E–G*) Apical four-chamber views. [If the LVOT is visible, the septal and anterior TV leaflets are likely to be in view (panel *F*). If the coronary sinus (CS) is seen, the septal and posterior TV leaflets are likely to be imaged (panel *G*).] (*H* and *I*) Parasternal long-axis (PLAX) RV inflow views. If the interventricular septum (IVS) and CS can be seen, the image will most likely demonstrate the septal and anterior leaflets of the TV (panel *H*). If the septum and CS are not seen, it is likely to be the anterior and posterior leaflets that are imaged (panel *I*). (*G*) Sub-costal view. (*K–M*) Parasternal short-axis (SAX) views (see *H* and *I*). A, anterior leaflet; P, posterior leaflet; S, septal leaflet.
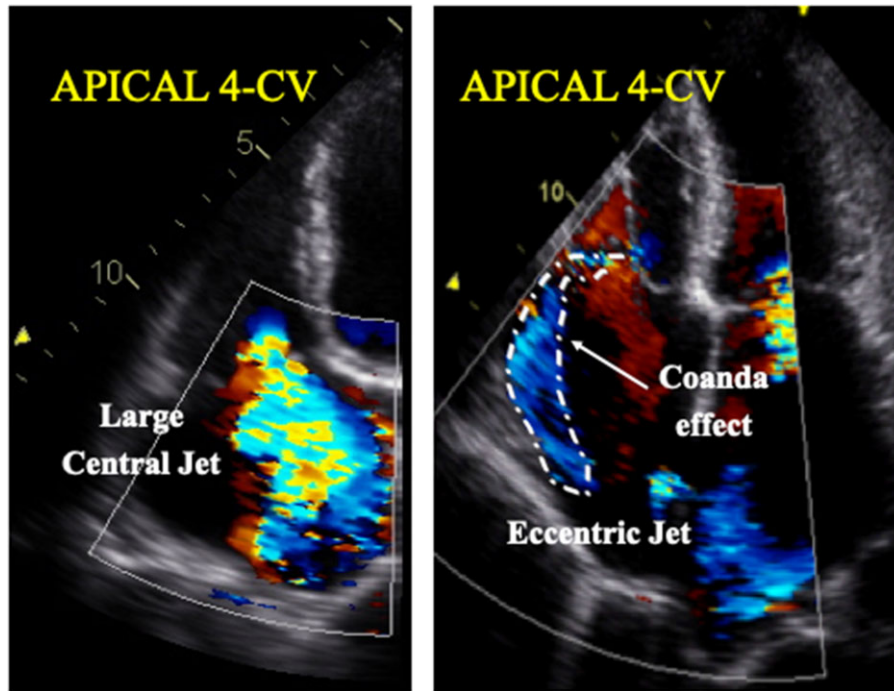
Figure 46 Visual assessment of tricuspid regurgitant jet using colour-flow imaging. (*A*) Large central jet. (*B*) Eccentric jet with a clear Coanda effect. CV, four-chamber view.
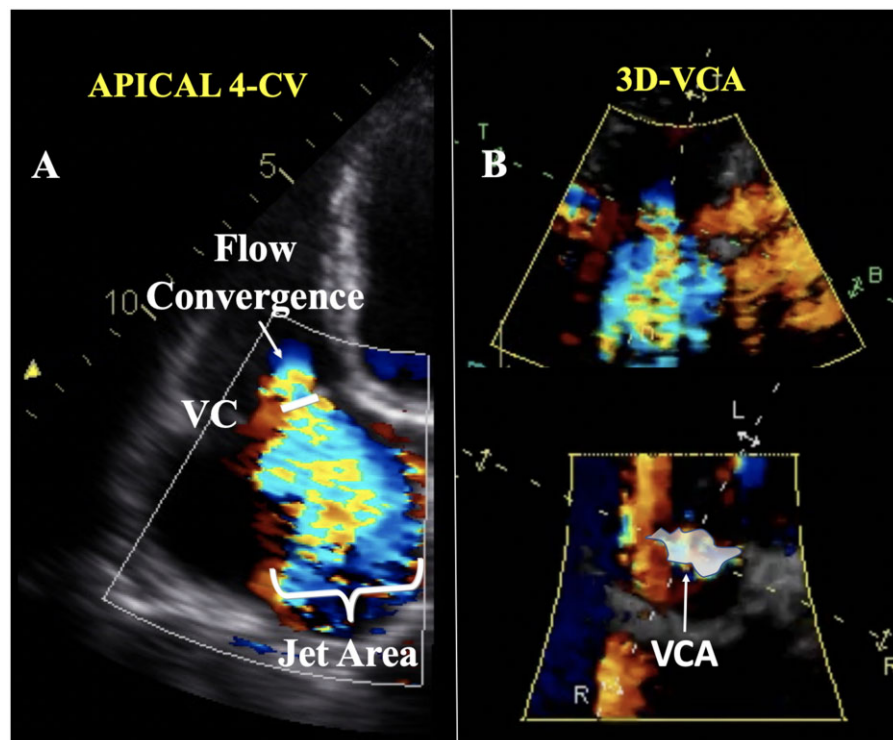
Figure 47 (*A*) Semi-quantitative assessment of TR severity using the vena contracta width (VC). The three components of the regurgitant jet (flow convergence zone, vena contracta, jet turbulence) are obtained. (*B*) 3D VC shape. CV: chamber view.
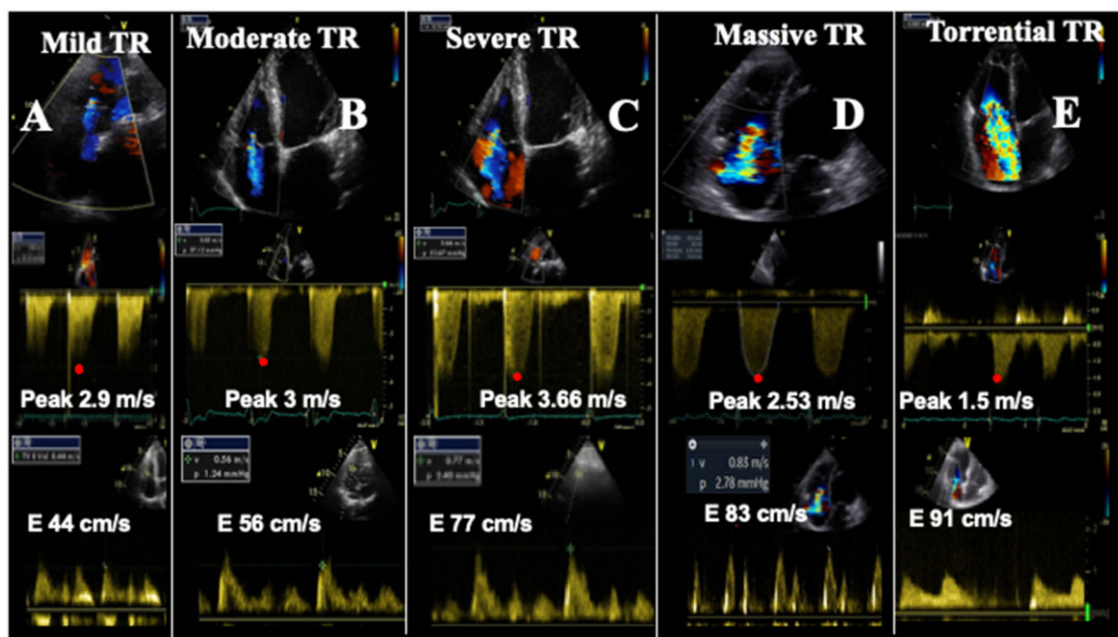
Figure 48 Five examples of various degrees of TR, mild (*A*), moderate (*B*), severe (*C*), massive (*D*), and torrential (*E*) are provided. The regurgitant jet area (RJA) as well as the tricuspid E wave velocity increase with the severity of TR. In severe TR, the continuous wave Doppler signal of the regurgitant jet is truncated, triangular and intense. The peak velocity of TR (continuous wave Doppler) allows the estimation of pulmonary pressure except in case of massive/torrential TR, since the Bernouilli equation is not applicable.
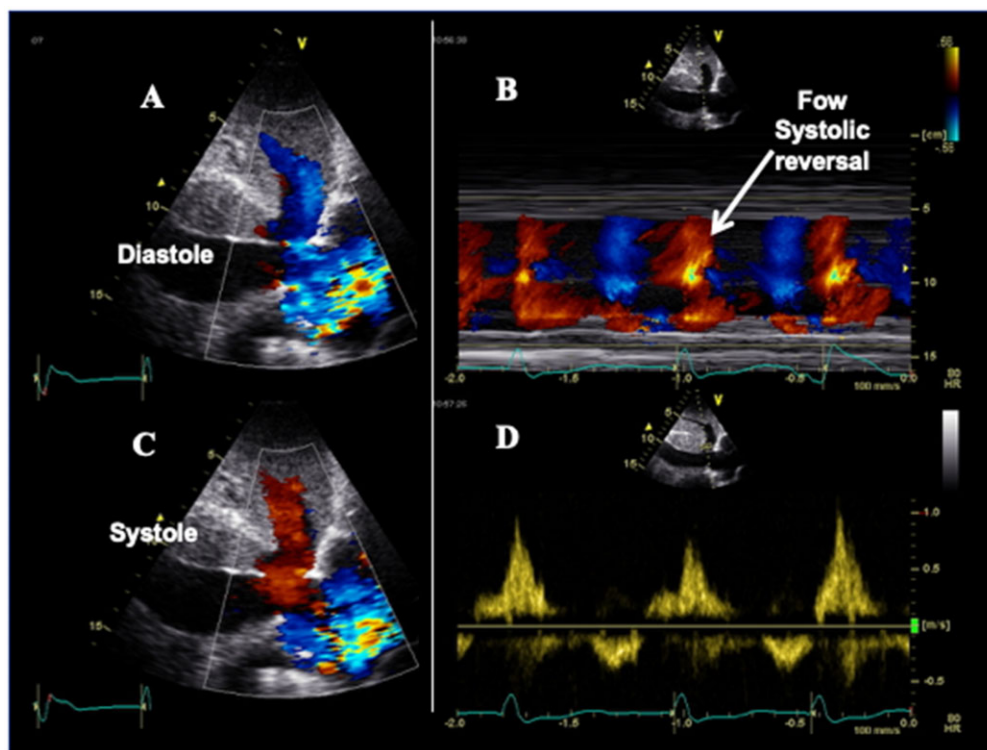
Figure 49 Subcostal echocardiogram recorded in a patient with severe TR. (*A–C*) The colour Doppler confirms retrograde flow into the vena cava and hepatic vein in systole consistent with TR (red). (*D*) A spectral Doppler recording from a hepatic vein, also confirming the systolic retrograde flow.
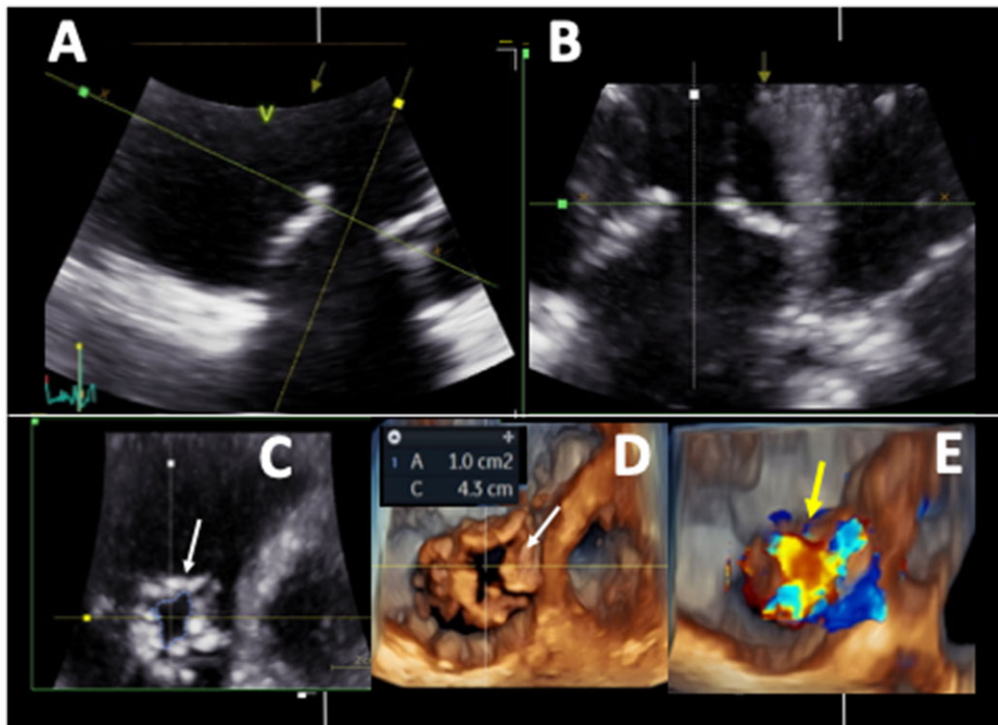
Figure 50 3D TTE acquisition in a patient with pulmonary hypertension and secondary TR. (*A* and *B*) Apical views showing the extent of leaflet tethering. (*C* and *D*) Quantitative assessment of the anatomic regurgitant orifice area using anatomically oriented cut planes to obtain and planimeter the true anatomical orifice area. (*E*) Size and shape of the VC obtained using 3D colour Doppler.
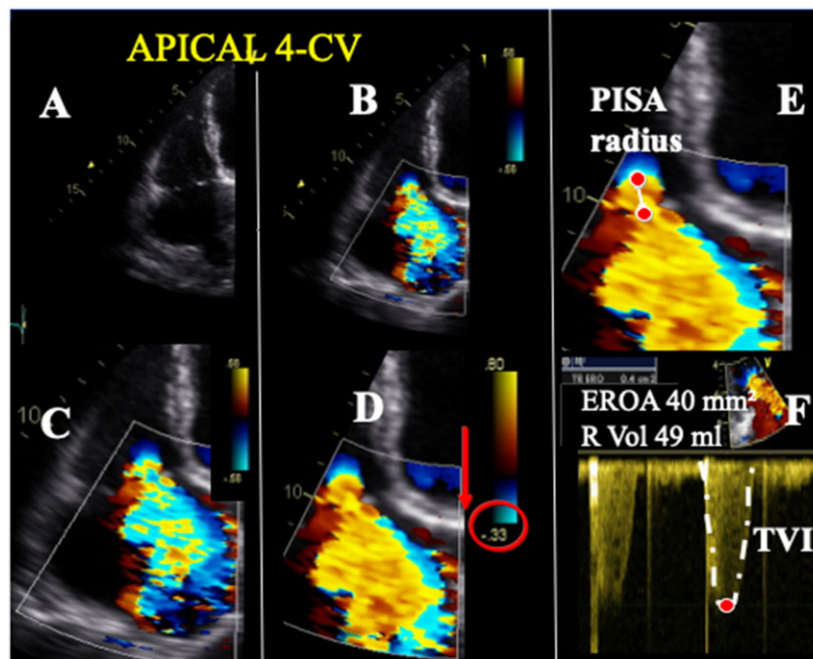
Figure 51 Quantitative assessment of TR severity using the PISA method. Stepwise analysis of TR. (*A*) Apical four-chamber view (CV); (*B*) colour-flow display; (*C*) zoom of the selected zone; (*D*) downward shift of zero baseline to obtain a hemispheric PISA; (*E*) measure of the PISA radius using the first aliasing; and (*F*) continuous wave Doppler of TR jet allowing calculation the effective regurgitant orifice area (EROA) and regurgitant volume (R Vol). TVI, time-velocity integral.
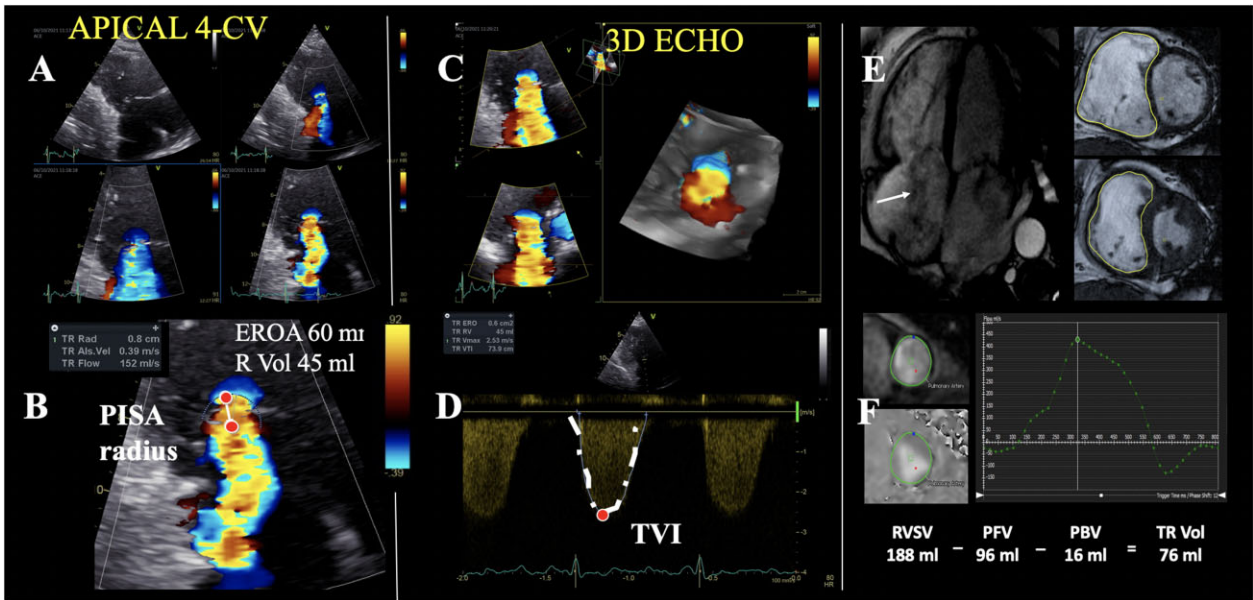
Figure 52 Quantitative assessment of TR severity using the PISA method (*A–D*) and the indirect CMR method (*E* and *F*). White arrow: extent of the signal loss on cine CMR. (*E*) Assessment of LV volumes using cine images. (*I*) Phase-contrast velocity mapping at the aortic root level and flow-time curves computing forward aortic flow.
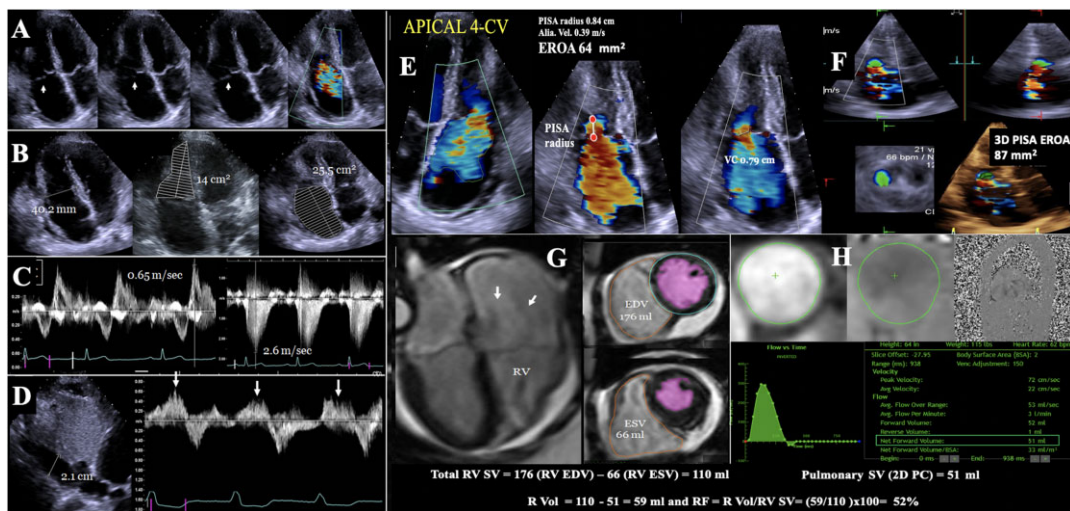
Figure 53 Assessment of TR severity and consequences compiling 2D/3D echocardiography and CMR data.
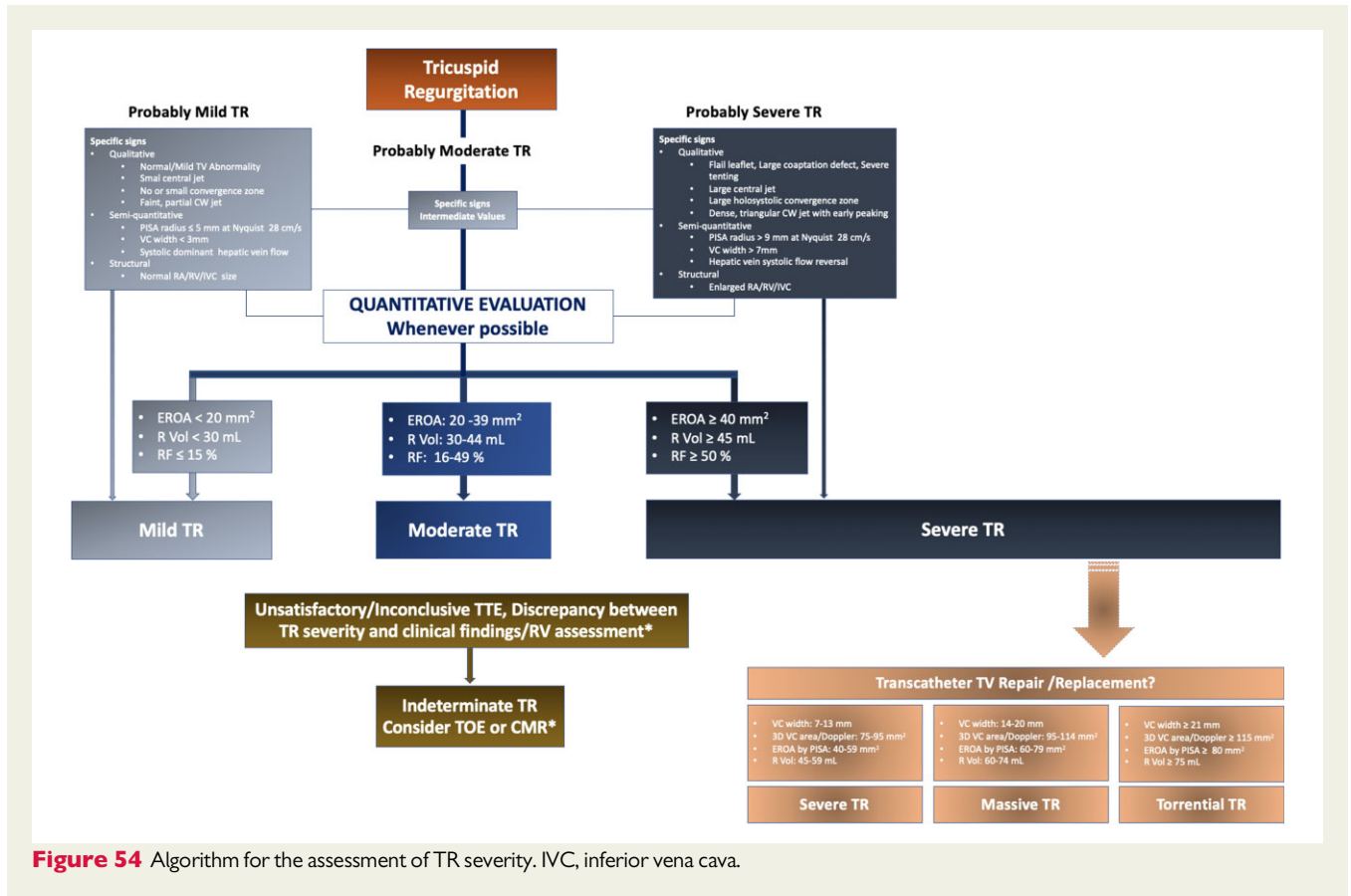
Figure 54 Algorithm for the assessment of TR severity. IVC, inferior vena cava.

Table 15   Grading the severity of TR

TR Severity classes	Mild	Moderate	Severe
Qualitative parameters			
Tricuspid valve morphology	Normal or mildly abnormal leaflets	Moderately abnormal leaflets	Severe valve lesions/**flail/large coaptation defect//severe tenting**
Colour flow TR jet[a]	Small, narrow, central	Moderate central	**Large central jet** or eccentric wall impinging jet of variable size
Flow convergence zone	Not visible, transient or small	Intermediate in size and duration	**Large throughout systole**
CW signal of TR jet	Faint/partial/parabolic	Dense/parabolic, or triangular	**Dense/often triangular with early peaking** (peak <2 m/s in massive TR)
Semi-quantitative parameters			
Hepatic vein flow[b]	Systolic dominance	Systolic blunting	**Systolic flow reversal**
Tricuspid inflow	A-wave dominant	Variable	E wave dominant (≥1 m/s)[e]
PISA radius (mm)[c]	≤5	6-9	**>9**
VC width (mm)[a,d]	<3	3–6.9	**>7**
3D VC area or quantitative Doppler EROA (mm^2)			75–94
Quantitative parameters			
EROA (mm^2)	<20	20–39	≥40
R Vol (mL)	<30	30–44	≥ 45
RF (%)	≤15	16–49	≥50
CMR parameters			
RF (%)	≤15	16–49	≥50
Structural parameters			
RV, RA, IVC size[e]	Usually normal	Normal of mild dilation	Usually dilated

CW, continuous-wave; EROA, effective regurgitant orifice area; R Vol, regurgitant volume; RA, right atrium; RF, regurgitant fraction; RV, right ventricle; TR, tricuspid regurgitation; VC, vena contracta.
In bold: specific signs for severe TR.
[a]At a Nyquist limit of 50–60 cm/s.
[b]Unless other reasons of systolic blunting (atrial fibrillation, elevated RA pressure).
[c]Baseline Nyquist limit shift of 28 cm/s.
[d]When VC width is assessed as an average of measurements performed biplane the threshold value for severe TR is > 9 mm.
[e]In the absence of other causes of elevated RA pressure.
[f]Unless for other reasons, the RA and RV size and IVC are usually normal in patients with mild TR. An end-systolic RV eccentricity index >2 is in favour of severe TR. In acute severe TR, the RV size is often normal. In chronic severe TR, the RV is classically dilated. *Accepted cut-off values for non-significant right-sided chambers enlargement (measurements obtained from the apical four-chamber view)*: mid RV dimension ≤33 mm, RV end-diastolic area ≤28 cm^2, RV end-systolic area ≤16 cm^2, RV fractional area change >32%, maximal 2D RA volume ≤33 mL/m^2.
An IVC diameter <2.1 cm is considered normal. The IVC is dilated when the diameter is >2.5 cm.

Table 16   Grading the severity of TR in the context of transcatheter TV repair/replacement

	Severe	Massive	Torrential
Semi-quantitative parameters			
VC width (mm)[a]	7–13	14–20	≥21
3D VC area or quantitative Doppler EROA (mm^2)	75–94	95–114	≥115
Quantitative parameters			
EROA by PISA (mm^2)[b]	40–59	60–79	≥80
R Vol (mL)	40–59	60–74	≥75

EROA, effective regurgitant orifice area; RF, regurgitant fraction; R Vol, regurgitant volume.
[a]At a Nyquist limit of 50–60 cm/s.
[b]Baseline Nyquist limit shift of 28 cm/s.
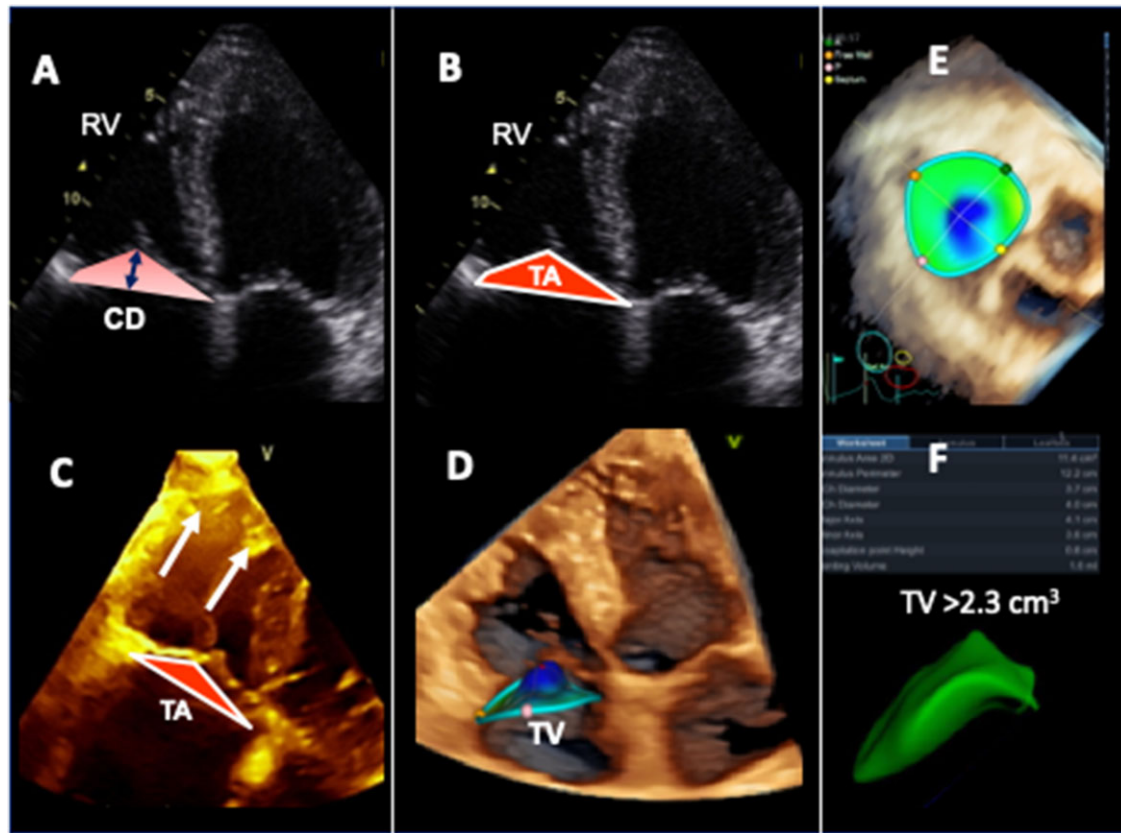
Figure 55 (*A–D*) 2D/3D echo morphologic parameters that are measured in secondary TR. (*A–D, F*) Evaluation of the tethering (coaptation) distance (CD), systolic tenting area (TA), and systolic tenting volume; (*E*) 3D derived tricuspid annulus.

References

1. Zoghbi WA, Adams D, Bonow RO, Enriquez-Sarano M, Foster E, Grayburn PA *et al.* Recommendations for noninvasive evaluation of native valvular regurgitation. *J Am Soc Echocardiogr* 2017;**30**:303–71.
2. Lancellotti P, Tribouilloy C, Hagendorff A, Popescu BA, Edvardsen T, Pierard LA *et al.*; Scientific Document Committee of the European Association of Cardiovascular Imaging. Recommendations for the echocardiographic assessment of native valvular regurgitation. *Eur Heart J Cardiovasc Imaging* 2013;**14**: 611–44.
3. Robinson S, Ring L, Augustine DX, Rekhraj S, Oxborough D, Harkness A *et al.* The assessment of mitral valve disease. *Echo Res Pract* 2021;**8**:G87–136.
4. Zaidi A, Oxborough D, Augustine DX, Bedair R, Harkness A, Rana B *et al.* Echocardiographic assessment of the tricuspid and pulmonary valves. *Echo Res Pract* 2020;**7**:G95–122.
5. Vahanian A, Beyersdorf F, Praz F, Milojevic M, Baldus S, Bauersachs J *et al.* 2021 ESC/EACTS Guidelines for the management of valvular heart disease. *Eur Heart J* 2021;**28**:ehab395.
6. Lang RM, Badano LP, Tsang W, Adams DH, Agricola E, Buck T *et al.*; European Association of Echocardiography. EAE/ASE recommendations for image acquisition and display using three-dimensional echocardiography. *Eur Heart J Cardiovasc Imaging* 2012;**13**:1–46.
7. Carpentier A, Chauvaud S, Fabiani JN, Deloche A, Relland J, Lessana A *et al.* Reconstructive surgery of mitral valve incompetence: ten-year appraisal. *J Thorac Cardiovasc Surg* 1980;**79**:338–48.
8. Lancellotti P, Pellikka PA, Budts W, Chaudhry FA, Donal E, Dulgheru R *et al.* The clinical use of stress echocardiography in non-ischaemic heart disease. *Eur Heart J Cardiovasc Imaging* 2016;**17**:1191–229.
9. Chambers JB, Garbi M, Nieman K, Myerson S, Pierard LA, Habib G *et al.* Appropriateness criteria for the use of cardiovascular imaging in heart valve disease in adults. *Eur Heart J Cardiovasc Imaging* 2017;**18**:489–98.
10. Chambers JB, Lancellotti P. Heart valve clinics, centers, and networks. *Cardiol Clin* 2020;**38**:65–74.
11. Petersen SE, Khanji MY, Plein S, Lancellotti P, Bucciarelli-Ducci C. European Association of Cardiovascular Imaging expert consensus paper: a comprehensive review of cardiovascular magnetic resonance normal values of cardiac chamber size and aortic root in adults and recommendations for grading severity. *Eur Heart J Cardiovasc Imaging* 2019;**20**:1321–31.
12. Schulz-Menger J, Bluemke DA, Bremerich J, Flamm SD, Fogel MA, Friedrich MG *et al.* Standardized image interpretation and post-processing in cardiovascular magnetic resonance—2020 update. *J Cardiovasc Magn Reson* 2020; **22**:19.
13. Blanken CPS, Farag ES, Boekholdt SM, Leiner T, Kluin J, Nederveen AJ *et al.* Advanced cardiac MRI techniques for evaluation of left-sided valvular heart disease. *J Magn Reson Imaging* 2018;**48**:318–29.
14. Myerson SG. CMR in evaluating valvular heart disease: diagnosis, severity, and outcomes. *JACC Cardiovasc Imaging* 2021;**14**:2020–32.
15. Guglielmo M, Fusini L, Muscogiuri G, Baessato F, Loffreno A, Cavaliere A *et al.* T1 mapping and cardiac magnetic resonance feature tracking in mitral valve prolapse. *Eur Radiol* 2021;**31**:1100–9.
16. Wagner S, Auffermann W, Buser P, Lim TH, Kircher B, Pflugfelder P *et al.* Diagnostic accuracy and estimation of the severity of valvular regurgitation from the signal void on cine magnetic resonance images. *Am Heart J* 1989;**118**: 760–7.
17. Buchner S, Debl K, Poschenrieder F, Feuerbach S, Riegger GAJ, Luchner A *et al.* Cardiovascular magnetic resonance for direct assessment of anatomic regurgitant orifice in mitral regurgitation. *Circ Cardiovascular Imaging* 2008;**1**:148–55.

18. Pelc NJ, Herfkens RJ, Shimakawa A, Enzmann DR. Phase contrast cine magnetic resonance imaging. *Magn Reson Q* 1991;**7**:229–54.

19. Hudsmith L, Petersen S, Francis J, Robson M, Neubauer S. Normal human left and right ventricular and left atrial dimensions using steady state free precession magnetic resonance imaging. *J Cardiovasc Magn Reson* 2005;**7**:775–82.

20. Clarke CJ, Gurka MJ, Norton PT, Kramer CM, Hoyer AW. Assessment of the accuracy and reproducibility of RV volume measurements by CMR in congenital heart disease. *JACC Cardiovasc Imaging* 2012;**5**:28–37.

21. Bolen MA, Popovic ZB, Rajiah P, Gabriel RS, Zurick AO, Lieber ML et al. Cardiac MR assessment of aortic regurgitation: holodiastolic flow reversal in the descending aorta helps stratify severity. *Radiology* 2011;**260**:98–104.

22. Malahfji M, Senapati A, Tayal B, Nguyen DT, Graviss EA, Nagueh SF et al. Myocardial scar and mortality in chronic aortic regurgitation. *JAHA* 2020;**9**: e018731.

23. Tayal B, Debs D, Nabi F, Malahfji M, Little SH, Reardon M et al. Impact of myocardial scar on prognostic implication of secondary mitral regurgitation in heart failure. *JACC Cardiovasc Imaging* 2021;**14**:812–22.

24. Kitkungvan D, Nabi F, Kim RJ, Bonow RO, Khan MA, Xu J et al. Myocardial fibrosis in patients with primary mitral regurgitation with and without prolapse. *J Am Coll Cardiol* 2018;**72**:823–34.

25. Wang J, Fleischmann D. Improving spatial resolution at CT: development, benefits, and pitfalls. *Radiology* 2018;**289**:261–2.

26. Litmanovich DE, Kirsch J. Computed tomography of cardiac valves. *Radiol Clin North Am* 2019;**57**:141–64.

27. Lang RM, Badano LP, Mor-Avi V, Afilalo J, Armstrong A, Ernande L et al. Recommendations for cardiac chamber quantification by echocardiography in adults: an update from the American Society of Echocardiography and the European Association of Cardiovascular Imaging. *Eur Heart J Cardiovasc Imaging* 2015;**16**:233–70.

28. Muraru D, Badano LP, Vannan M, Iliceto S. Assessment of aortic valve complex by three-dimensional echocardiography: a framework for its effective application in clinical practice. *Eur Heart J Cardiovasc Imaging* 2012;**13**:541–55.

29. de Waroux JB, Pouleur AC, Goffinet C, Vancraeynest D, Van Dyck M, Robert A et al. Functional anatomy of aortic regurgitation: accuracy, prediction of surgical repairability, and outcome implications of transesophageal echocardiography. *Circulation* 2007;**116**:I264–9.

30. Feuchtner GM, Dichtl W, Schachner T, Müller S, Mallouhi A, Friedrich GJ et al. Diagnostic performance of MDCT for detecting aortic valve regurgitation. *Am J Roentgenol* 2006;**186**:1676–81.

31. Blondheim DS, Vassilenko L, Glick Y, Asif A, Nachtigal A, Meisel SR et al. Aortic dimensions by multi-detector computed tomography vs. echocardiography. *J Cardiol* 2016;**67**:365–70.

32. Tribouilloy CM, Enriquez-Sarano M, Bailey KR, Seward JB, Tajik AJ. Assessment of severity of aortic regurgitation using the width of the vena contracta: a clinical color Doppler imaging study. *Circulation* 2000;**102**:558–64.

33. Perry GJ, Helmcke F, Nanda NC, Byard C, Soto B. Evaluation of aortic insufficiency by Doppler colour flow mapping. *J Am Coll Cardiol* 1987;**9**:952–9.

34. Eren M, Eksik A, Gorgulu S, Norgaz T, Dagdeviren B, Bolca O. Determination of vena contracta and its value in evaluating severity of aortic regurgitation. *J Heart Valve Dis* 2002;**11**:567–75.

35. Fang L, Hsiung MC, Miller AP, Nanda NC, Yin WH, Young MS et al. Assessment of aortic regurgitation by live three-dimensional transthoracic echocardiographic measurements of vena contracta area: usefulness and validation. *Echocardiography* 2005;**22**:775–81.

36. Tribouilloy C, Avinée P, Shen WF, Rey JL, Slama M, Lesbre JP. End diastolic flow velocity just beneath the aortic isthmus assessed by pulsed Doppler echocardiography: a new predictor of the aortic regurgitant fraction. *Br Heart J* 1991; **65**:37–40.

37. Samstad SO, Hegrenaes L, Skjaerpe T, Hatle L. Half time of the diastolic aortoventricular pressure difference by continuous wave Doppler ultrasound: a measure of the severity of AR? *Br Heart J* 1989;**61**:336–43.

38. Griffin BP, Flachskampf FA, Siu S, Weyman AE, Thomas JD. The effects of regurgitant orifice size, chamber compliance, and systemic vascular resistance on aortic regurgitant velocity slope and pressure half-time. *Am Heart J* 1991; **122**:1049–56.

39. Debl K, Djavidani B, Buchner S, Heinicke N, Fredersdorf S, Haimerl J et al. Assessment of the anatomic regurgitant orifice in aortic regurgitation: a clinical magnetic resonance imaging study. *Heart* 2008;**94**:e8.

40. Tribouilloy CM, Enriquez-Sarano M, Fett SL, Bailey KR, Seward JB, Tajik AJ. Application of the proximal flow convergence method to calculate the effective regurgitant orifice area in aortic regurgitation. *J Am Coll Cardiol* 1998;**32**:1032–9.

41. Pouleur AC, de Waroux JB, Goffinet C, Vancraeynest D, Pasquet A, Gerber BL et al. Accuracy of the flow convergence method for quantification of aortic regurgitation in patients with central versus eccentric jets. *Am J Cardiol* 2008;**102**: 475–80.

42. Myerson SG, d'Arcy J, Mohiaddin R, Greenwood JP, Karamitsos TD, Francis JM et al. Aortic regurgitation quantification using cardiovascular magnetic resonance: association with clinical outcome. *Circulation* 2012;**126**:1452–60.

43. Yang LT, Anand V, Zambito EI, Pellikka PA, Scott CG, Thapa P et al. Association of echocardiographic left ventricular end-systolic volume and volume-derived ejection fraction with outcome in asymptomatic chronic aortic regurgitation. *JAMA Cardiol* 2021;**6**:189–98.

44. Ewe SH, Haeck MLA, Ng ACT, Witkowski TG, Auger D, Leong DP et al. Detection of subtle left ventricular systolic dysfunction in patients with significant aortic regurgitation and preserved left ventricular ejection fraction: speckle tracking echocardiographic analysis. *Eur Heart J Cardiovasc Imaging* 2015;**16**: 992–9.

45. Lee JKT, Franzone A, Lanz J, Siontis GCM, Stortecky S, Gräni C et al. Early detection of subclinical myocardial damage in chronic aortic regurgitation and strategies for timely treatment of asymptomatic patients. *Circulation* 2018;**137**: 184–96.

46. Le Polain de Waroux JB, Pouleur AC, Robert A, Pasquet A, Gerber BL, Noirhomme P et al. Mechanisms of recurrent aortic regurgitation after aortic valve repair: predictive value of intraoperative transesophageal echocardiography. *JACC Cardiovasc Imaging* 2009;**2**:931–9.

47. Erbel R, Aboyans V, Boileau C, Bossone E, Bartolomeo RD, Eggebrecht H et al.; ESC Committee for Practice Guidelines. ESC Guidelines on the diagnosis and treatment of aortic diseases. *Eur Heart J* 2014 ;**35**:2873–926.

48. Bouzas B, Kilner PJ, Gatzoulis MA. Pulmonary regurgitation: not a benign lesion. *Eur Heart J* 2005;**26**:433–9.

49. Kelly NFA, Platts DG, Burstow DJ. Feasibility of pulmonary valve imaging using three-dimensional transthoracic echocardiography. *J Am Soc Echocardiogr* 2010; **23**:1076–80.

50. Hadeed K, Hascoët S, Amadieu R, Dulac Y, Breinig S, Cazavet A et al. 3D transthoracic echocardiography to assess pulmonary valve morphology and annulus size in patients with tetralogy of Fallot. *Arch Cardiovasc Dis* 2016;**109**: 87–95.

51. Maciel BC, Simpson IA, Valdes-Cruz LM, Recusani F, Hoit B, Dalton N et al. Color flow Doppler mapping studies of "physiologic" pulmonary and tricuspid regurgitation: evidence for true regurgitation as opposed to a valve closing volume. *J Am Soc Echocardiogr* 1991;**4**:589–97.

52. Kobayashi J, Nakano S, Matsuda H, Arisawa J, Kawashima Y. Quantitative evaluation of pulmonary regurgitation after repair of tetralogy of Fallot using real-time flow imaging system. *Jpn Circ J* 1989;**53**:721–7.

53. Williams RV, Minich LL, Shaddy RE, Pagotto LT, Tani LY. Comparison of Doppler echocardiography with angiography for determining the severity of pulmonary regurgitation. *Am J Cardiol* 2002;**89**:1438–41.

54. Puchalski MD, Askovich B, Sower CT, Williams RV, Minich LL, Tani LY. Pulmonary regurgitation: determining severity by echocardiography and magnetic resonance imaging. *Congenit Heart Dis* 2008;**3**:168–75.

55. Van Berendoncks A, Van Grootel R, McGhie J, van Kranenburg M, Menting M, Cuypers JAAE et al. Echocardiographic parameters of severe pulmonary regurgitation after surgical repair of tetralogy of Fallot. *Congenit Heart Dis* 2019;**14**: 628–37.

56. Pothineni KR, Wells BJ, Hsiung MC, Nanda NC, Yelamanchili P, Suwanjutah T et al. Live/real time three-dimensional transthoracic echocardiographic assessment of pulmonary regurgitation. *Echocardiography* 2008;**25**:911–7.

57. Goldberg SJ, Allen HD. Quantitative assessment by Doppler echocardiography of pulmonary or aortic regurgitation. *Am J Cardiol* 1985;**56**:131–5.

58. Lei MH, Chen JJ, Ko YL, Cheng JJ, Kuan P, Lien WP. Reappraisal of quantitative evaluation of pulmonary regurgitation and estimation of pulmonary artery pressure by continuous wave Doppler echocardiography. *Cardiology* 1995;**86**: 249–56.

59. Silversides CK, Veldtman GR, Crossin J, Merchant N, Webb GD, McCrindle BW et al. Pressure Halftime predicts hemodynamically significant pulmonary regurgitation in adult patients with repaired tetralogy of Fallot. *J Am Soc Echocardiogr* 2003;**16**:1057–62.

60. Li W, Davlouros PA, Kilner PJ, Pennell DJ, Gibson D, Henein MY et al. Doppler-echocardiographic assessment of pulmonary regurgitation in adults with repaired tetralogy of Fallot: comparison with cardiovascular magnetic resonance imaging. *Am Heart J* 2004;**147**:165–72.

61. Mercer-Rosa L, Yang W, Kutty S, Rychik J, Fogel M, Goldmuntz E. Quantifying pulmonary regurgitation and right ventricular function in surgically repaired tetralogy of Fallot: a comparative analysis of echocardiography and magnetic resonance imaging. *Circ Cardiovascular Imaging* 2012;**5**: 637–43.

62. Oosterhof T, van Straten A, Vliegen HW, Meijboom FJ, van Dijk APJ, Spijkerboer AM et al. Preoperative thresholds for pulmonary valve replacement in patients with corrected tetralogy of Fallot using cardiovascular magnetic resonance. *Circulation* 2007;**116**:545.

63. Baumgartner H, De Backer J, Babu-Narayan SV, Budts W, Chessa M, Diller GP et al.; ESC Scientific Document Group. 2020 ESC Guidelines for the management of adult congenital heart disease. *Eur Heart J* 2021;**42**:563–645.

64. O'Gara P, Sugeng L, Lang R, Sarano M, Hung J, Raman S et al. The role of imaging in chronic degenerative mitral regurgitation. *JACC Cardiovasc Imaging* 2008;**1**: 221–37.

65. Lancellotti P, Lebrun F, Piérard LA. Determinants of exercise-induced changes in mitral regurgitation in patients with coronary artery disease and left ventricular dysfunction. *J Am Coll Cardiol* 2003;**42**:1921–8.

66. Agricola E, Oppizzi M, Pisani M, Meris A, Maisano F, Margonato A. Ischemic mitral regurgitation: mechanisms and echocardiographic classification. *Eur J Echocardiogr* 2008;**9**:207–21.

67. Mesi O, Gad MM, Crane AD, Ramchand J, Puri R, Layoun H et al. Severe atrial functional mitral regurgitation: clinical and echocardiographic characteristics, management, and outcomes. *J AmColl Cardiol Img* 2021;**14**:797–808.

68. Dejgaard LA, Skjølsvik ET, Lie ØH, Ribe M, Stokke MK, Hegbom F et al. The mitral annulus disjunction arrhythmic syndrome. *J Am Coll Cardiol* 2018;**72**:1600–9.

69. Han Y, Peters DC, Salton CJ, Bzymek D, Nezafat R, Goddu B et al. Cardiovascular magnetic resonance characterization of mitral valve prolapse. *JACC Cardiovasc Imaging* 2008;**1**:294–303.

70. Chaliki HP, Nishimura RA, Enriquez-Sarano M, Reeder GS. A simplified, practical approach to assessment of severity of mitral regurgitation by Doppler color flow imaging with proximal convergence: validation with concomitant cardiac catheterization. *Mayo Clin Proc* 1998;**73**:929–35.

71. McCully RB, Enriquez-Sarano M, Tajik AJ, Seward JB. Overestimation of severity of ischemic/functional mitral regurgitation by color Doppler jet area. *Am J Cardiol* 1994;**74**:790–3.

72. Tribouilloy C, Shen WF, Quéré JP, Rey JL, Choquet D, Dufossé H et al. Assessment of severity of mitral regurgitation by measuring regurgitant jet width at its origin with transesophageal Doppler color flow imaging. *Circulation* 1992;**85**:1248–53.

73. Hall SA, Brickner ME, Willett DL, Irani WN, Afridi I, Grayburn PA. Assessment of mitral regurgitation severity by Doppler color flow mapping of the vena contracta. *Circulation* 1997;**95**:636–42.

74. Matsumura Y, Fukuda S, Tran H, Greenberg NL, Agler DA, Wada N et al. Geometry of the proximal isovelocity surface area in mitral regurgitation by 3-dimensional color Doppler echocardiography: difference between functional mitral regurgitation and prolapse regurgitation. *Am Heart J* 2008;**155**:231–8.

75. Song JM, Kim MJ, Kim YJ, Kang SH, Kim JJ, Kang DH et al. Three-dimensional characteristics of functional mitral regurgitation in patients with severe left ventricular dysfunction: a real-time three-dimensional colour Doppler echocardiography study. *Heart* 2008;**94**:590–6.

76. Yosefy C, Hung J, Chua S, Vaturi M, Ton-Nu TT, Handschumacher MD et al. Direct measurement of vena contracta area by real-time 3-dimensional echocardiography for assessing severity of mitral regurgitation. *Am J Cardiol* 2009;**104**:978–83.

77. Kahlert P, Plicht B, Schenk IM, Janosi RA, Erbel R, Buck T. Direct assessment of size and shape of noncircular vena contracta area in functional versus organic mitral regurgitation using real-time three-dimensional echocardiography. *J Am Soc Echocardiogr* 2008;**21**:912–21.

78. Goebel B, Heck R, Hamadanchi A, Otto S, Doenst T, Jung C et al. Vena contracta area for severity grading in functional and degenerative mitral regurgitation: a transoesophageal 3D colour Doppler analysis in 500 patients. *Eur Heart J Cardiovasc Imaging* 2018;**19**:639–46.

79. Tribouilloy C, Shen WF, Rey JL, Adam MC, Lesbre JP. Mitral to aortic velocity-time integral ratio. A non-geometric pulsed-Doppler regurgitant index in isolated pure mitral regurgitation. *Eur Heart J* 1994;**15**:1335–9.

80. Enriquez-Sarano M, Dujardin KS, Tribouilloy CM, Seward JB, Yoganathan AP, Bailey KR et al. Determinants of pulmonary venous flow reversal in mitral regurgitation and its usefulness in determining the severity of regurgitation. *Am J Cardiol* 1999;**83**:535–41.

81. Enriquez-Sarano M, Miller FA Jr, Hayes SN, Bailey KR, Tajik AJ, Seward JB. Effective mitral regurgitant orifice area: clinical use and pitfalls of the proximal isovelocity surface area method. *J Am Coll Cardiol* 1995;**25**:703–9.

82. Lancellotti P, Marwick T, Pierard LA. How to manage ischaemic mitral regurgitation. *Heart* 2008;**94**:1497–502.

83. Iwakura K, Ito H, Kawano S, Okamura A, Kurotobi T, Date M et al. Comparison of orifice area by transthoracic three-dimensional Doppler echocardiography versus proximal isovelocity surface area (PISA) method for assessment of mitral regurgitation. *Am J Cardiol* 2006;**97**:1630–7.

84. Stone GW, Lindenfeld J, Abraham WT, Kar S, Lim DS, Mishell JM et al. Transcatheter mitralvalve repair in patients with heart failure. *N Engl J Med* 2018;**379**:2307–18.

85. Asch FM, Grayburn PA, Siegel RJ, Kar S, Lim DS, Zaroff JG et al. Echocardiographic outcomes after transcatheter leaflet approximation in patients with secondary mitral regurgitation: the COAPT trial. *J Am Coll Cardiol* 2019;**74**:2969–79.

86. Obadia JF, Messika-Zeitoun D, Leurent G, Iung B, Bonnet G, Piriou N et al. Percutaneous repair or medical treatment for secondary mitral regurgitation. *N Engl J Med* 2018;**379**:2297–306.

87. Lancellotti P, Troisfontaines P, Toussaint AC, Piérard LA. Prognostic importance of exercise-induced changes in mitral regurgitation in patients with chronic ischemic left ventricular dysfunction. *Circulation* 2003;**108**:1713–17.

88. Bartko PE, Arfsten H, Heitzinger G, Pavo N, Toma A, Strunk G et al. A unifying concept for the quantitative assessment of secondary mitral regurgitation. *J Am Coll Cardiol* 2019;**73**:2506–17.

89. Gelfand EV, Hughes S, Hauser TH, Yeon SB, Goepfert L, Kissinger KV et al. Severity of mitral and aortic regurgitation as assessed by cardiovascular magnetic resonance: optimizing correlation with Doppler echocardiography. *J Cardiovasc Magn Reson* 2006;**8**:503–7.

90. Myerson SG, d'Arcy J, Christiansen JP, Dobson LE, Mohiaddin R, Francis JM et al. Determination of clinical outcome in mitral regurgitation with cardiovascular magnetic resonance quantification. *Circulation* 2016;**133**:2287–96.

91. Cavalcante JL, Kusunose K, Obuchowski NA, Jellis C, Griffin BP, Flamm SD et al. Prognostic impact of ischemic mitral regurgitation severity and myocardial infarct quantification by cardiovascular magnetic resonance. *J Am Coll Cardiol Img* 2020;**13**:1489–150.

92. Uretsky S, Gillam L, Lang R, Chaudhry FA, Argulian E, Supariwala A et al. Discordance between echocardiography and MRI in the assessment of mitral regurgitation severity: a prospective multicenter trial. *J Am Coll Cardiol* 2015;**65**: 1078–88.

93. Witkowski TG, Thomas JD, Debonnaire PJMR, Delgado V, Hoke U, Ewe SH et al. Global longitudinal strain predicts left ventricular dysfunction after mitral valve repair. *Eur Heart J Cardiovasc Imaging* 2013;**14**:69–76.

94. Omran AS, Woo A, David TE, Feindel CM, Rakowski H, Siu SC. Intraoperative transesophageal echocardiography accurately predicts mitral valve anatomy and suitability for repair. *J Am Soc Echocardiogr* 2002;**15**:950–7.

95. Kongsaerepong V, Shiota M, Gillinov AM, Song JM, Fukuda S, McCarthy PM et al. Echocardiographic predictors of successful versus unsuccessful mitral valve repair in ischemic mitral regurgitation. *Am J Cardiol* 2006;**98**:504–8.

96. Agricola E, Ancona F, Brochet E, Donal E, Dweck M, Faletra F et al. The structural heart disease interventional imager rationale, skills and training: a position paper of the European Association of Cardiovascular Imaging. *Eur Heart J Cardiovasc Imaging* 2021;**22**:471–9.

97. Topilsky Y, Maltais S, Medina Inojosa J, Oguz D, Michelena H, Maalouf J et al. Burden of tricuspid regurgitation in patients diagnosed in the community setting. *JACC Cardiovasc Imaging* 2019;**12**:433–42.

98. Santoro C, Marco Del Castillo A, González-Gómez A, Monteagudo JM, Hinojar R, Lorente A et al. Mid-term outcome of severe tricuspid regurgitation: are there any differences according to mechanism and severity? *Eur Heart J Cardiovasc Imaging* 2019;**20**:1035–42.

99. Muraru D, Previtero M, Ochoa-Jimenez RC, Guta AC, Figliozzi S, Gregori D et al. Prognostic validation of partition values for quantitative parameters to grade functional tricuspid regurgitation severity by conventional echocardiography. *Eur Heart J Cardiovasc Imaging* 2021;**22**:155–65.

100. Hahn RT, Weckbach LT, Noack T, Hamid N, Kitamura M, Bae R et al. Proposal for a standard echocardiographic tricuspid valve nomenclature. *JACC Cardiovasc Imaging* 2021;**14**:1299–305.

101. Rogers JH, Bolling SF, The tricuspid valve: current perspective and evolving management of tricuspid regurgitation. *Circulation* 2009;**119**:2718–25.

102. Muraru D, Guta A-C, Ochoa-Jimenez RC, Bartos D, Aruta P, Mihaila S et al. Functional regurgitation of atrioventricular valves and atrial fibrillation: an elusive pathophysiological link deserving further attention. *J Am Soc Echocardiogr* 2020;**33**:42–53.

103. Muraru D, Badano LP, Sarais C, Solda E, Iliceto S. Evaluation of tricuspid valve morphology and function by transthoracic three-dimensional echocardiography. *Curr Cardiol Rep* 2011;**13**:242–9.

104. Toh H, Mori S, Izawa Y, Toba T, Nishii T, Hirata KI. Revival of mitral and tricuspid annular disjunctions: are these really abnormal findings? *JACC Cardiovasc Imaging* 2021;**14**:1682–4.

105. Prihadi EA, Delgado V, Leon MB, Enriquez-Sarano M, Topilsky Y, Bax JJ. Morphologic types of tricuspid regurgitation: characteristics and prognostic implications. *JACC Cardiovasc Imaging* 2019;**12**:491–9.

106. Guta AC, Badano LP, Tomaselli M, Mihalcea D, Bartos D, Parati G et al. The pathophysiological link between right atrial remodeling and functional tricuspid regurgitation in patients with atrial fibrillation: a three-dimensional echocardiography study. *J Am Soc Echocardiogr* 2021;**34**:585–94.

107. Badano LP, Agricola E, Perez de Isla L, Gianfagna P, Zamorano JL. Evaluation of the tricuspid valve morphology and function by transthoracic real-time three-dimensional echocardiography. *Eur J Echocardiogr* 2009;**10**:477–84.

108. Addetia K, Harb SC, Hahn RT, Kapadia S, Lang RM. Cardiac implantable electronic device lead-induced tricuspid regurgitation. *JACC Cardiovasc Imaging* 2019; **12**:622–36.

109. Stankovic I, Daraban AM, Jasaityte R, Neskovic AN, Claus P, Voigt JU. Incremental value of the en face view of the tricuspid valve by two-dimensional and three-dimensional echocardiography for accurate identification of tricuspid valve leaflets. *J Am Soc Echocardiogr* 2014;**27**:376–84.

110. Addetia K, Yamat M, Mediratta A, Medvedofsky D, Patel M, Ferrara P *et al.* Comprehensive two-dimensional interrogation of the tricuspid valve using knowledge derived from three-dimensional echocardiography. *J Am Soc Echocardiogr* 2016;**29**:74–82.

111. Addetia K, Muraru D, Veronesi F, Jenei C, Cavalli G, Besser SA *et al.* 3-Dimensional echocardiographic analysis of the tricuspid annulus provides new insights into tricuspid valve geometry and dynamics. *JACC Cardiovasc Imaging* 2019;**12**:401–12.

112. Kim HK, Kim YJ, Park JS, Kim KH, Kim KB, Ahn H *et al.* Determinants of the severity of functional tricuspid regurgitation. *Am J Cardiol* 2006;**98**:236–42.

113. Kwan J, Kim GC, Jeon MJ, Kim DH, Shiota T, Thomas JD *et al.* 3D geometry of a normal tricuspid annulus during systole: a comparison study with the mitral annulus using real-time 3D echocardiography. *Eur J Echocardiogr* 2007;**8**:375–83.

114. Gonzalez-Vilchez F, Zarauza J, Vazquez de Prada JA M, Durán, R, Ruano, J Delgado, C *et al.* Assessment of tricuspid regurgitation by Doppler color flow imaging: angiographic correlation. *Int J Cardiol* 1994;**44**:275–83.

115. Hahn RT, Thomas JD, Khalique OK, Cavalcante JL, Praz F, Zoghbi WA. Imaging assessment of tricuspid regurgitation severity. *JACC Cardiovasc Imaging* 2019;**12**:469–90.

116. Muraru D, Hahn RT, Soliman OI, Faletra FF, Basso C, Badano LP. 3-Dimensional echocardiography in imaging the tricuspid valve. *JACC Cardiovasc Imaging* 2019;**12**:500–15.

117. Dahou A, Ong G, Hamid N, Avenatti E, Yao J, Hahn RT. Quantifying tricuspid regurgitation severity: a comparison of proximal isovelocity surface area and novel quantitative doppler methods. *JACC Cardiovasc Imaging* 2019;**12**:560–2.

118. Nagueh SF, Kopelen HA, Zoghbi WA. Relation of mean right atrial pressure to echocardiographic and Doppler parameters of right atrial and right ventricular function. *Circulation* 1996;**93**:1160–9.

119. Minagoe S, Rahimtoola SH, Chandraratna PA. Significance of laminar systolic regurgitant flow in patients with tricuspid regurgitation: a combined pulsed-wave, continuous-wave Doppler and two-dimensional echocardiographic study. *Am Heart J* 1990;**119**:627–35.

120. Lopes BBC, Sorajja P, Hashimoto G, Fukui M, Bapat VN, Du Y *et al.* Tricuspid anatomic regurgitant orifice area by functional DSCT: a novel parameter of tricuspid regurgitation severity. *JACC Cardiovasc Imaging* 2021;**14**:1669–72.

121. Tribouilloy CM, Enriquez-Sarano M, Capps MA, Bailey KR, Tajik AJ. Contrasting effect of similar effective regurgitant orifice area in mitral and tricuspid regurgi-

122. tation: a quantitative Doppler echocardiographic study. *J Am Soc Echocardiogr* 2002;**15**:958–65.

122. Grossmann G, Stein M, Kochs M, Höher M, Koenig W, Hombach V *et al.* Comparison of the proximal flow convergence method and the jet area method for the assessment of the severity of tricuspid regurgitation. *Eur Heart J* 1998;**19**:652–9.

123. Rivera JM, Vandervoort P, Mele D, Weyman A, Thomas JD. Value of proximal regurgitant jet size in tricuspid regurgitation. *Am Heart J* 1996;**131**:742–7.

124. Hahn RT, Zamorano JL. The need for a new tricuspid regurgitation grading scheme. *Eur Heart J Cardiovasc Imaging* 2017;**18**:1342–43.

125. Vieitez JM, Monteagudo JM, Mahia P, Perez L, Lopez T, Marco I *et al.* New insights of tricuspid regurgitation: a large-scale prospective cohort study. *Eur Heart J Cardiovasc Imaging* 2021;**22**:196–202.

126. Fortuni F, Dietz MF, Prihadi EA, van der Bijl P, De Ferrari GM, Knuuti J *et al.* Prognostic implications of a novel algorithm to grade secondary tricuspid regurgitation. *JACC Cardiovasc Imaging* 2021;**14**:1085–95.

127. Park JB, Kim HK, Jung JH, Klem I, Yoon YE, Lee SP *et al.* Prognostic value of cardiac MR imaging for preoperative assessment of patients with severe functional tricuspid regurgitation. *Radiology* 2016;**280**:723–34.

128. Kim HK, Kim YJ, Park EA, Bae JS, Lee W, Kim KH *et al.* Assessment of haemodynamic effects of surgical correction for severe functional tricuspid regurgitation: cardiac magnetic resonance imaging study. *Eur Heart J* 2010;**31**:1520–8.

129. Badano LP, Muraru D, Parati G, Haugaa K, Voigt JU. How to do right ventricular strain. *Eur Heart J Cardiovasc Imaging* 2020;**21**:825–7.

130. Shimada YJ, Shiota M, Siegel RJ, Shiota T. Accuracy of right ventricular volumes and function determined by three-dimensional echocardiography in comparison with magnetic resonance imaging: a meta-analysis study. *J Am Soc Echocardiogr* 2010;**23**:943–53.

131. Muraru D, Spadotto V, Cecchetto A, Romeo G, Aruta P, Ermacora D *et al.* New speckle-tracking algorithm for right ventricular volume analysis from three-dimensional echocardiographic data sets: validation with cardiac magnetic resonance and comparison with the previous analysis tool. *Eur Heart J Cardiovasc Imaging* 2016;**17**:1279–89.

132. Matsunaga A, Duran CM. Progression of tricuspid regurgitation after repaired functional ischemic mitral regurgitation. *Circulation* 2005;**112**:I453–7.

133. Fukuda S, Gillinov AM, McCarthy PM, Stewart WJ, Song JM, Kihara T *et al.* Determinants of recurrent or residual functional tricuspid regurgitation after tricuspid annuloplasty. *Circulation* 2006;**114**:I582–7.

134. Lurz P, Stephan von Bardeleben R, Weber M, Sitges M, Sorajja P, Hausleiter J *et al.* Transcatheter edge-to-edge repair for treatment of tricuspid regurgitation. *J Am Coll Cardiol* 2021;**77**:229–239.